

*Genetics and epigenetics of memory functions:  
from nematodes to human health and disease*

**Inauguraldissertation**

zur

Erlangung der Würde eines Doktors der Philosophie

vorgelegt der

Philosophisch-Naturwissenschaftlichen Fakultät

der Universität Basel

von

Vanja Vukojevic

Belgrade, Serbia

Basel, 2012

Original document stored on the publication server of the University of Basel

**edoc.unibas.ch**

This work is licensed under the agreement „Attribution Non-Commercial No Derivatives –2.5

Switzerland“. The complete text may be viewed here:

**[creativecommons.org/licenses/by-nc-nd/2.5/ch/deed.en](https://creativecommons.org/licenses/by-nc-nd/2.5/ch/deed.en)**

Genehmigt von der Philosophisch Naturwissenschaftlichen Fakultät auf Antrag  
von

Prof. Dr. Heinrich Reichert

Prof. Dr. Andreas Papassotiropoulos

Basel, den 18.09.2012

Prof. Dr. Jörg Schibler

Dekan



## Attribution-Noncommercial-No Derivative Works 2.5 Switzerland

### You are free:



to Share — to copy, distribute and transmit the work

### Under the following conditions:



**Attribution.** You must attribute the work in the manner specified by the author or licensor (but not in any way that suggests that they endorse you or your use of the work).



**Noncommercial.** You may not use this work for commercial purposes.



**No Derivative Works.** You may not alter, transform, or build upon this work.

- For any reuse or distribution, you must make clear to others the license terms of this work. The best way to do this is with a link to this web page.
- Any of the above conditions can be waived if you get permission from the copyright holder.
- Nothing in this license impairs or restricts the author's moral rights.

#### Your fair dealing and other rights are in no way affected by the above.

This is a human-readable summary of the Legal Code (the full license) available in German:  
<http://creativecommons.org/licenses/by-nc-nd/2.5/ch/legalcode.de>

#### Disclaimer:

The Commons Deed is not a license. It is simply a handy reference for understanding the Legal Code (the full license) — it is a human-readable expression of some of its key terms. Think of it as the user-friendly interface to the Legal Code beneath. This Deed itself has no legal value, and its contents do not appear in the actual license. Creative Commons is not a law firm and does not provide legal services. Distributing, displaying of, or linking to this Commons Deed does not create an attorney-client relationship.

## ACKNOWLEDGMENTS

I would like to gratefully and sincerely thank to Prof. Dr. Heinrich Reichert, Prof. Dr. Andreas Pappasotiropoulos, Prof. Dr. Dominique J.-F. de Quervain and Dr. Attila Stetak for their guidance, understanding, patience, and most importantly, their friendship and support during my graduate studies at the Biozentrum of the University of Basel. During the years I have spent working on my thesis they constantly encouraged me to grow as a scientist, as an instructor and an independent thinker. I strongly believe that not many graduate students are given the opportunity to develop their own individuality and self-sufficiency by being allowed to work with such independence on multidisciplinary projects. Memory: From Mind to Molecules. For everything you've done for me, dear Andreas, Dominique, Heinrich and Attila, I thank you.

This dissertation could also not be done without the wonderful support of all the people from the Departments of Molecular and Cognitive Neurosciences, as well as the LSTF Core Facility. It was a long journey, and I couldn't have come this far without the assistance of many dear colleagues. I want to express my deepest appreciation to them. Thank you for all the beautiful science and also for some much needed humor and entertainment in what could have otherwise been a somewhat stressful laboratory environment.

My great gratitude goes to the Werner Siemens Foundation PhD Program "Opportunities for excellence" and the Biozentrum of University of Basel. I feel honored being prized with this prestigious scholarship, and would like to express my deepest appreciation for the dedication and generosity of the people standing behind it. The people I have met while in the Biozentrum graduate school have become my closest and dearest friends, counselors and collaborators, and to all of you I give my love and thanks.

Finally, I would like to thank the dear people that have brought me to science and supported me along the way for many years. Among many, it was Dr. Aneta and Dr. Marko Sabovljevic, loving friends and caring supervisors that have stood by my side from the beginnings. Theirs and my PhD supervisors' examples, as researchers and teachers, continue to serve as guidelines for my academic career.

Above all, I want to thank my family and friends for their support, encouragement, quiet patience and unwavering love. Those were undeniably the bedrock upon which my life has been built. They always had faith in my ambitions and me. I owe them everything and I wish I could show them more just how much I love and appreciate them.

**“Neither psychology nor biology alone can satisfactorily address the questions of memory, but the combined strength of both disciplines is providing a fresh and exciting picture of how the brain learns and remembers.”**

Larry R.Squire and Eric R.Kandel, *Memory: From Mind to Molecules*



## Table of Contents

<b>Plastic cytoskeleton: Actin interplay with synaptic form and function .....</b>	<b>11</b>
<b>A role for <math>\alpha</math>-adducin (ADD-1) in nematode and human memory .....</b>	<b>15</b>
<b>1 Abstract .....</b>	<b>16</b>
<b>2 Introduction .....</b>	<b>17</b>
<b>3 Results .....</b>	<b>20</b>
3.1.1 Loss of adducin ( <i>add-1</i> ) causes impairment of short and long-term memory.....	20
3.1.2 Adducin expression in neurons overlaps with AMPA-type glutamate receptor, GLR-1 .....	27
3.1.3 Sustained consolidation of synaptic plasticity depends on adducin.....	30
3.1.4 Changes of GLR-1 dynamics during associative learning is regulated by adducin.....	32
3.1.5 GLR-1 function in AVA is essential for memory formation .....	34
3.1.6 <i>Adducin function is essential for sustained changes of AVA neuron         activity upon learning.....</i>	<i>36</i>

3.1.7	Adducin function in AVA interneuron is essential for sustained changes in RIM motor neuron activity upon learning and memory.	40
3.1.8	Stabilization of actin filaments by ADD-1 is essential for memory	44
3.1.9	Behavioral genetic studies support a role for $\alpha$ -adducin in human memory.....	46
<b>4</b>	<b>Discussion .....</b>	<b>49</b>
<b>5</b>	<b>Experimental procedures .....</b>	<b>53</b>
5.1.1	General methods and strains used.....	53
5.1.2	Molecular biology.....	54
5.1.3	Real-time RT-PCR.....	54
5.1.4	Chemotaxis.....	54
5.1.5	Olfactory conditioning.....	54
5.1.6	Chemotaxis to water-soluble compounds .....	55
5.1.7	Microscopy.....	55
5.1.8	Human studies.....	56
5.1.9	Array-based SNP genotyping.....	57
<b>6</b>	<b>Acknowledgments.....</b>	<b>58</b>
<b>7</b>	<b>References .....</b>	<b>59</b>
	<b>Epigenetics of human memory: Linking memory to the fifth base.....</b>	<b>670</b>
	<b>DNA methylation at glucocorticoid receptor gene promoter is linked to the PTSD risk in genocide survivors.....</b>	<b>70</b>
<b>8</b>	<b>Abstract.....</b>	<b>71</b>



<b>9</b>	<b>Introduction .....</b>	<b>72</b>
<b>10</b>	<b>Results .....</b>	<b>75</b>
	10.1.1 DNA methylation of the GR promoter gene in traumatized survivors of the Rwandan genocide.....	75
	10.1.2 Expression of the GR correlates with DNA methylation at the <i>NR3C1</i> gene promoter .....	79
	10.1.3 <i>LINE-1</i> element methylation.....	81
<b>11</b>	<b>Discussion.....</b>	<b>83</b>
<b>12</b>	<b>Material and methods .....</b>	<b>86</b>
	12.1.1 Subjects: Rwanda Sample .....	86
	12.1.2 DNA isolation and bisulfite conversion .....	87
	12.1.3 Pyrosequencing analysis .....	87
	12.1.4 <i>LINE-1</i> HRM qPCR analysis.....	88
	12.1.5 RNA isolation and expression analysis.....	89
	12.1.6 Statistical analyses .....	90
<b>13</b>	<b>Acknowledgments .....</b>	<b>91</b>
<b>14</b>	<b>References .....</b>	<b>92</b>



## **Plastic cytoskeleton: Actin interplay with synaptic form and function**

Synapses are highly specialized intercellular junctions specialized for transmission of signals between neuron and its target cells. One of the most profound characteristics of synapses is the extraordinary degree of morphological and functional plasticity under basal conditions and also in response to neuronal activity. Synaptic plasticity is a long studied mechanism that is thought to be in the center of memory formation and maintenance. The significance of synapse morphological dynamics for the synaptic plasticity and therefore memory still remains unclear (Dillon & Goda, 2005).

Actin is the main structural component of the neurons and their synaptic terminals. The role of actin and other cytoskeleton components for the formation and function of cells is immense. The remodeling of these filaments by multiple intrinsic and extrinsic cues, via conserved signaling pathways, enables the cytoskeleton to control the amazing diversity of eukaryotic cellular morphologies and modify cellular behaviors (Dillon & Goda, 2005). Actin is also highly enriched at axon terminals and dendritic spines, neuronal compartments that mediate the most of excitatory synaptic transmission in the brain (Matus, 2000; Capani *et al*, 2001; Yuste & Bonhoeffer, 2004). Taken together, remodeling of synapses necessarily depends on actin dynamics.

Actin is present in two different states in the cell: monomeric G-actin and asymmetric F-actin - two stranded helical filament that is composed of G-actin (Figure S1). The polymerization and disassembly processes are rapid due to weak non-covalent interaction of the G-actin. At the basal state, F-actin preferentially polymerizes at the barbed end, while G-actin monomers are constantly lost at the opposite, pointed end. As the result of different speed of two processes the molecules there is a constant net turnover of actin filaments. Furthermore actin dynamic is additionally altered and filaments are hierarchically organized in higher structures by numerous actin-binding proteins (Pollard & Borisy, 2003; Revenu *et al*, 2004; Ethell & Pasquale, 2005; Cingolani, 2008).

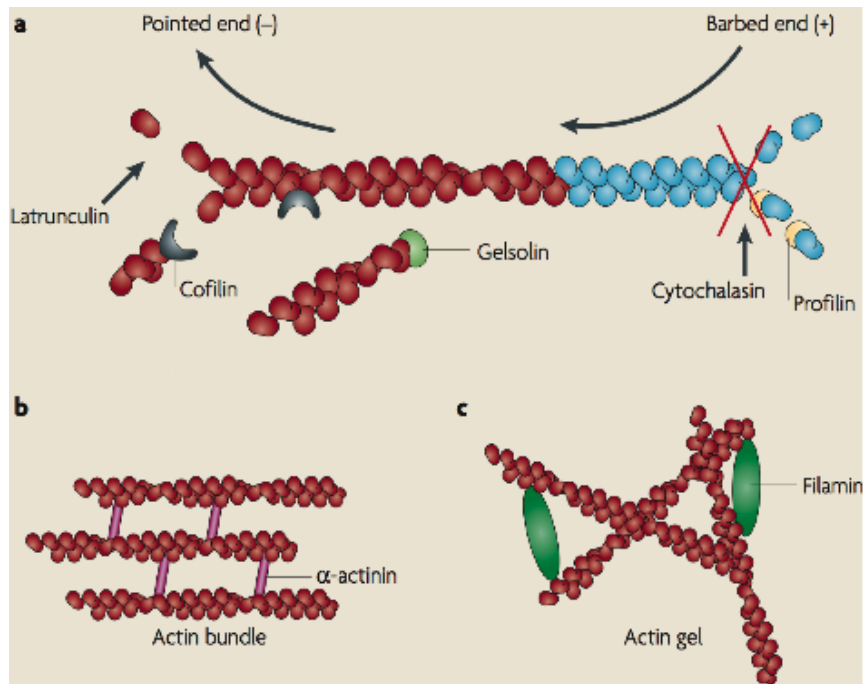


**Figure S1. Actin dynamics** (from (Cingolani, 2008)). Monomeric G-actin is the building block of F-actin. G-actin bound to ATP (panel a of the figure, blue) spontaneously self-associates through weak non-covalent interactions to form asymmetric filaments that have distinct ends because of the polarity of their constituent actin monomers (ADP-bound G-actin is shown in red). Polymerization occurs preferentially at the barbed (or ‘plus’) end over the pointed (or ‘minus’) end. At steady-state and at a given cellular G-actin concentration, the difference in polymerization rates at the two ends gives rise to a net loss of actin monomers at the pointed end and a simultaneous gain of monomers at the barbed end. This creates a net flow of newly acquired G-actin through the filament in a phenomenon that is known as actin tread milling, resulting in a dynamic turnover of actin filaments while filament length is maintained. A variety of actin-binding proteins (ABPs) influence the structure and organization of the actin cytoskeleton. Capping proteins (for example, tropomodulin and CapZ) bind to filament ends and can modify filament turnover to affect their length, whereas crosslinking proteins (for example,  $\alpha$ -actinin (see figure, part b), filamin (see figure, part c) and spectrin) can arrange F-actin into distinct networks, such as actin bundles and gels (see figure, parts b and c). Other ABPs affect F-actin by promoting its depolymerization (for example, ADF/cofilin), its severing (for example, gelsolin and ADF/cofilin) or its polymerization (for example, profilin) (see figure, part a).

The organization of actin filaments at synapses is very conserved. Main cytoskeleton features are essentially very similar among different type of synapses, consistent with the uniform appearance of the synaptic architecture. F-actin filaments are abundantly distributed in the presynaptic terminal and often associated with synapsin filaments (Landis *et al*, 1988). Actin is also an important component of the active zone (Phillips *et al*, 2001; Hirokawa *et al*, 1989; Morales *et al*, 2000; Bloom *et al*, 2003) (Figure S2). Fluorescence, microscopy studies showed that F-actin is focused in the vesicle release site and excluded from the synaptic vesicle cluster in the center. In the postsynaptic terminal, actin is clustered in 3 pools: Post Synaptic Density (PSD) actin pool that is crucial for the normal signal transduction; additional network of actin filaments throughout the spine volume; and finally a pool of actin filaments spanning from the cell body towards dendritic spine (Figure S2, for review see (Dillon & Goda, 2005)).

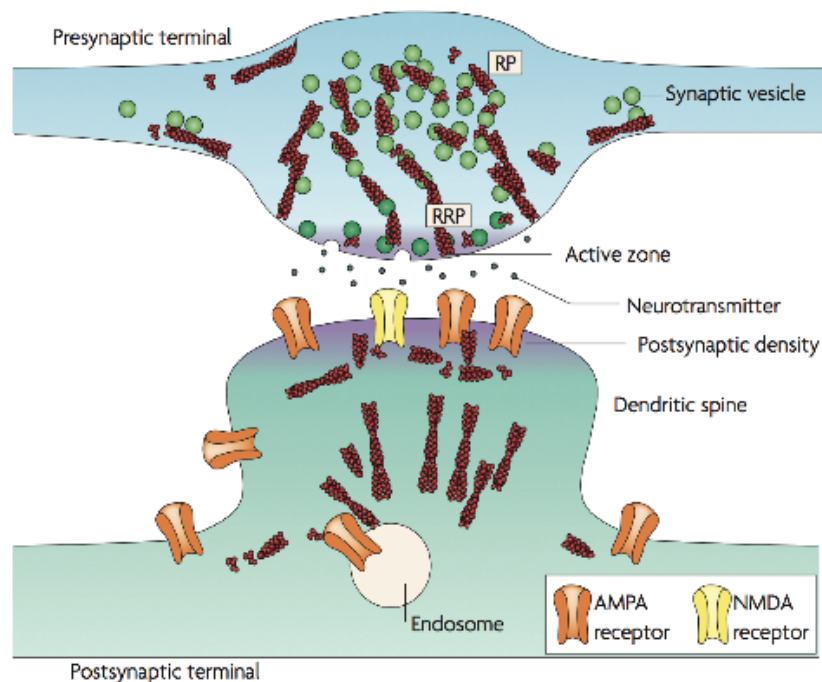


**Figure S2. Overview of actin at the excitatory synapse** (from (Cingolani, 2008)). At the presynaptic terminal (top), some synaptic vesicles (those belonging to the readily releasable pool (RRP); dark green) are found docked at the active zone, where they undergo exocytosis to release neurotransmitters. Numerous vesicles that presumably belong to the reserve pool (RP; light green) are located centrally, where they are interlinked to each other by short actin filaments (shown in red) and by synapsin (not shown) in a manner that suggests

subgrouping within the cluster. The subgroups are linked to longer filaments that extend from the plasma membrane, some of them from the active zone. At the postsynaptic terminal (bottom), the dendritic spine harbors AMPA ( $\alpha$ -amino-3-hydroxy-5-methyl-4-isoxazole propionic acid) and NMDA (N-methyl-d-aspartate) receptors at the postsynaptic density (PSD), which lies opposite the presynaptic active zone. A sub-membranous actin network that interlinks scaffolding proteins (not shown) organizes the PSD. Actin filaments are also found longitudinally along the spine axis. Actin is a key component of dendritic spines that defines their shape. Furthermore, actin filaments regulate surface-receptor diffusion and the exo- and endocytic trafficking of receptors, thus determining their abundance at the postsynaptic membrane (a key parameter of postsynaptic efficacy). Plasticity is elicited by altering actin dynamics, leading to active remodeling of both the pre- and the postsynaptic actin scaffold, the organization of synaptic vesicle pools or the organization of the postsynaptic receptors that are supported by the scaffold. In addition, altered actin dynamics could modulate steps of the synaptic vesicle cycle and postsynaptic receptor activity or traffic, which are directly regulated by actin turnover. Overall, these changes would affect the efficacy of synaptic transmission and, thus, of synaptic plasticity.

The properties of the cytoskeleton and actin as its main constituent are crucial for different levels of synapse anatomy and function. Cytoskeleton remodeling tightly regulates synapse structure formation and organization. The maintenance of synaptic structure is supposed to be crucial for sustained cellular memory and also depends on cytoskeleton. Additionally, vesicles cycling, including trafficking, exo- and endocytosis depends on active dynamics of the cellular skeleton. Finally, activation dependent plasticity and remodeling of synaptic structures, crucially important for learning and memory of new information, is also dependent on actin dynamics action in neuronal cells (Dillon & Goda, 2005).

In the current work, using the nematode *C.elegans* as a model system, we investigated the role of adducin (*add-1*), an acting capping protein, in synaptic plasticity during aversive learning and memory. Loss of *add-1* resulted in short- and long-term memory impairments, possibly through changed actin stability and altered synapse dynamics. Additionally, the human ortholog  $\alpha$ -adducin showed remarkable functional conservation in human episodic memory. The study presented here is an important contribution to our understanding of synaptic plasticity and the role of cytoskeleton remodeling in learning and memory. Furthermore, it emphasizes the importance of translational approach and usefulness of *C.elegans* as a model system for neuroscience research.

## A role for $\alpha$ -adducin (ADD-1) in nematode and human memory

Vanja Vukojevic<sup>1,2</sup>, Leo Gschwind<sup>1,3</sup>, Christian Vogler<sup>1,4</sup>, Fabian Peter<sup>1,2</sup>, Philippe Demougin<sup>1,2</sup>, Dominique J.-F. de Quervain<sup>3,4</sup>, Andreas Papassotiropoulos<sup>1,2,4,5</sup> and Attila Stetak<sup>1,2,4,5</sup>

<sup>1</sup>*University of Basel, Department of Psychology, Division of Molecular Neuroscience, Missionsstrasse 62, 4055 Basel, Switzerland*

<sup>2</sup>*University of Basel, Department Biozentrum, Life Sciences Training Facility, Klingelbergstrasse 50/70, 4056 Basel, Switzerland*

<sup>3</sup>*University of Basel, Department of Psychology, Division of Cognitive Neuroscience, Birmannsgasse 8, 4055 Basel, Switzerland*

<sup>4</sup>*University of Basel, University Psychiatric Clinics, Wilhelm Klein-Strasse 27, 4055 Basel, Switzerland*

Keywords: episodic memory, adducin, glutamate, synaptic plasticity, *C. elegans*, actin cytoskeleton

## **A role for $\alpha$ -adducin (ADD-1) in nematode and human memory**

### **1 Abstract**

Identifying the molecular mechanisms that underlie learning and memory is one of the major challenges in neuroscience. Taken the advantages of the nematode *C. elegans*, we investigated  $\alpha$ -adducin (*add-1*) in aversive olfactory associative learning and memory. Loss of *add-1* function selectively impaired short- and long-term memory without causing acquisition, sensory or motor deficits. We showed that  $\alpha$ -adducin is required for consolidation of synaptic plasticity, for sustained synaptic increase of AMPA-type glutamate receptor (GLR-1) content and altered GLR-1 turnover dynamics. ADD-1 controlled the storage of memories presumably through actin capping activity in a splice form and tissue specific manner. In support of the *C. elegans* results, genetic variability of the human *ADD1* gene was significantly associated with episodic memory performance in healthy young subjects. Finally, human *ADD1* expression in nematodes restored loss of *C. elegans add-1* gene function. Taken together, our findings support a role for  $\alpha$ -adducin in memory from nematodes to humans. Studying the molecular and genetic underpinnings of memory over distinct species may be helpful in the development of novel strategies to treat memory-related diseases.



## 2 Introduction

Dynamic changes including the formation of new synapses, morphological changes of dendrites, and the redistribution of synaptic proteins during long-term potentiation (LTP) as well as regulation of long-term depression (LTD) create the remarkable plasticity of the nervous system (Matus, 2000; Okamoto et al, 2004). Stimulation of the neuronal network among others, triggers sustained changes in size of existing synaptic areas through the remodeling of the actin cytoskeleton (Matsuzaki et al, 2004). An elegant study by Honkura *et al.* (Honkura et al, 2008) demonstrated the existence of at least three pools of F-actin in synaptic spines. These different actin pools tightly regulate synapse morphology, in addition, actin filaments are particularly dynamic near the post-synaptic density (PSD) but not near endocytic zones (Frost et al, 2010), suggesting that stability of the PSD is conferred by an active process of continuous turnover in the actin network.

Adducin in vertebrates is a ubiquitously expressed membrane cytoskeletal protein localized at spectrin-actin junctions (Bennett et al, 1988; Kuhlman et al, 1996; Li et al, 1998) where it promotes assembly of the spectrin-actin cytoskeleton. Three closely related genes termed  $\alpha$ ,  $\beta$  and  $\gamma$  encode adducins in vertebrates. These forms are differentially expressed;  $\alpha$  and  $\gamma$  forms are highly expressed in most tissues including the nervous system while the  $\beta$  form is most abundant in the erythrocytes and the brain (Citterio et al, 2003). All adducin forms share a similar domain structure, composed of an N-terminal aldolase domain, and a tail region that contains critical phosphorylation sites and a lysine-rich region at the extreme C-terminal end of the protein. The head and tail regions are connected by the neck-domain that is critical for the function of adducins (Li et al, 1998). The native adducin is a mixture of heterodimers and higher oligomers comprised of  $\alpha/\beta$  or  $\alpha/\gamma$  subunit combinations. Oligomerized adducin caps the fast growing barbed ends of actin filaments (Kuhlman et al, 1996), recruits spectrin to actin filaments (Bennett et al, 1988; Gardner & Bennett, 1987; Hughes & Bennett, 1995), and bundles actin (Mische et al, 1987). In vertebrates, adducin activity is inhibited by protein kinase C (PKC) (Matsuoka et al, 1998), cyclic AMP (cAMP)-dependent protein kinase (PKA) (Matsuoka et al, 1996) and  $\text{Ca}^{2+}$ -calmodulin (Gardner & Bennett, 1987; Kuhlman et al, 1996; Porro et al) that blocks interactions of adducin with F-actin and spectrin resulting exposure of free barbed ends (Matsuoka et al, 1998). In contrast, Rho-associated kinase (ROCK) enhances adducin-actin interactions (Fukata et al, 1999;

Kimura et al, 1998). The role of the adducin family proteins in learning and memory was demonstrated by the results of Rabenstein and co-workers (Rabenstein et al, 2005) who investigated the role of  $\beta$ -adducin in behavior and found that  $\beta$ -adducin knockout mice show deficits in Morris water-maze test. However, further experiments demonstrated that knock out of  $\beta$ -adducin in mice alters the expression of  $\alpha$  and  $\gamma$  forms (Porro et al, 2010), therefore, the specific role of the adducin forms in learning and memory remains less clear. Furthermore, recent studies demonstrated the role of adducin in the degradation and assembly of new synapses in mice hippocampus and *drosophila* neuromuscular junctions (Bednarek & Caroni, 2011; Pielage et al, 2011).

*C. elegans* reacts among others to several olfactory (Colbert & Bargmann, 1995; Nuttley et al, 2002), gustatory (Saeki et al, 2001), and thermal (Mori et al, 2007) cues. In addition, the relatively simple nervous system of *C. elegans* composed of 302 neurons allows associative learning between a variety of volatile or soluble chemoattractants, or cultivation temperature, and food (Morrison & van der Kooy, 1997; Morrison & van der Kooy, 2001; Tomioka et al, 2006). Previous studies have also shown that regulators of learning and memory are conserved between mammals and *C. elegans* (Kuhara & Mori, 2006; Morrison & van der Kooy, 1997; Morrison & van der Kooy, 2001; Rose et al, 2003; Stetak et al, 2009). For example, AMPA type of ionotropic glutamate receptors not only play a critical role in vertebrate synaptic plasticity, but glutamate neurotransmission has also been shown to be involved in habituation of the tap withdrawal response as well as in olfactory associative learning in *C. elegans* (Morrison & van der Kooy, 2001; Rose et al, 2003). Therefore, the analysis of genes in *C. elegans* can provide important insights into the mechanisms of learning and memory also for vertebrates, including humans.

Taken the advantages of the nematode *C. elegans*, in the current work we investigated the role of the single worm ortholog of  $\alpha$ -adducin, *add-1* in synaptic plasticity during aversive associative learning (defined here as the acquisition of the aversive behavior; immediate recall of conditioned behavior after training) and memory (defined here as the retention of the conditioned behavior over time; short- or long-term delayed recall). We found that *add-1* loss of function mutant worms show normal chemotaxis, locomotor behavior, and aversive olfactory associative learning but they have impaired short- and long-term memory. Specifically, adducin is required *in vivo* for consolidation of synaptic size expansion, changes in the post-synaptic density, and sustained increase of AMPA-type glutamate receptor (GLR-1) content in the synapses. ADD-1 also plays an important role in changes of GLR-1 turnover dynamics at the synapse. ADD-1 presumably functions through capping of the fast growing

barbed end of actin filaments. The role of ADD-1 in synaptic plasticity is splice-form specific, and the lysine-rich C-terminal end of the protein is essential for ADD-1 function. Finally, using tissue specific rescue experiments we demonstrate that  $\alpha$ -adducin likely controls the storage of memories cell-autonomously in the AVA command interneuron by consolidating altered synaptic structures, and through the maintenance of increased amount of AMPA-type glutamate receptor at the synapses. Thus exposure to olfactory cues in combination with food withdrawal modifies the aversive olfactory neural network that may increase for a longer time period the responsiveness of the command interneuron AVA that is the main regulator of backward movements.

In addition to the *C. elegans* experiments, data obtained in humans also support a role for  $\alpha$ -adducin in memory. Genetic variability of the *ADD1* gene (encoding human adducin alpha) was significantly associated with episodic memory performance. Finally, expression of human  $\alpha$ -adducin in *C. elegans* efficiently compensated for loss of nematode *add-1* gene, suggesting that despite the differences in the amino-acid sequences between worms and humans, the molecular function of  $\alpha$ -adducin is conserved.

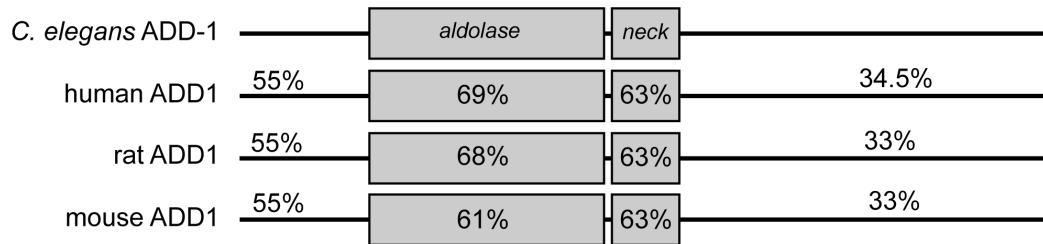
Taken together our findings support a role for  $\alpha$ -adducin in memory in such diverse species as nematodes and humans. Furthermore, we demonstrate that capping of actin filaments at the fast growing barbed-end is likely required for long-term consolidation of synaptic plasticity, suggesting that dynamic remodeling of the actin cytoskeleton in synapses during learning has to be followed by stabilization of actin filaments for efficient memory storage.

### 3 Results

#### 3.1.1 Loss of adducin (*add-1*) causes impairment of short and long-term memory

To study the physiological function of worm  $\alpha$ -adducin (ADD-1) ortholog (Figure 1), we analyzed the defects in aversive associative learning and memory using an *add-1* deletion allele (*tm3760*) (National BioResource Project, Japan). The *tm3760* deletion removes 312 bp of the *add-1* coding region that covers exon 10 and exon-intron boundaries, which causes insertion of the remaining intronic sequences and gives an in frame deletion (Figure 2B). The deletion in *tm3760* mutants alters all *add-1* splice forms and removes the conserved neck region including the dimerization sequence (Figure 1A, B, and Figure 2A, B), which has been shown to be essential for the function of vertebrate adducins (Li et al, 1998). Furthermore, the deletion affects the correct splicing of the mRNA as we observed a reduction of *add-1* mRNA compared to wild type expression (Figure 2C). Finally, *add-1(tm3760)* mutation placed over a deficiency shows similar phenotype to the homozygous mutants (Figure 3), which suggests that the *tm3760* deletion is likely a loss-of-function (*lf*) mutant of the *C. elegans* ortholog of  $\alpha$ -adducin (*add-1*) gene. *add-1(tm3760)* mutants appear healthy, fertile and display no obvious morphological or locomotory defects (Figure 4B and data not shown).

**A**



**B**



**C**



**D**

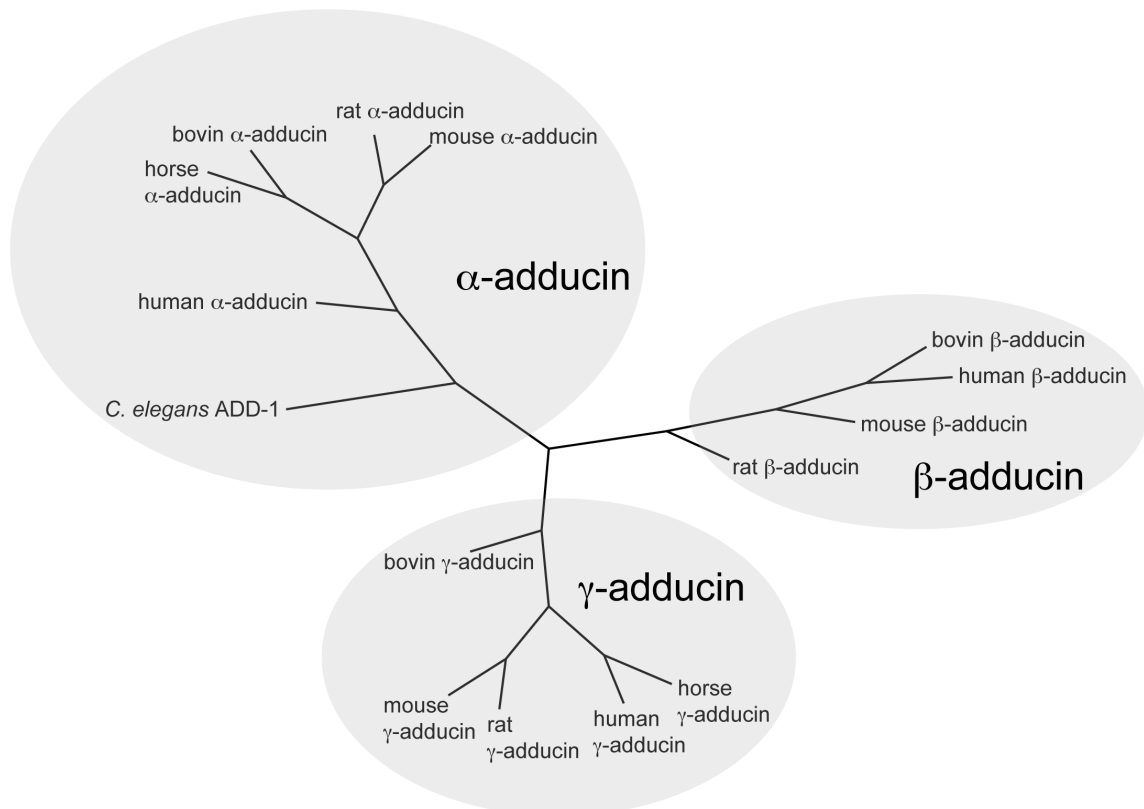


**Figure 1. *C. elegans* ADD-1 is orthologous to vertebrate  $\alpha$ -adducins.** **A.** Similarity of the ADD1 protein sequence across species. **B.** Alignment of the neck region of worm and human  $\alpha$ -adducin. Identity is highlighted in grey, similarity with open boxes. The critical

methionine required for dimerization is depicted in red. **C.** Alignment of the C-terminal MARCKS region of worm and human  $\alpha$ -adducin. Identity is highlighted in grey, similarity with open boxes. **D.** Phylogenetic classification of the adducin gene family.

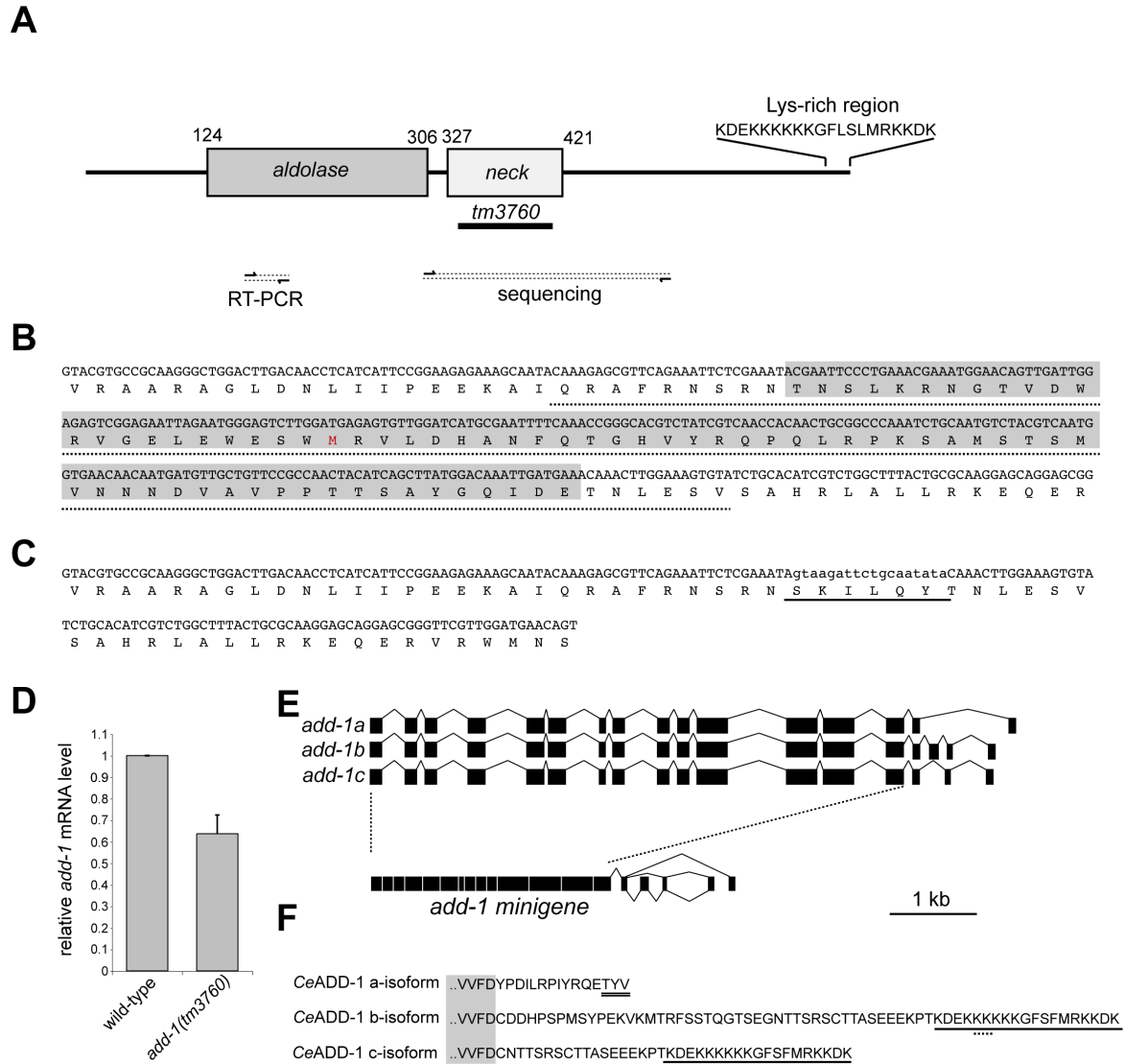


**Figure 2. Characterization of the *add-1(tm3760)* deletion.** **A.** Domain structure of the worm ADD-1. The deletion is highlighted with solid bar, and the position of primers is shown. **B.** The amino-acid sequence of ADD-1 covering the deletion region. Position of the deletion is highlighted in grey and the neck domain is shown with dotted line. The critical methionine required for dimerization is depicted in red. **C.** Protein structure in the *add-1(tm3760)* mutants. Insertion of the intronic region is highlighted with solid bar. **D.** Relative abundance of the ADD-1 transcript. **E.** Genomic structure of the different *add-1* splice forms and *add-1* minigene. Region between the dotted lines were replaced with cDNA in the *add-1* minigene used in this study. **F.** C-terminal sequence of the different worm ADD-1 isoforms. **Vukojević Vanja 2012**

The MARCKS domain is underlined, dotted line shows the putative spectrin-binding site, and double line labels the PDZ-binding motif.

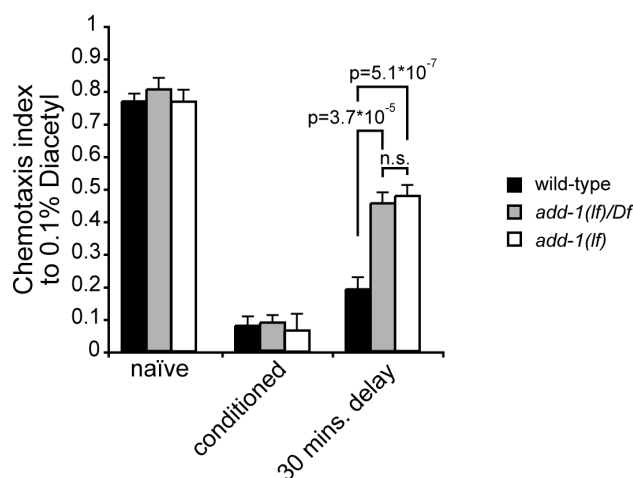


**Figure 3. Phenotypic characterization of the *add-1(tm3760)* allele.** The aversive olfactory associative learning (conditioned) and memory (30 mins. delay) using paired treatment of starvation and DA was tested as described in Materials and Methods in wild type, *add-1(tm3760)* homozygous (*add-1(lf)*), or in *add-1(tm3760)/syDf1* hemizygous (*add-1(lf)/Df*) mutant worms. All experiments were done in triplicate and repeated three times. Error bars indicate mean  $\pm$  SEM. Significance between datasets as indicated was tested with two-tailed Student's t-test (n.s.  $p > 0.05$ ).

To test the role of *add-1* in aversive olfactory associative learning, we first analyzed the chemotaxis behavior of *add-1(tm3760)* mutant worms towards three chemoattractants (diacetyl, benzaldehyde, and isoamyl-alcohol) and a repellent (octanol) as described previously (Bargmann et al, 1993). As shown on Figure 4A, *add-1(tm3760)* mutant worms exhibited efficient chemotaxis similar to wild type animals. Furthermore, both wild type and *add-1(tm3760)* mutants showed the same motility and responded similarly to food starvation (Mohri et al, 2005; Sawin et al, 2000), indicating that *add-1(tm3760)* mutants have no sensory or motor defects (Figure 4B).

We next, tested the role of ADD-1 in aversive olfactory associative learning, using established context-dependent starvation conditioning protocol (Cassata et al, 2000; Kuhara & Mori, 2006; Wicks et al, 2000). In this assay, combination of a one-hour starvation period in the presence of diacetyl, or benzaldehyde (conditioned) dramatically reduced the attraction towards chemoattractants both in wild type animals and *add-1(tm3760)* mutants to a similar

extent, while starvation alone had no effect, and adaptation (DA treatment alone) showed only a minor decrease in chemotaxis. These results suggest that *add-1* function is not required for the acquisition process (Figure 4C, D).

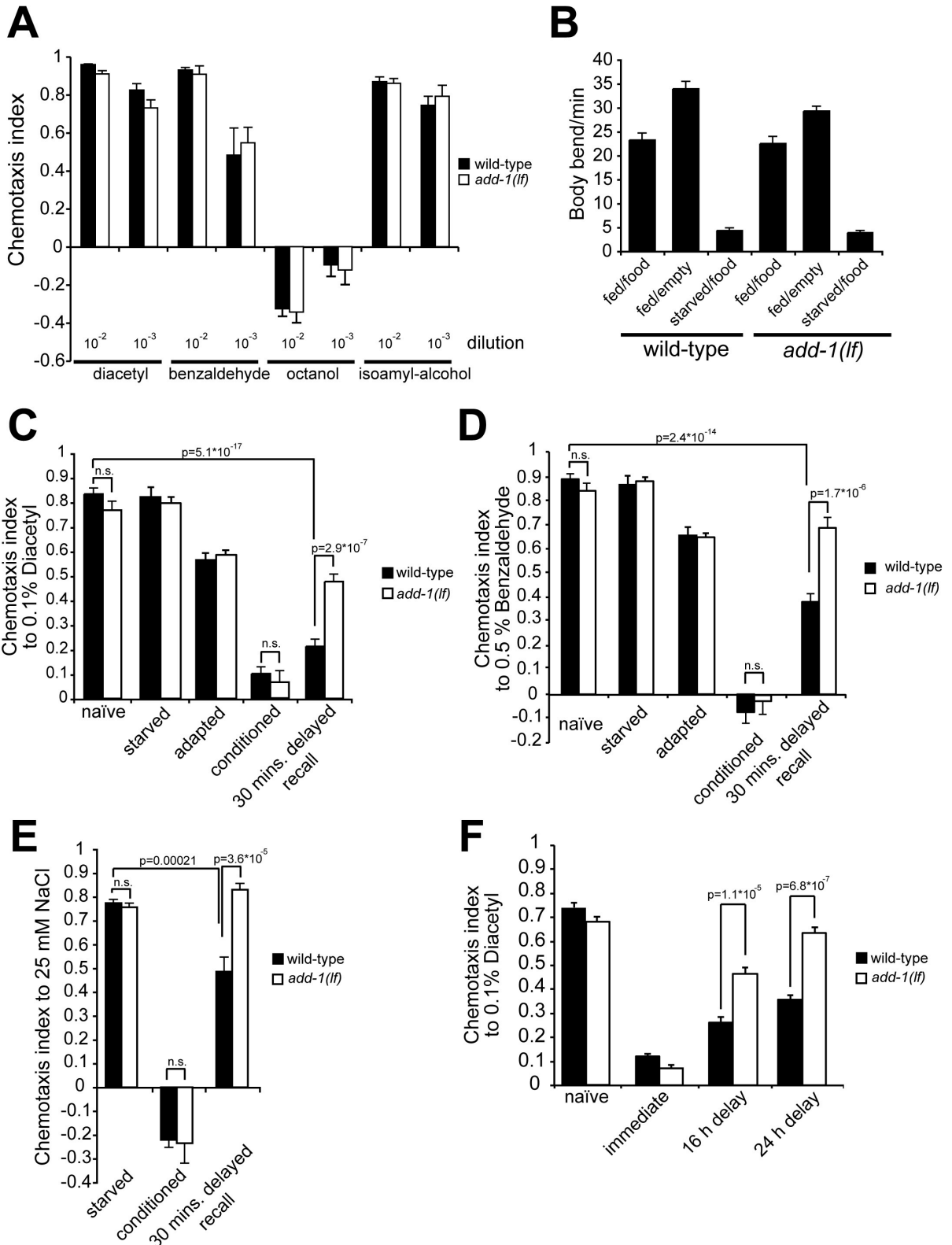




**Figure 4. ADD-1 regulates for short- and long-term memory.** (A) Chemotaxis wild type or mutant worms was assayed towards 1% or 0.1% diacetyl, benzaldehyde, or isoamyl-alcohol volatile chemo-attractant, and 1% or 0.1% octanol as repellent. Chemotaxis index was calculated as  $CI = (\text{worms at the attractant} - \text{worms at the solvent}) / \text{total number of worms}$ . (B) locomotor behavior and response to starvation of wild type and *add-1(tm3760)* mutant worms was tested by counting body bends of well fed (fed) or starved (starved) young adults on empty (empty) or seeded (food) NGM agar plates (C-E) Starvation, adaptation, associative learning (conditioned), and memory after a 30 minutes recovery period in absence of attractant (30 mins. delayed recall) of *add-1(tm3760)* and wild type animals was tested with starvation conditioning assay using (C) diacetyl, (D) benzaldehyde, or (E) NaCl. (F) long-term memory was tested as shown on Figure 5. Conditioned wild type and *add-1(tm3760)* mutant worms were tested for their preference towards diacetyl immediately after the conditioning (immediate), after a 16 hours (16h delay), or after a 24 hours delay (24h delay). All experiments were done in triplicate and repeated at least three times. Error bars indicate mean  $\pm$  SEM. Significance between datasets as indicated was tested with two-tailed Student's t-test.

We also tested short-term aversive memory by conditioning the animals with diacetyl or benzaldehyde and letting the animals recover for 30 NaCl as attractant, in gustatory starvation conditioning assay (Wicks et al, 2000) (Figure 4E). In order to test the role of ADD-1 during long-term aversive associative memory (LTAM), we performed multiple conditioning training consisting of food withdrawal in combination with diacetyl (Figure 5A). Worms were tested for chemotaxis towards DA immediately following the conditioning phase, after 16 hours, or 24 hours delay. This repetitive conditioning induced long-term memory that persisted for at least 24 hours (Figure 4F) and required transcription and translation (Figure 5B) similar to previous findings (Kauffman et al, 2010; Segal et al, 1971; Squire & Barondes, 1970). While the learning of *add-1* mutant worms was effective and comparable to wild type animals, we observed significant decrease in long-term memory in *add-1* mutant compared to wild type worms after 16 hours or 24 hours delay period (Figure 4F). Taken together these results show that loss of *add-1* function impairs both short- and long-term aversive associative memory but not learning, regardless of the sensory input.

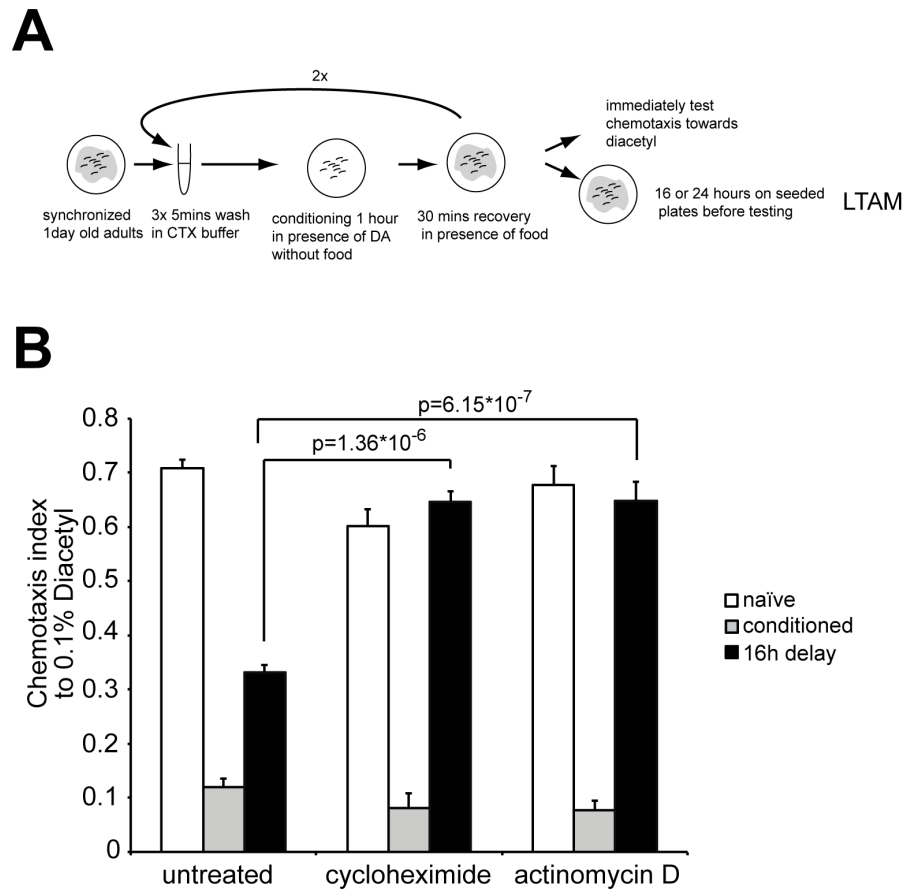


**Figure 5. Long-term aversive olfactory memory requires transcription and translation.** **A.** Flow chart of the long-term aversive olfactory memory protocol (LTAM). **B.** Naïve, or conditioned wild type worms using the LTAM protocol were tested for their preference towards diacetyl immediately after the conditioning (conditioned), or after 16 hours (16h delay). For translational or transcriptional inhibition, 800  $\mu\text{g}/\text{ml}$  cycloheximide or 100  $\mu\text{g}/\text{ml}$  actinomycin D was applied in all washing steps prior and between conditioning steps. All experiments were done in triplicate and repeated three times. Error bars indicate mean  $\pm$  SEM. Significance between datasets as indicated was tested with two-tailed Student's t-test.

### 3.1.2 Adducin expression in neurons overlaps with AMPA-type glutamate receptor, GLR-1

To identify the cellular focus of ADD-1, we first investigated the expression pattern of a rescuing translational *add-1* reporter construct, using the endogenous 3.1 kb promoter region fused to ADD-1 minigene with an N-terminal tRFP (Figure 6A-O, Q). ADD-1 was expressed throughout the life cycle of *C. elegans* in several tissues, including the intestine and rectal epithelia (Fig. 2C), the coelomocytes (Figure 6E), the seam cells (Figure 6F), as well as the nervous system (Figure 6A-B, D, G-L). In the head ganglia, ADD-1 expression largely overlapped with the ionotropic glutamate receptor, GLR-1 (Figure 6G-I) including AVA, AVE and AVD command interneurons and PVC neuron (Figure 6J-L, P). These interneurons project their axons along the ventral nerve cord where they are interconnected through GLR-1 containing synapses. In order to test the subcellular localization of ADD-1, we observed simultaneously the localization of tRFP labeled ADD-1, and GFP tagged GLR-1 in the ventral nerve cord (VNC). ADD-1 colocalized with GLR-1 along the VNC (Figure 6M-O) and ADD-1 accumulated at the synaptic areas. This subcellular distribution suggests a structural role of ADD-1 in the GLR-1 containing synapses of AVA,

In order to further investigate the cellular focus of ADD-1, we performed tissue-specific rescue experiments by using *add-1* minigene, which consists of a cDNA encoding the N-terminal part of the *add-1* gene, fused to a 1 kb C-terminal genomic piece that encodes all splicing forms (Figure 2). The *add-1* minigene was reintroduced into *add-1(tm3760)* mutant worms under the control of a 940 bp fragment of the *nmr-1* promoter, a 2.6 kb piece of the AVD, and AVE command interneurons. *lim-4*, a 3.2 kb fragment of the *rig-3*, a 3.4 kb fragment of the *odr-2*, or a 780 bp of the *tdc-1* promoters (Figure 6P, Q). The activity of these promoters overlaps with certain ADD-1 expressing neurons (Figure 6P). In the short-term aversive memory test, *Pnmr-1*, and *Prig-3*-driven *add-1* minigene rescued the memory defects of *add-1(tm3760)* mutants, while no rescue was observed with *Plim-4*-, *Podr-2*-, or *Ptdc-1*-driven *add-1* minigene (Figure 6Q).

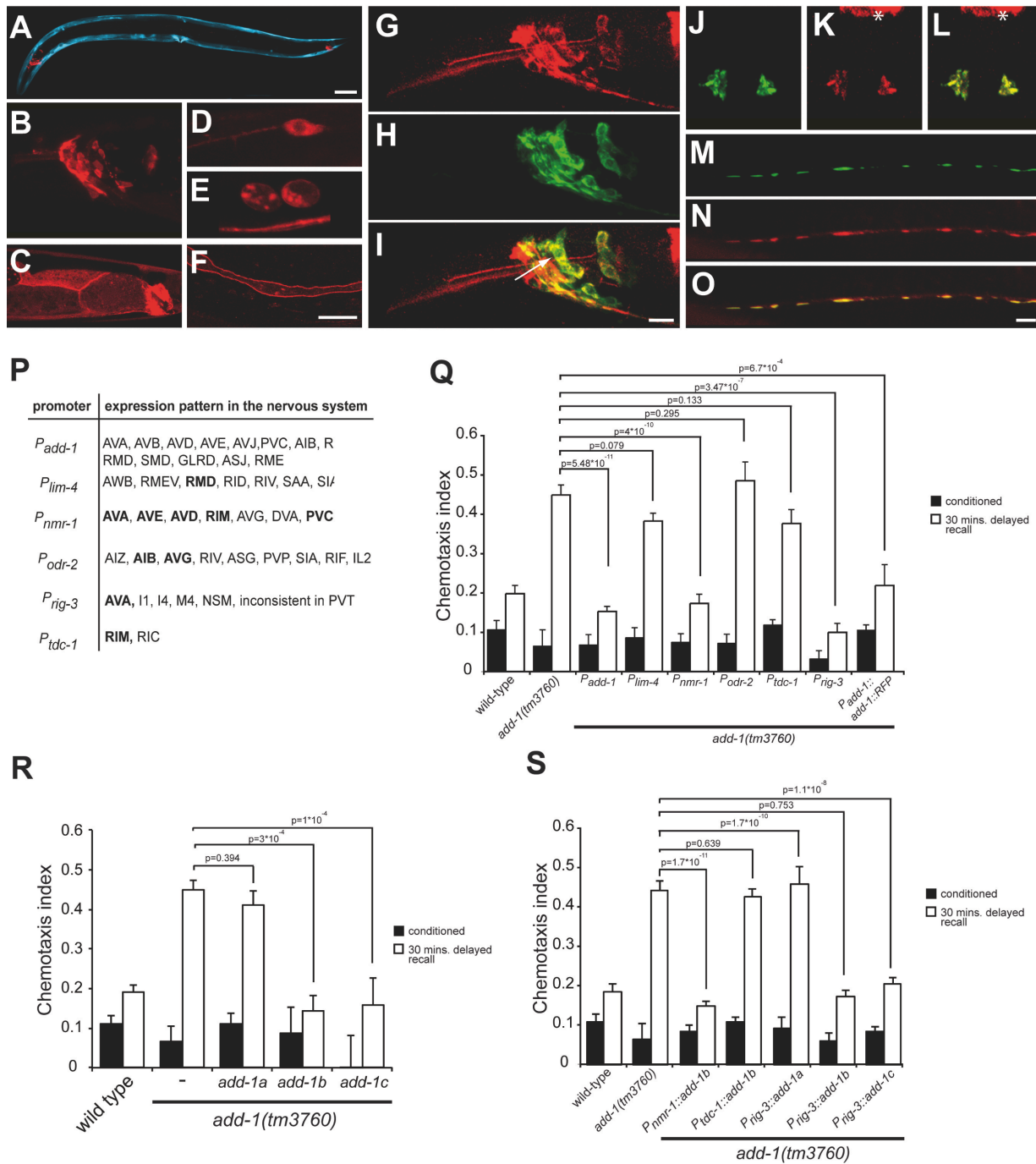


**Figure 6. Expression pattern and sub-cellular localization of tRFP::ADD-1. (A)** *add-1* (red) expression in adult worm (blue: *myo-3::gfp* coinjection marker). **(B)** Localization of ADD-1::tRFP in the head ganglia. **(C-F)** *add-1* expression was also detected in **(C)** the gut, **(D)** the CAN neurons, in **(E)** coelomocytes, and **(F)** seam cells. Co-localization of **(G)** ADD-1::tRFP with **(H)** the glutamate-receptor (GLR-1) fused to GFP driven by endogenous

promoter. Merged image of panels **G** and **H** is shown in **I**. Arrow points to AVA command interneuron. (**J**) ADD-1::tRFP expression overlaps with (**K**) GLR-1 in PVC neuron. Merged image of panels **J** and **K** is shown in **L**. Asterisk labels intestine. **M-O**, The subcellular localization of (**N**) ADD-1 was observed along the ventral nerve cord, where it colocalizes with (**M**) GLR-1 positive glutamatergic synapses. Merged image of panels **M** and **N** is shown in **O**. Scale bars represent 50  $\mu\text{m}$  on panel **A**, 10  $\mu\text{m}$  on panel **F** 5  $\mu\text{m}$  on panel **I**, and 1  $\mu\text{m}$  on panel **O**. (**P**) Expression pattern of the different neural promoters used in **Q** and **S**. ADD-1::tRFP expressing neurons are highlighted in bold. (**Q**) Tissue-specific rescue of the memory defect of *add-1(tm3760)* mutant worms carrying the *add-1* minigene under the control of different promoters. Young adult worms of each transgenic line were conditioned with DA and their preference towards DA was tested immediately (conditioned) or following 30 minutes recovery in the absence of DA (30 min. delayed recall). (**R**) Splice form specific rescue of the memory defect was tested in *add-1(tm3760)* mutant worms carrying different arrays for their preference towards DA immediately (conditioned) or following 30 minutes recovery in the absence of DA (30 min. delayed recall). (**S**) Splice form specific rescue of the memory defect in *add-1(tm3760)* mutant worms carrying arrays as indicated using DA immediately (conditioned) or following 30 minutes recovery in the absence of DA (30 min. delayed recall). All experiments were done in triplicate and repeated in three independent experiments. At least two independent transgenic lines were tested for each construct. Error bars indicate mean  $\pm$  SEM. Datasets were compared as indicated using two-tailed Student's t-test.

The *C. elegans add-1* locus encodes for several splice forms that differ in their C-terminal end (Figure 2E). The *add-1a* splice form contains an extreme C-terminal PDZ-binding motif while the *add-1b* and *add-1c* forms include the lysine-rich region that is important for binding of vertebrate  $\alpha$ -adducin to spectrin and actin *in vitro* (Li et al, 1998). Interestingly, similar alternative isoforms of the  $\alpha$ -adducin mRNA are present in the vertebrate genomes that differ in their C-terminal part including the lysine-rich region. We therefore wondered which of the splice forms are required for synaptic plasticity. Thus, we generated isoform specific rescuing constructs that contained the cDNA encoding *add-1a*, *b*, or *c* isoform fused to *add-1* promoter region, and reintroduced them into *add-1(tm3760)* mutant worms. In the olfactory memory test, both *add-1b* and *add-1c* splice forms rescued the memory defects of *add-1(tm3760)* mutants, while no rescue was observed with the *add-1a* form (Figure 2E, 2R). We further confirmed these results, by introducing *add-1a*, *b*, or *c*

isoforms under the control of the *rig-3* promoter. Similar to the endogenous promoter, both *add-1b* and *add-1c* splice forms rescued the memory defects of *add-1(tm3760)* mutants when expressed under the control of the *rig-3* promoter (Figure 6S). Finally, in order to exclude possible regulatory elements in the intronic sequences of the *add-1* minigene we fused the longest *add-1b* isoform to *nmr-1*, *rig-3*, or *tdc-1* promoters. In conjunction with the results observed for the minigene construct, *Pnmr-1*, and *Prig-3*-driven *add-1b* rescued the memory defects of *add-1(tm3760)* mutants, while no rescue was observed with *Ptdc-1*-driven *add-1b* gene (Figure 6S).

Taken together, ADD-1 expression was detected among others in AVA, and neuron specific rescue studies demonstrate that the function of *add-1* in memory is likely required predominantly in AVA command interneuron. Furthermore, AVA requires specific ADD-1 splice forms that contain the lysine-rich region for efficient memory.

### 3.1.3 Sustained consolidation of synaptic plasticity depends on adducin

Previously, we demonstrated that GLR-1 positive synapses in *C. elegans* VNC changes their size upon associative learning and memory consolidation (Stetak et al, 2009). Furthermore, persistent alteration in synaptic size correlates with memory retention capability. Therefore, we investigated the role of ADD-1 in synaptic structure, first by analyzing the subcellular localization of ADD-1 during associative learning. Quantitative analysis of the tRFP signal intensity showed a three-fold increase in ADD-1 content upon conditioning (Figure 7B) while the number of synapses was not affected (Figure 7A). Furthermore, the observed change in fluorescence intensity persisted during the 30 minutes delay phase (Figure 7B).

Since ADD-1 function is required in AVA neurons for memory consolidation, and we found an increase in the amount of ADD-1 at the glutamatergic synapses, we next asked whether remodeling of GLR-1 containing synapses in the VNC during associative learning and memory require ADD-1 function. We therefore investigated GLR-1 fluorescence intensities and GLR-1 punctae volume posterior to the vulva in naïve, diacetyl conditioned, and memory consolidated wild type and *add-1(tm3760)* mutant worms (Figure 7 C, D). Loss of adducin had no effect on synapse number and morphology (data not shown), and we observed an increase in the fluorescence intensity of GLR-1::GFP signal upon associative

learning both in wild type and in *add-1(tm3760)* animals but not following starvation or DA treatment alone (Figure 7C). While conditioning induced a similar increase in GLR-1::GFP intensity in both genotypes, GLR-1::GFP intensity in *add-1(tm3760)* animals reverted after 30 minutes to nearly the level observed in unconditioned animals, but persisted in wild type animals (Figure 7C). We found similar results when we analyzed GLR-1::GFP positive synapse volumes (Figure 7D) where changes in *add-1(tm3760)* mutant worms reverted to the level of unconditioned animals after 30 minutes of delay. Thus, ADD-1 consolidates changes in GLR-1 content and synapse volume during memory formation.

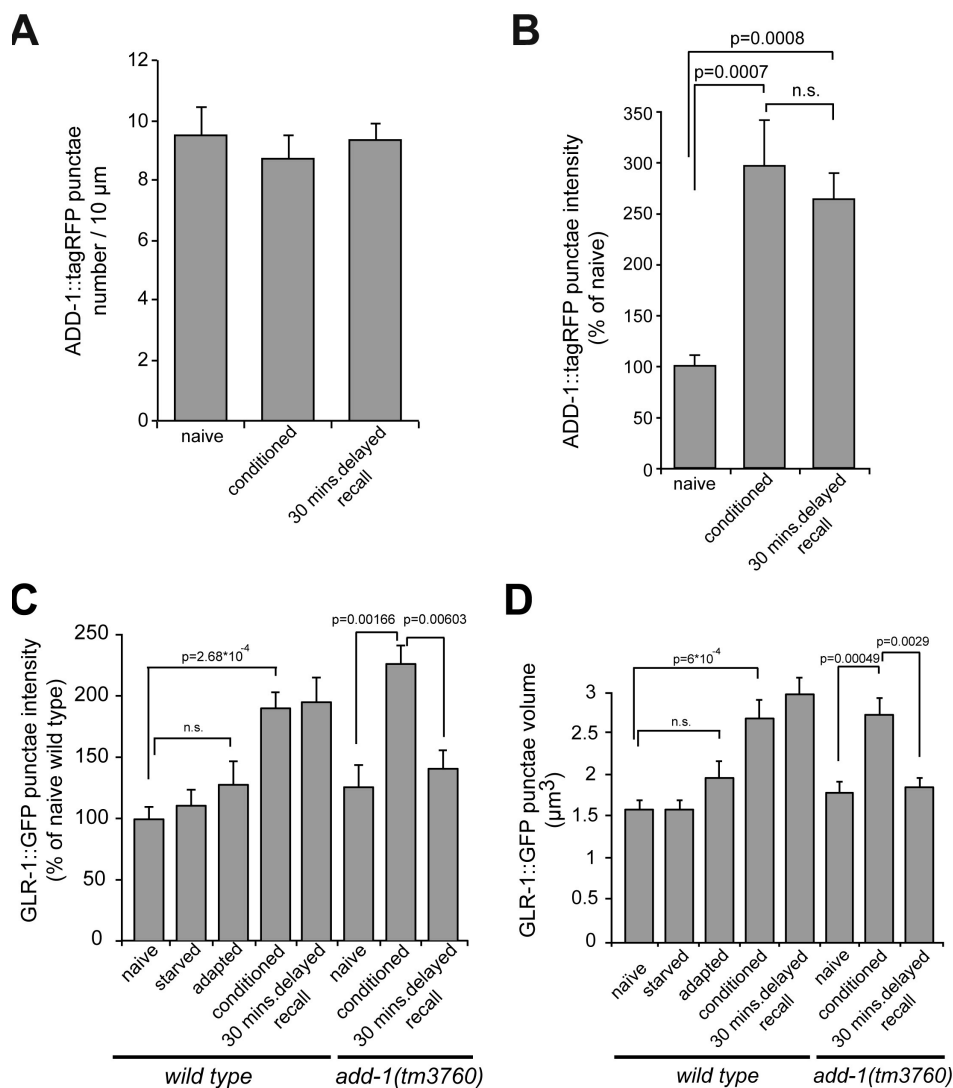


**Figure 7. ADD-1 regulates consolidation of structural plasticity in glutamatergic synapses.** (A) Number of ADD-1 containing punctae along the ventral nerve chord, in untrained, conditioned with DA and after 30 minutes recovery in wild type worms. (B) Average fluorescence intensity of ADD-1::tagRFP in the posterior VNC upon starvation without

(naïve) or with 0.1% DA (conditioned) or conditioning followed by 30 minutes recovery in the absence of DA (30 mins. delayed recall) in wild type adults. (C) Average fluorescence intensity of GLR-1::GFP in the posterior VNC in naïve, upon starvation without (starved) or with 0.1% DA (conditioned), upon treatment with 0.1% DA without starvation (adapted), or after conditioning followed by 30 minutes recovery in the absence of DA (30 mins. delayed recall) in wild type and *add-1(tm3760)* animals. (E) Average volume of GLR-1::GFP synapses in the posterior VNC in naïve, upon starvation without (starved) or with 0.1% DA (conditioned), upon treatment 0.1% DA in presence of food (adapted), or after conditioning followed by 30 minutes recovery in the absence of DA (30 mins. delayed recall) in wild type and *add-1(tm3760)* animals. Synapse volumes were measured using ImageJ on confocal images (voxel size: 0.11x0.11x0.44  $\mu\text{m}$ ). Error bars indicate mean  $\pm$  SEM. Significance between datasets as indicated was tested with two-tailed Student's t-test (n.s.  $p > 0.05$ ).

### 3.1.4 Changes of GLR-1 dynamics during associative learning is regulated by adducin

Our results demonstrate that ADD-1 stabilizes changes in GLR-1 containing synaptic structures and the increase in glutamate receptor abundance along the VNC. As a next step, we asked whether adducin regulates GLR-1 diffusion and trafficking at the synapses as this could lead to an increase in receptor density during associative learning. Indeed, we observed a significant decrease of GLR-1::GFP mobility following conditioning with DA using fluorescence recovery after photobleaching (FRAP) in the synapses along the ventral nerve cord (Figure 8A, B and Table 1). A single training with DA paired with starvation evoked a long lasting change in GLR-1 mobility that remained for at least four hours after the conditioning phase (Figure 8B and Table 1). Finally, we could not detect any change in GLR-1 mobility after starvation, or after conditioning wild type animals with DA in the presence of abundant food (adaptation) (Figure 8C and Table 1). These results demonstrate that associative learning specifically causes a long-lasting decrease in GLR-1 mobility, which could lead to an activity dependent receptor accumulation at synapses. In contrast to wild type, we could not detect change in GLR-1 mobility upon conditioning in *add-1(tm3760)* mutants (Figure 8D and Table 1). These results suggest that associative learning, through the function of ADD-1 causes a long-lasting decrease in GLR-1 mobility, which could lead to receptor accumulation at synapses.



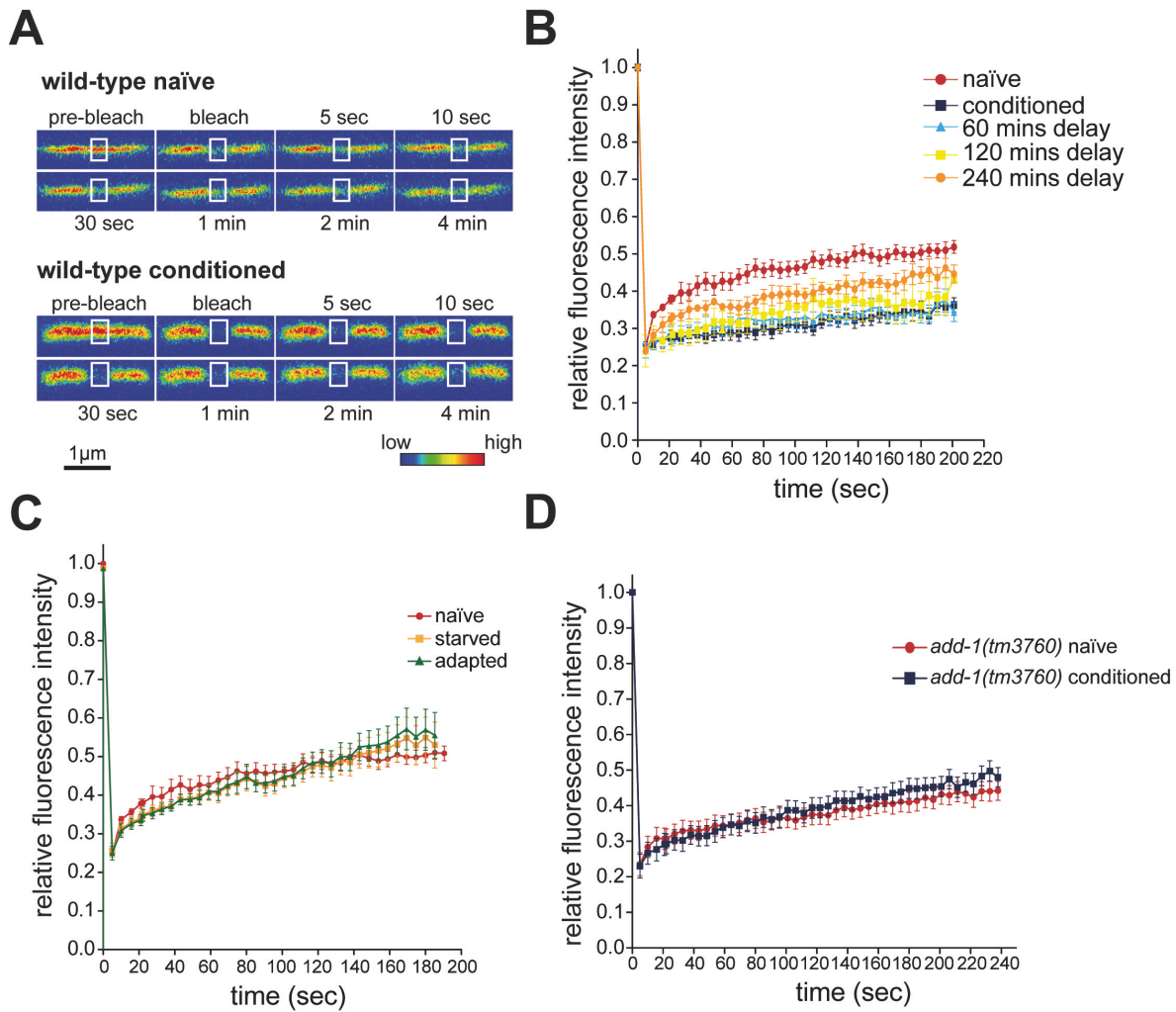


**Figure 8. GLR-1 dynamics changes in ADD-1 dependent manner upon associative learning and memory.** (A) Fluorescence recovery after photobleaching (FRAP) of GLR-1 was monitored in wild type naïve (upper panels) or conditioned (lower panels) worms. Scale represents the relative fluorescence intensity. (B) FRAP signal of GLR-1 in wild type animals was quantitatively analyzed in untrained, conditioned, or after the indicated recovery phase following conditioning (naïve: n= 12; conditioned= 13; 60 minutes delay: n=6; 120 minutes delay: n=5; 240 minutes delay: n=5). (C) FRAP signal of GLR-1 in wild type animals starved for 1 hour or upon treatment with 0.1% DA without starvation (adapted) (naïve: n= 12; starved: n=7; adapted: n=9). (D) FRAP signal of GLR-1 in naïve, or conditioned *add-1(tm3760)* animals (naïve: n= 9; starved: n=6). Error bars indicate mean +/- SEM.

	Mobile fraction*	D mm <sup>2</sup> s <sup>-1</sup> (*10 <sup>-3</sup> ) <sup>†</sup>	n
naïve wild-type	36.13±0.501	0.15405±0.0139	5
conditioned wild-type	12.21±0.56	0.0155±0.0012	8
starved wild-type	35.21±1.18	0.128±0.0258	4
adapted wild-type	39.23±1.44	0.1557±0.0522	5
60 min delay	13.56±0.338	0.01282±0.0114	6
120 min delay	17.99±0.62	0.0182±0.0273	4
240 min delay	25.08±0.564	0.131±0.0182	4
naïve <i>add-1(lf)</i>	28.36±0.74	0.1593±0.038	6
conditioned <i>add-1(lf)</i>	30.31±0.998	0.1565±0.047	4

**Table 1.** Quantitative analysis of GLR-1 mobility at the synapses along the ventral nerve chord. \* The mobile fraction was determined as described (Kim et al., 2002), using  $Mf=(Ne_{(final)} - Ne_0)/(Ne_1 - Ne_0)$  formula, where  $Ne_{(final)}$  is the final intensity after full recovery and  $Ne_1$  is the intensity immediately after photobleaching. Graphpad Prism software (GraphPad Software, San Diego CA) was used for curve fitting in order to estimate the  $Ne_{(final)}$  value. † Diffusion coefficient was determined as  $D=w^2 \ln 2 / 4t_{1/2}$  where  $w_2$  is the bleached area,  $t_{1/2}$  is the recovery half time, and D is the diffusion coefficient.

### 3.1.5 GLR-1 function in AVA is essential for memory formation

GLR-1 has been shown to have a role in nose touch response (Figure 9D) as well as in associative olfactory learning (Hart et al, 1995; Morrison & van der Kooy, 2001) (Figure 9F) that later defect unable investigation of the specific role of GLR-1 in memory. In our study we found that adducin regulates GLR-1 positive synapses and GLR-1 turnover in AVA interneuron specifically during memory formation, thus we wondered if selective deletion of GLR-1 function in AVA could lead to memory defects. A GLR-1::GFP transgene (Rongo et al, 1998) (*nuls25*) fully rescued both nose touch defect and learning deficiency of the *glr-1* loss of function mutant (Hart et al, 1995) (Figure 9D and F). In order to get AVA specific knockdown of GLR-1, we introduced an interfering GFP hairpin (GFPhp) under the control of the *rig-3* promoter in *glr-1(lf); nuls25* mutant worms. Efficient and specific knockdown of the

**Vukojević Vanja 2012**

rescuing GLR-1::GFP in otherwise *glr-1* deficient worms was monitored by measuring the GFP signal in different neurons (Figure 9A-D). In such genetic background, the strong reduction in the amount of GLR-1::GFP from AVA neuron resulted a nose touch defect in accordance to previous findings (Figure 9E) (Hart et al, 1995). Next, we tested short-term aversive memory by conditioning the animals with diacetyl and testing chemotaxis immediately, or following a 30 minutes delay. In conjunction with our hypothesis, we observed a specific memory defect in worms with reduction of GLR-1 function in AVA neurons (Figure 9F). Thus, memory formation requires the function of GLR-1 in AVA interneuron that is likely dependent on ADD-1 mediated stabilization of the synapses.

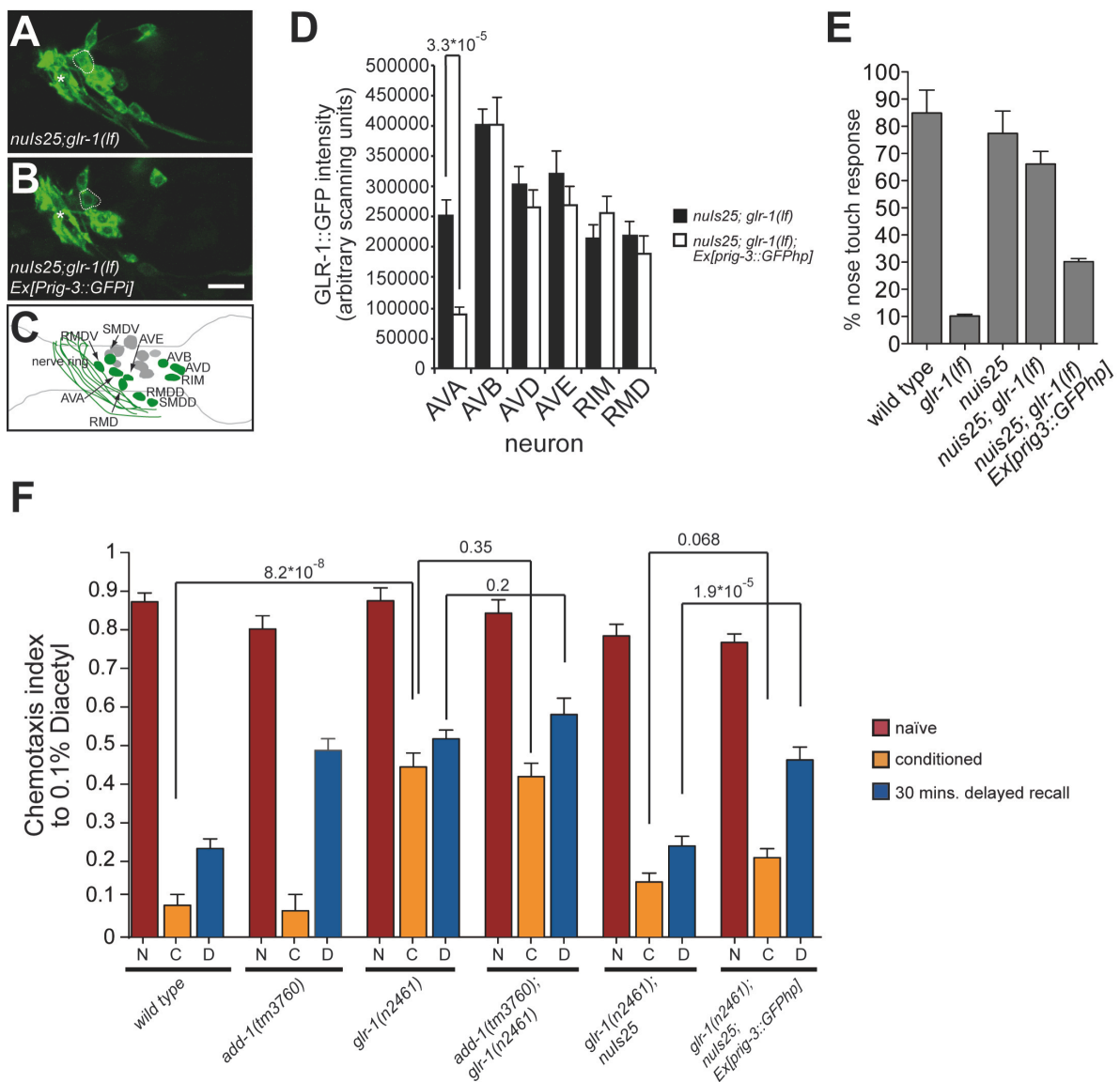


**Figure 9. The function of GLR-1 in AVA is essential for memory formation. (A-B)** Representative expression of the rescuing GLR-1::GFP protein in the head ganglia in (A)

*glr-1(n2461)*, *nuIs25*, or (B) in *glr-1(n2461); nuIs25; Ex[prig-3::GFP<sub>hairpin</sub>]* transgenic worms. AVA neuron is highlighted with dotted line and asterisk labels the nerve ring. Scale bar represents 5  $\mu\text{m}$ . (C) schematic representation of GLR-1 expressing neurons in the head ganglia. (D) Quantification of the GLR-1::GFP fluorescence intensities in different neurons with or without *rig-3* promoter driven GFP hairpin construct (n=10 for each genotype). (E) Percentage of nose touch response of different mutant worms as indicated (n=61-124). (F) Chemotaxis (naïve, N), associative learning (conditioned, C), and memory after a 30 minutes recovery period in absence of attractant (delayed recall, D) of wild type and different mutants as indicated were tested with aversive olfactory conditioning assay using diacetyl. All experiments were done in triplicate and repeated in three independent experiments. At least two independent transgenic lines were tested for the *prig-3::GFP<sub>hairpin</sub>* extrachromosomal array. Error bars indicate mean  $\pm$  SEM. Significance between datasets as indicated was tested with two-tailed Student's t-test.

### 3.1.6 *Adducin function is essential for sustained changes of AVA neuron activity upon learning*

In neurons, changes in glutamate receptors activity during synaptic transmission trigger large and rapid changes in cytoplasmic-free calcium concentrations resulting in  $\text{Ca}^{2+}$  transients. Therefore, we tested if adducin dependent, sustained changes in the GLR-1 function in AVA interneuron, is also reflected in changed neuronal activity. Genetically encoded calcium indicators (GECIs) can be used to visualize activity in defined neuronal populations<sup>14,15</sup>. In order to monitor the changes in  $\text{Ca}^{2+}$  transients we used GCaMP3, an improved, single fluorescent protein-based GECI from the GCaMP family of calcium indicators, with increased baseline fluorescence, increased dynamic range and higher affinity for calcium<sup>16</sup>. We monitored calcium transients specifically in AVA neuron by expressing GCaMP3 calcium indicator under the control of *rig-3* promoter in wild type animals and *add-1(tm3760)* mutants. AVA interneuron is the main regulator of the backward movement having a crucial role in avoidance behavior. Indeed, the activity of this interneuron is down-regulated upon exposure to diacetyl in naïve, wild type worms (Figure 10 A and B). Interestingly, upon conditioning followed by a 30 minutes delay (short-term aversive memory), the AVA activity is oppositely regulated, with up-regulation of  $\text{Ca}^{2+}$  upon exposure to diacetyl (Figure 10 C and

D). Therefore, following conditioning a sustained increase in synaptic sensitivity in this neuron due to memory towards negative cue, could lead to increased reversals and backward movement upon repeated exposure to the chemoattractant.

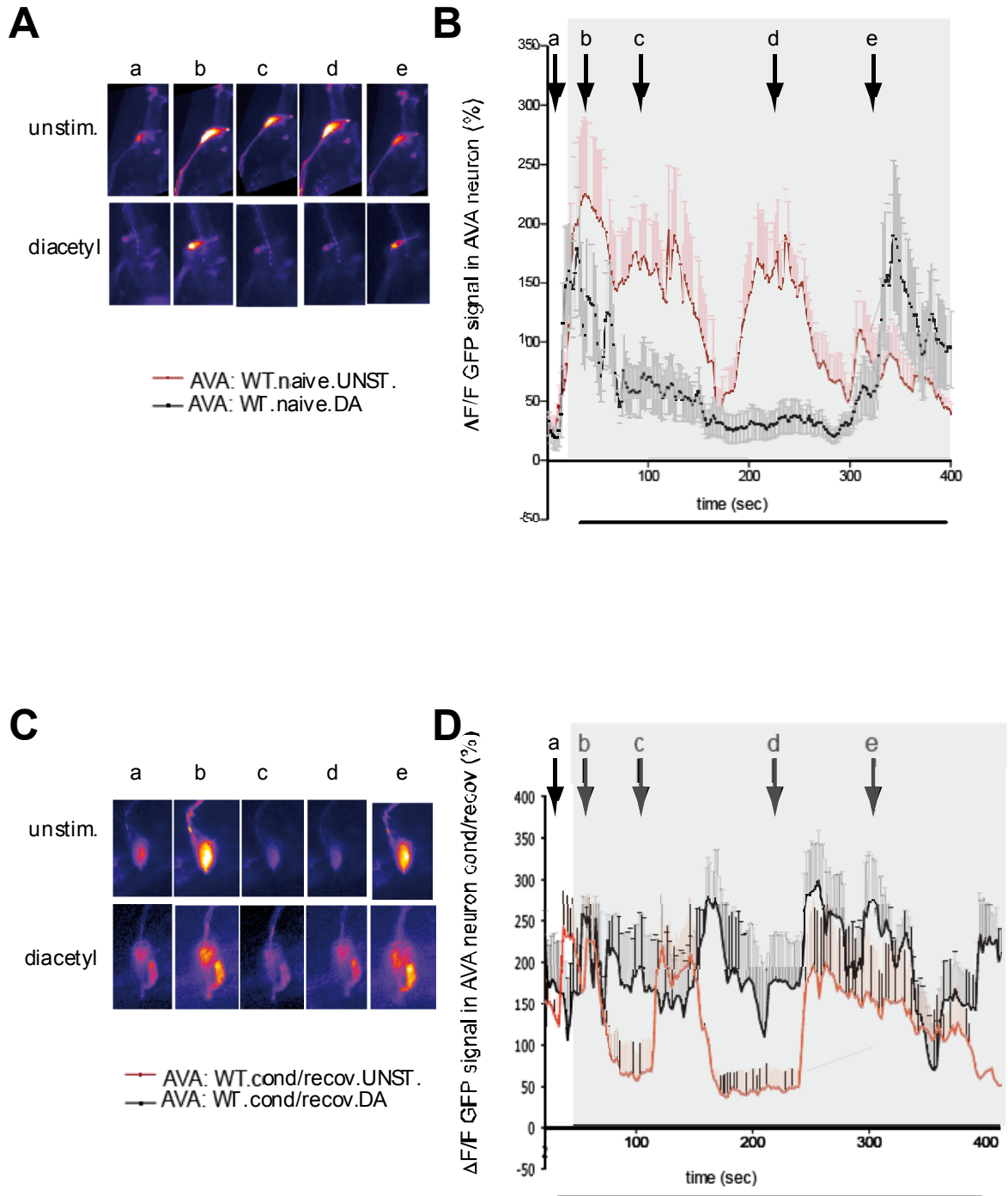


**Figure 10. Neuronal activity of the AVA interneuron in aversive olfactory associative learning and memory.** (A, C) Representative fluorescence images of AVA interneuron  $\text{Ca}^{2+}$  transients in naïve (A) and conditioned/recovered (C) wild type animals. Upper and lower panels represent un-stimulated (basal activity) and diacetyl-stimulated

Vukojević Vanja 2012

activity, respectively. **(B, E)** GCaMP3 signal summary in AVA interneuron in un-stimulated (red line) and diacetyl-stimulated (black line) naïve **(B)** and conditioned/recovered **(D)** wild type animals (naïve: n= 11; conditioned + 30 minutes delay for recovery: n= 12). The arrows marked a to e correspond to time-points representative fluorescence images under **A** and **C** were taken. The gray-shaded box marks acquisition post to exposure with diacetyl or just solvent. Scale represents the relative fluorescence intensity. Error bars indicate mean +/- SEM.

Taken together, the method implemented enabled us to get the insight of function and integration at the level of a single neuron. Moreover, we were able to caught in-vivo, a single neuronal cell in learning and memory formation. Next, we tested *add-1(tm3760)* mutants using the same method. In accordance with our previous findings, we didn't observe significant difference in neuronal activity of AVA in wild type or naïve *add-1(tm3760)* animals, after diacetyl exposure (Figure 11 A and B). Additionally, as we have shown with glutamate receptor dynamics and turnover, conditioning of *add-1(tm3760)* induced changes in AVA  $Ca^{2+}$  transients that are similar to wild type (Figure 11 C and D, and data not shown). Remarkably, the learning phase induced changes in AVA neuronal activity fails to be consolidated after 30 minutes recovery in the absence of adducin. As opposed to the wild type, the  $Ca^{2+}$  transients are reversed to the level observed in naïve animals (Figure 11 E and F). Therefore we were also capable caught *in vivo* a neuron in the act of forgetting. These findings further support the role of ADD-1 in the stabilization of synapses, changes in GLR-1 dynamics and finally modulations of neuronal activity patterns.

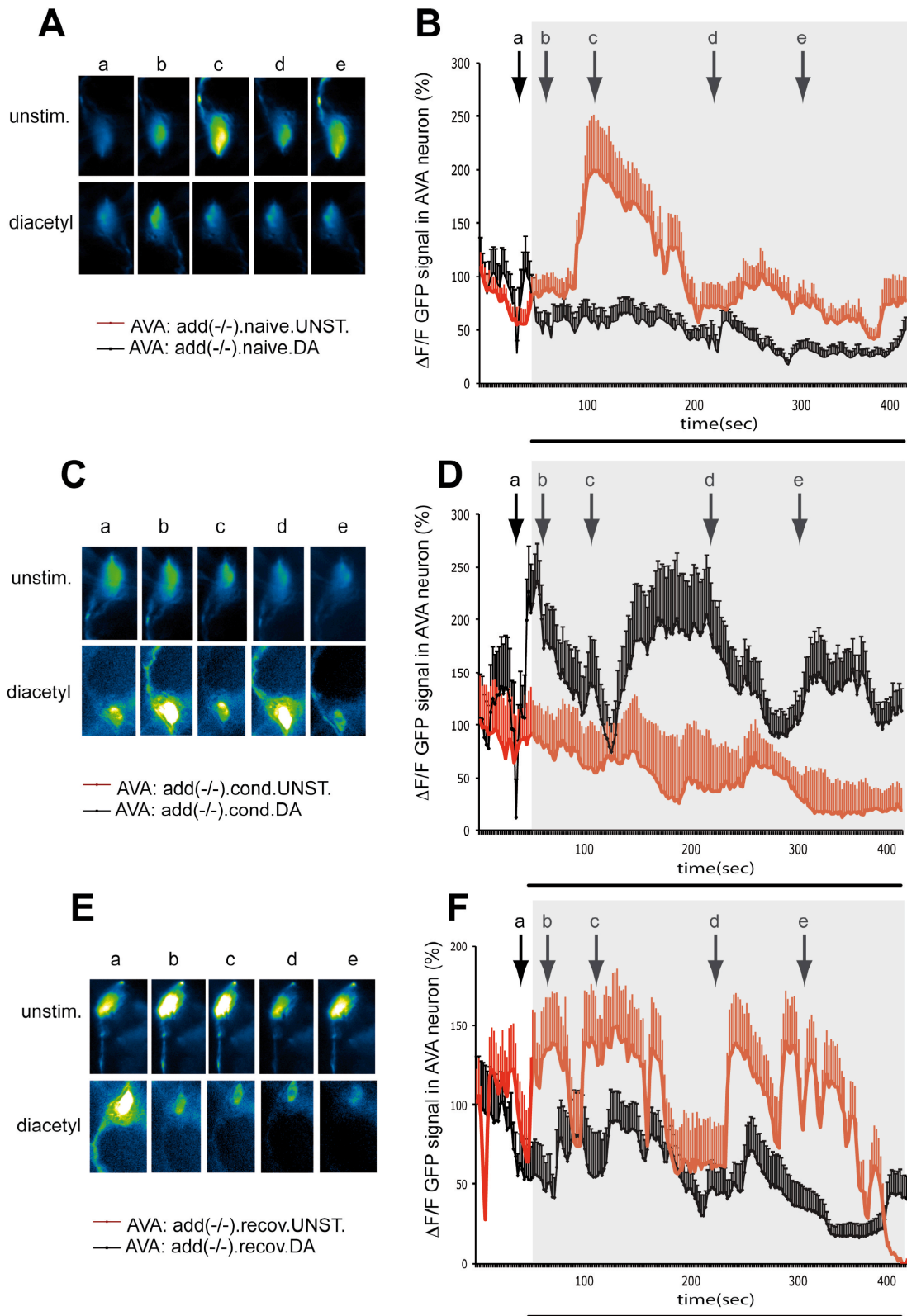


**Figure 11. The function ADD-1 in AVA is essential for memory, and for sustained changes in neuronal activity. (A, C, E) Representative fluorescence images of AVA**

interneuron  $\text{Ca}^{2+}$  transients in naïve (**A**), conditioned (**C**) and recovered (**E**) wild type animals. Upper and lower panels represent unstimulated (basal activity) and diacetyl-stimulated activity, respectively. (**B, D, F**) GCaMP3 signal summary in AVA interneuron in unstimulated (red line) and diacetyl-stimulated (black line) naïve (**B**), conditioned (**D**) or recovered (**F**) wild type animals (naïve: n= 11; conditioned: n= 8; recovery: n= 12). The arrows marked a to e correspond to time-points representative fluorescence images under **A**, **C** and **E** were taken. The gray-shaded box marks acquisition post to exposure with diacetyl or just solvent. Scale represents the relative fluorescence intensity. Error bars indicate mean +/- SEM.

### 3.1.7 Adducin function in AVA interneuron is essential for sustained changes in RIM motor neuron activity upon learning and memory

AVA interneuron is an important component of the *C.elegans* motor network. We therefore wanted to test if the adducin deficiency impairment in AVA interneuron is also reflected in the other members of the network. RIM motor neuron is positioned downstream of the AVA command interneuron. RIM inhibits the initiation of reversals, and its activity is suppressed during reversals. It is under direct upstream control of the AIB command interneuron. Additionally, the AVA circuit is also involved in the regulation of RIM activity via crosstalk signaling to RIM. Both AIB and AVA interneurons trigger reversals by inhibiting RIM activity<sup>17-19</sup>. Therefore, we monitored calcium transients specifically in RIM neuron by expressing GCaMP3 calcium indicator under the control *tdc-1* promoter in wild type animals and *add-1(tm3760)* mutants. In accordance with our hypothesis, neuronal activity of RIM was oppositely regulated as compared to AVA interneuron. In naïve, wild type animals exposure to diacetyl enhanced the activity of the RIM neuron (Figure 12 A and B). Upon conditioning and following 30 minutes recovery phase this effect was reversed, probably as the consequence of new aversive memory and changed AVA activity (Figure 12 C and D).



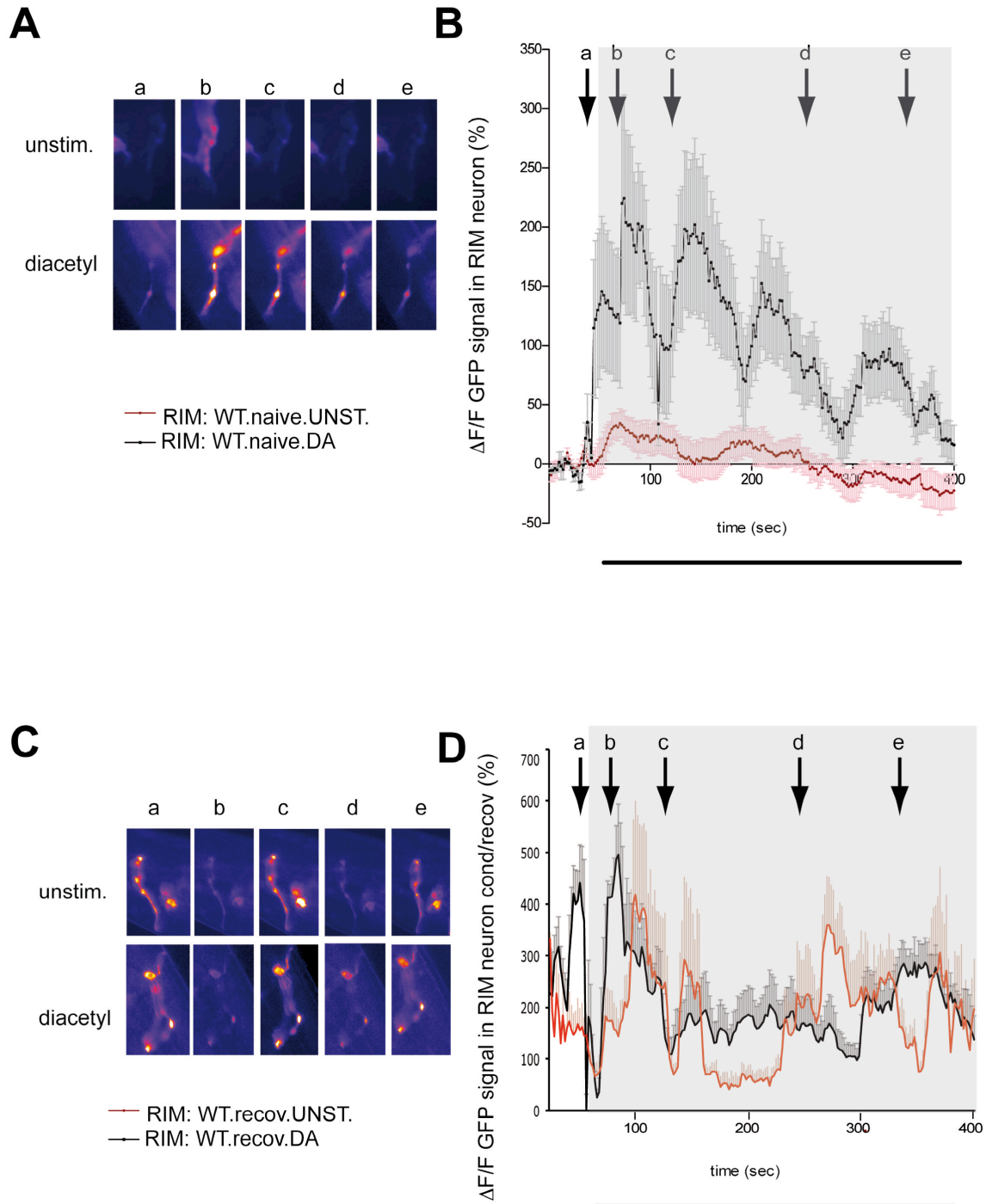


**Figure 12. Neuronal activity of the RIM motor neuron in aversive olfactory associative learning and short-term memory.** (A, C) Representative fluorescence images of RIM interneuron  $\text{Ca}^{2+}$  transients in naïve (A) and conditioned/recovered (C) wild type animals. Upper and lower panels represent unstimulated (basal activity) and diacetyl-stimulated activity, respectively. (B, D) GCaMP3 signal summary in RIM interneuron in unstimulated (red line) and diacetyl-stimulated (black line) naïve (B) and conditioned/recovered (D) wild type animals (naïve:  $n=9$ ; conditioned + 30 minutes delay for recovery:  $n=10$ ). The

arrows marked a to e correspond to time-points representative fluorescence images under **A** and **C** were taken. The gray-shaded box marks acquisition post to exposure with diacetyl or just solvent. Scale represents the relative fluorescence intensity. Error bars indicate mean +/- SEM.

Finally, we tested *add-1(tm3760)* mutants using the same method. Compared with the wild type, we didn't detect difference in RIM motor neuron activity of naïve *add-1(tm3760)* animals, after diacetyl exposure (Figure 13 A and B). Conditioning of *add-1(tm3760)* animals induced changes in RIM  $Ca^{2+}$  transients similar to wild type (Figure 13 C and D, and data not shown). Last, the learning phase induced changes in RIM neuronal activity fail to be consolidated after 30 minutes recovery in the absence of adducin. As in the case of AVA interneuron and opposed to the wild type, the  $Ca^{2+}$  transients were reversed to the level observed in naïve animals (Figure 13 E and F). Thus, lack of adducin causes impairments in learning and memory induced consolidation of neuronal activity also in RIM motor neuron. All together, our results suggest that the lack of adducin in AVA interneuron has consequences on synapse remodelling and changes of neuronal activity that are functionally reflected also in other members of the motor network.

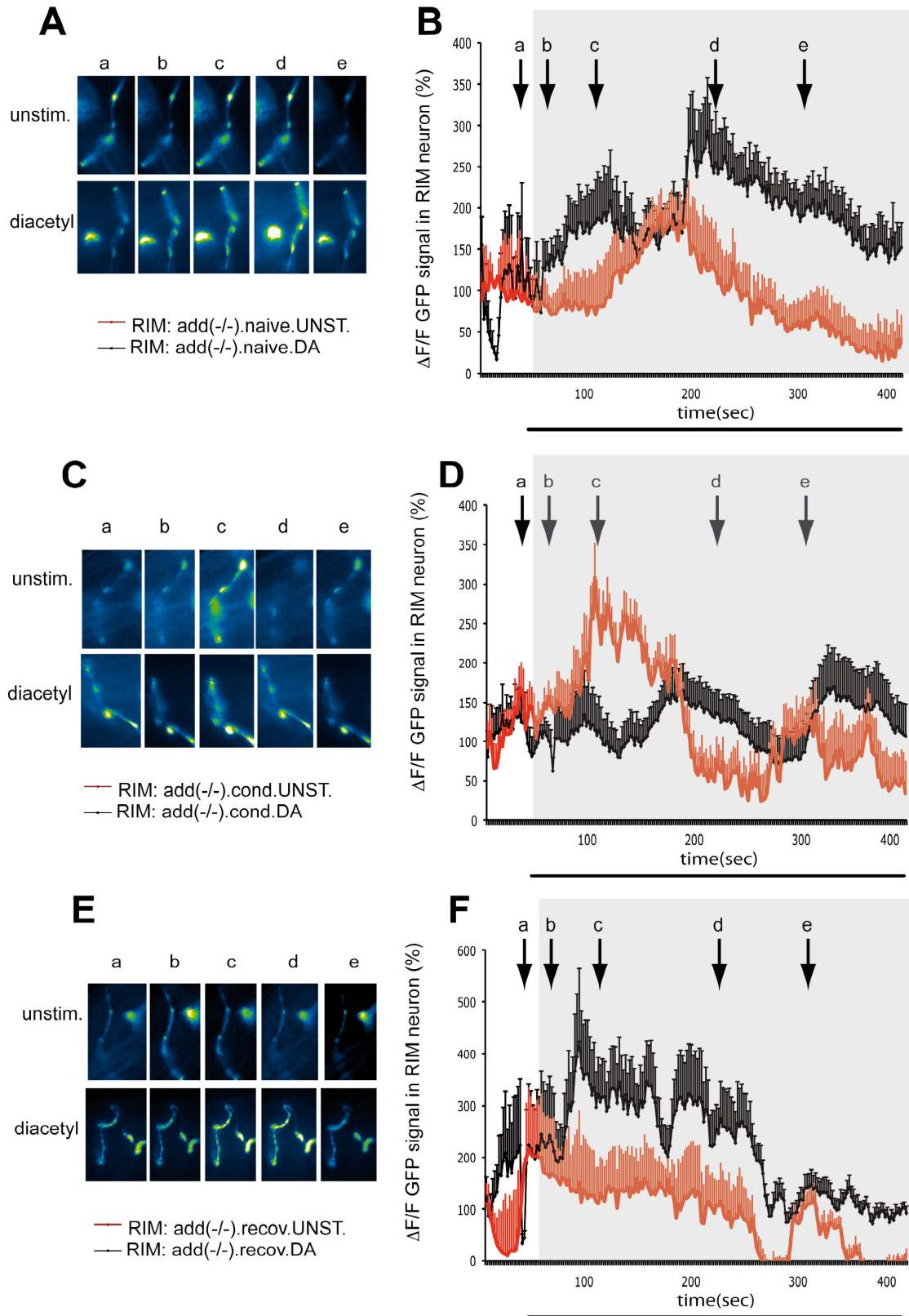


**Figure 13. Lack of ADD-1 impairs memory and sustained changes in neuronal activity of RIM motor neuron. (A, C, E) Representative fluorescence images of RIM**

interneuron  $\text{Ca}^{2+}$  transients in naïve (**A**) and conditioned (**C**) and recovered (**E**) wild type animals. Upper and lower panels represent un-stimulated (basal activity) and diacetyl-stimulated activity, respectively. (**B, D, F**) GCaMP3 signal summary in RIM interneuron in unstimulated (red line) and diacetyl-stimulated (black line) naïve (**B**), conditioned (**D**) recovered (**F**) wild type animals (naïve:  $n=8$ ; conditioned:  $n=10$ ; recovery:  $n=11$ ). The arrows marked a to e correspond to time-points representative fluorescence images under **A**, **C** and **E** were taken. The gray-shaded box marks acquisition post to exposure with diacetyl or just solvent. Scale represents the relative fluorescence intensity. Error bars indicate mean  $\pm$  SEM.

### 3.1.8 Stabilization of actin filaments by ADD-1 is essential for memory

Stabilization of the synaptic area may be achieved through the modification of the actin cytoskeleton that could be regulated by the barbed-end capping activity of ADD-1. Cytochalasin B (CCB) is a well-characterized fungal metabolite that inhibits actin polymerization by binding to the barbed end of actin filaments in broad variety of species from plants to vertebrates including *C. elegans* (Cowan & McIntosh, 1985; Flanagan & Lin, 1980; Goldstein, 1995; MacLean-Fletcher & Pollard, 1980) and may act analogous to actin-capping proteins. Therefore, we tested if pharmacological inhibition of actin polymerization could compensate for loss of *add-1* gene function. Application of different concentrations of CCB had no significant toxic side effect on chemotaxis (Figure 14A), or aversive olfactory associative learning (Figure 14B). Next, we applied increasing concentrations of CCB following conditioning and tested the associative memory after a 30 minutes delay period (Figure 14C). As suggested, 10 or 20  $\mu\text{M}$  CCB fully rescued the memory defect of *add-1(tm3760)* mutant worms, while it had no effect on memory in wild type animals (Figure 14C). We obtained similar results when we analyzed the effect of CCB on GLR-1 synapse volume along the VNC, where 10  $\mu\text{M}$  CCB had no effect on synaptic structures in wild type animals, but restored the defect in consolidation of synaptic volume observed in *add-1(tm3760)* mutant worms (Figure 14D). Thus, efficient memory and consolidation of synaptic plasticity likely requires the barbed-end capping activity of ADD-1.

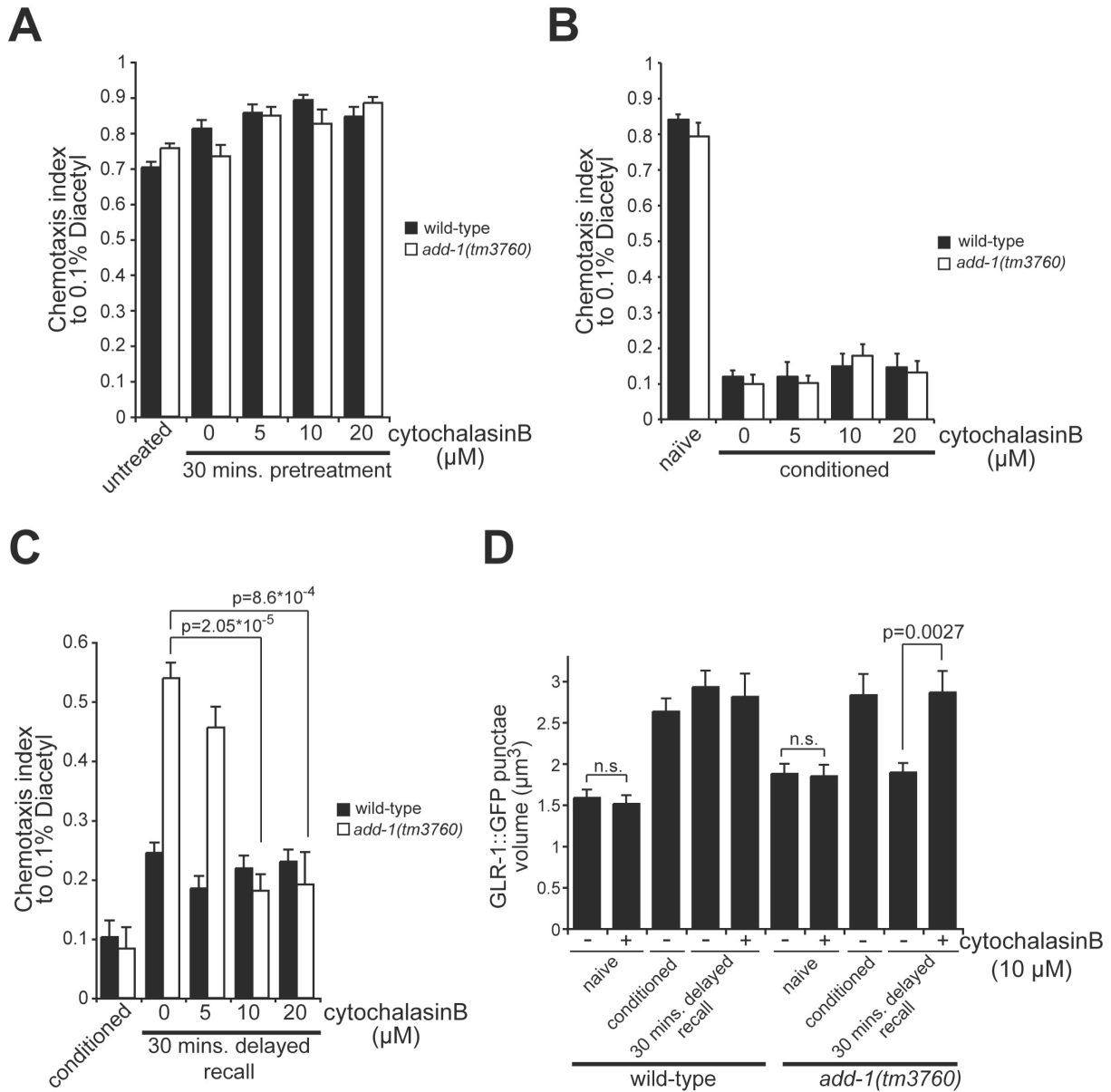


**Figure 14. Cytochalasin B suppresses memory defects of *add-1(tm3760)* mutant worms.** (A) Chemotaxis of wild type or mutant worms was assayed towards 0.1% diacetyl in absence or presence of cytochalasin B as indicated. (B) Associative learning (conditioned) of *add-1(tm3760)* and wild type animals in absence or presence of cytochalasin B as indicated was tested with starvation conditioning assay towards diacetyl. (C) Associative learning (conditioned) and memory after a 30 minutes recovery period in absence of attractant (delayed recall) of *add-1(tm3760)* and wild type animals in absence or presence of cytochalasin B. (D) Average volume of GLR-1::GFP synapses in the posterior VNC upon starvation without (naïve) or with 0.1% DA (conditioned) or conditioning followed by 30 minutes recovery in the absence of DA (30 mins delayed recall) in wild type and *add-*

*I(tm3760)* animals in absence or presence of cytochalasin B as indicated. Graphs indicate mean  $\pm$  SEM. Significance between datasets as indicated was tested with two-tailed Student's t-test (n.s.  $p > 0.05$ ).

### 3.1.9 Behavioral genetic studies support a role for $\alpha$ -adducin in human memory

In order to demonstrate a general evolutionary role of adducin in memory, we used a behavioral genetics approach to investigate the impact of genetic variability in the human  $\alpha$ -adducin homolog on human hippocampus-dependent episodic memory. Human  $\alpha$ -adducin (adducin 1, MIM:102680) is encoded by *ADD1*, which is located on chromosome 4p16.3 and spans an 86 kb large genomic region. To capture *ADD1*-related genetic variability we selected 21 tagging SNPs in Hardy–Weinberg equilibrium (HWE,  $P_{\text{HWE}} \geq 5\%$ ) with minor allele frequency (MAF)  $\geq 5\%$  and located within or very close to *ADD1* (Figure 15A–C). Genotype-phenotype correlations were run under the additive and dominant genetic model. SNP rs10026792 was significantly associated with episodic memory performance as quantified by a picture-based, delayed free recall task. *A* allele carriers recalled significantly more pictures 10 min after presentation than non-carriers ( $P = 0.0005$ ) (S). This result remained significant also after conservative Bonferroni correction for multiple comparisons (21 SNPs, 2 genetic models,  $P_{\text{Bonf}} = 0.021$ ) (Figure 15A). The genetic effect on memory performance was more pronounced for pictures with high emotional content, but was also observed for neutral pictures (Table 2). Five additional *ADD1* SNPs in linkage disequilibrium (LD) with rs10026792 were also associated with episodic memory performance, at least at a nominal, uncorrected significance level.

In addition to the 10 min delayed free recall task, participants also performed a free recall task 24 h after learning. Again, rs10026792 was significantly associated ( $P = 0.0005$ ) with performance in this task, which reflects, among others, protein synthesis-related memory consolidation. Interestingly, we observed no association of *ADD1* SNPs with cognitive phenotypes other than hippocampus-dependent episodic memory (i.e. attention and working memory; all  $P_s > 0.05$ , Table 3).

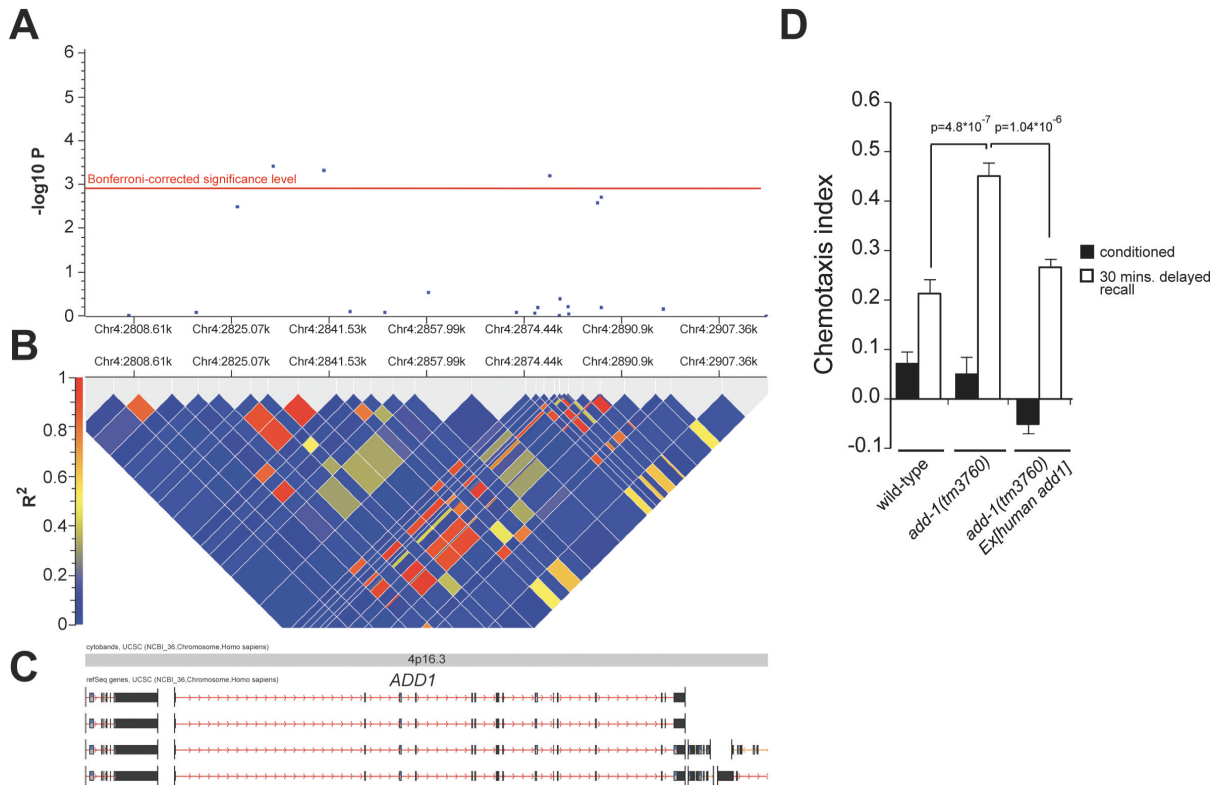


**Figure 15. Human  $\alpha$ -adducin, *ADD1* associates with memory performance. (A)** Significances (Y-axis,  $-\log_{10}P$ ) are shown for individually genotyped *ADD1* SNPs that were tested for association with episodic memory performance in 1085 healthy Swiss young adults. The red horizontal line indicates the Bonferroni-corrected significance level. **(B)** LD structure ( $r^2$  values) of the chromosomal region harboring *ADD1* as calculated in the entire sample of 1085 healthy Swiss young adults. **(C)** Visualization of known transcripts in the *ADD1* region. Chromosomal positions were retrieved from the March 2006 UCSC genome browser assembly. **(D)** Rescue of the memory defect of *add-1(tm3760)* mutant worms carrying the human *ADD1* under the control of *C. elegans add-1* promoter. Young adult worms were conditioned with DA and their preference towards DA was tested immediately (conditioned) or following 30 minutes recovery in the absence of DA (30 min. delayed recall). All experiments were done in triplicate and repeated in three independent experiments. Two independent transgenic lines were tested. Error bars indicate mean  $\pm$  SEM. Datasets were compared as indicated using two-tailed Student's t-test.

Genotype (rs10026792)	Emotional pictures	Neutral pictures	All pictures
	mean $\pm$ sem	mean $\pm$ sem	mean $\pm$ sem
GG (n = 515)	-0.11 $\pm$ 0.04	-0.04 $\pm$ 0.04	-0.10 $\pm$ 0.04
GA/AA (n = 571)	0.10 $\pm$ 0.04	0.09 $\pm$ 0.04	0.11 $\pm$ 0.04
	P = 0.0004	P = 0.038	P = 0.0005

**Table 2 Genotype-dependent memory performance<sup>¶</sup>** (n = 1086). <sup>¶</sup> Values are z-transformed to allow direct comparison between phenotypes.

In order to further support our findings, we generated a “humanized” *C. elegans add-1(tm3760)* strain carrying cDNA of the longest splice form of the human *add1* gene under the control of worm *add-1* regulatory sequences. We tested the worms carrying the extra-chromosomal array for short-term memory, and demonstrated that expression of the human *ADD1* in *add-1(tm3760)* mutants efficiently substituted the worm ADD-1 protein function (Figure 15D), suggesting that despite the divergence in the amino-acid composition, human adducin likely plays a similar molecular role in worms and in humans.

Genotype (rs10026792)	Attention (d2 task)	Working memory (digit span)
	mean $\pm$ sem	mean $\pm$ sem
GG (n = 180)	-0.05 $\pm$ 0.05	-0.04 $\pm$ 0.07
GA/AA (n = 224)	0.04 $\pm$ 0.08	0.01 $\pm$ 0.06
	P = 0.4	P = 0.6

**Table 3. Genotype-dependent attentional and working memory performance. <sup>¶</sup>** Values are z-transformed to allow direct comparison between phenotypes.



## 4 Discussion

Here, we investigated the role of the actin network regulating protein  $\alpha$ -adducin in aversive olfactory associative learning (acquisition of the aversive behavior; tested by immediate recall after conditioning) and in memory (retention of the conditioned behavior over time; short- or long-term delayed recall) in *C. elegans*. Phenotypic analysis of the  $\alpha$ -adducin (*add-1*) knockout mutant worms demonstrated the selective role of the gene in short and long-term memory but not in the learning (acquisition) process. Previous study in  $\beta$ -adducin knock-out mice showed a deficit in fear conditioning and Morris water maze paradigms that measured long-term (several days) acquisition and recall of altered behavior, and did not discriminate between, acquisition (immediate recall), short-term and long-term memories (Rabenstein et al, 2005). Memory, the retention of the conditioned behavior over time, likely requires ADD-1 function in the GLR-1 expressing AVA command interneuron (Figure 6). Furthermore, our results also show that the aversive olfactory memory requires the activity of GLR-1 in AVA neuron (Figure 9). AVA is the main regulator of backward movement and ablation of AVA was previously found to abolish long reversals (Chalfie et al, 1985), therefore following conditioning a sustained increase in synaptic sensitivity in this neuron could lead to increased reversals and backward movement upon repeated exposure to the chemoattractant, thus it could be the direct cause of the avoidance behavior. In good correlation with our previous findings (Stetak et al, 2009) and recent work of Ha *et al.* (Ha et al, 2010) explored the neural network of associative learning, AVA is not required for the learning process (acquisition). However, the data presented here together with our previous results (Stetak et al, 2009) suggests that the AVA command interneuron likely plays a central role in memory, and persistent modulation of synaptic strength in AVA is responsible for the formation of memories towards negative cues.

Analysis of the ADD-1 splice forms in *C. elegans* revealed the importance of the conserved C-terminal Lys-rich MARCKS-related domain in the formation of memory (Figure 6). In vertebrates, the MARCKS-related domain is required for all adducin functions identified up to now, and likely needed for association of adducin with spectrin and actin (Matsuoka et al, 2000). Interestingly, both human and *C. elegans add-1* locus encode for splice forms that differ in their C-terminal end with some forms lacking the MARCKS-related domain. These splice forms may therefore have functions unrelated to the organization of the actin cytoskeleton. The activity of vertebrate ADD-1 is regulated *in vitro* by PKC and PKA

through phosphorylation of residues in the neck and in the MARCKS-related domains, furthermore by binding of  $\text{Ca}^{2+}$ /Calmodulin to the C-terminal end of the protein (Matsuoka et al, 2000). PKC, PKA, as well as  $\text{Ca}^{2+}$  signaling have long been known to be critical for LTP formation and learning in several species including *Drosophila* and *C. elegans* (Drain et al, 1991; Li et al, 1996; Mehren & Griffith, 2004; Nakazawa et al, 1995), our results therefore suggest that they may exert their role at least in part through regulation of ADD-1 activity.

Previously, it has been shown in vertebrates that LTP induces increase in volume of existing dendritic spines (Matsuzaki et al, 2004; Okamoto et al, 2004) a feature that is strongly correlating with AMPARs content. Such structural plasticity requires the modification of the actin cytoskeleton. In contrast to habituation, associative learning in *C. elegans* increases synaptic sensitivity and causes a dynamic remodeling of synapses without formation of new synapses (Rose et al, 2003; Stetak et al, 2009). Here we show that ADD-1 is necessary *in vivo* for consolidating changes in the AMPA-type glutamate receptor, GLR-1 synapse size and receptor content. We found that olfactory associative learning regulates the average size and receptor content but not the number of GLR-1 positive synapses. On the other hand, the persisting changes in GLR-1 cluster size that correlate with memory consolidation require the presence of ADD-1 in AVA. GLR-1 positive synaptic rearrangements occur both in wild type and in *add-1(tm3760)* mutant worms, however *add-1(tm3760)* mutants fail to consolidate synapse rearrangement over time (Figure 7). These results are in accord with our previous findings, with the *C. elegans* behavioral results presented here (Figure 4), and with the hypothetical role of adducin in vertebrates (Matsuoka et al, 2000). Furthermore, our findings expand recent results on the role of  $\beta$ -adducin in the formation and elimination of synapses in mice and in *Drosophila* (Bednarek & Caroni; Pielage et al). Besides the proposed role of adducins in the degradation and assembly of new synapses, ADD-1 could be an important element in existing GLR-1 containing synapses where it controls persistent changes in actin cytoskeleton and thereby could contribute to the consolidation of changes in synapse structure and composition, both of which is required for memory.

Besides the function of  $\alpha$ -adducin in the maintenance of increased synapse volume upon associative learning, here we also demonstrate that ADD-1 plays a role in AMPA-type glutamate receptor mobility. It was previously shown in vertebrates that LTP induction *in vitro* results in a stimulation-dependent decrease of the GluR1 recovery rate suggesting that the reduction of the synaptic receptor exchange ultimately allows synaptic trapping of AMPA receptors (Sharma et al, 2006; Tardin et al, 2003). Our *in vivo* FRAP results in worms (Figure

8) are consistent with vertebrate findings, as we observed a reduced recovery rate upon learning in worms that could lead to the long-term accumulation of AMPA-type glutamate receptor GLR-1 at the synapses. A single training results in long-lasting changes on GLR-1 dynamics that is specific for associative learning. In contrast, loss of  $\alpha$ -adducin prevents the decrease of GLR-1 recovery rate and may interfere with the long-term accumulation of GLR-1 at the synapses. Upon associative learning insertion of GLR-1 from intracellular pools into the PSD may occur independently of ADD-1 function as we observed increase in the amount of GLR-1 signals together with synaptic size expansion, however stabilization of the actin cytoskeleton and consolidation of membrane bound GLR-1 requires the function of ADD-1. This hypothesis is further supported by computational modeling, which suggests that slight local shifts in receptor density could lead to large changes in the postsynaptic response. According to these models (Earnshaw & Bressloff, 2006; Lisman & Raghavachari, 2006) the actin cytoskeleton mediated rapid and continuous changes of the synaptic architecture. Upon associative learning, a transient signal could activate effectors, such as ADD-1 that induces long-lasting modification of the synaptic structure required for the formation of memory. Additionally, our measurements of  $Ca^{2+}$  transients in AVA neuron pointed to changes in neuronal activity upon acquiring and consolidating new information. Sustained changes are dependent on ADD-1 function, and also have implications to motor network members downstream of AVA, like RIM motor neuron. Thus, the changes in glutamate receptor dynamics due to cytoskeleton remodeling are reflected persistent changes in neuronal activity.

As predicted from our hypothesis, loss of ADD-1 function was fully rescued at different levels by the application of an actin filament-stabilizing drug. While cytochalasin B was not toxic, we observed a dose dependent rescue of the memory defect in behavioral assays. Furthermore, the drug consolidated the increase of synapse volumes otherwise abrogated in *add-1(tm3760)* mutants (Figure 14). Altogether, our results strongly suggest that barbed-end capping of F-actin is critical for memory consolidation. In accord with this result, disruption of actin filaments in vertebrates by depolymerizing agents, such as latrunculin A, inhibits LTP (Chen et al, 2007; Krucker et al, 2000; Lang et al, 2004). In a similar way latrunculin A inhibits the long-lasting synapse enlargement that takes place after LTP induction (Matsuzaki et al, 2004). Thus integrity of the actin cytoskeleton is necessary for functional and structural plasticity. Hence, ADD-1 could be one of the molecular determinants that indirectly control glutamate receptor signaling by consolidating rearrangement of the actin cytoskeleton through the barbed-end capping activity of ADD-1 and thereby maintain the changes in synapse structure and composition following learning.

Finally, the behavioral genetics findings support an association of genetic variability in the human homolog of ADD-1 (*ADD1*) with memory-related phenotypes. *ADD1* SNPs were significantly associated with performance in delayed free recall tasks (i.e. 10 min and 24 h after learning), suggesting that in humans, *ADD1* plays a role in hippocampus-dependent memory. Interestingly, no association was found between *ADD1* SNPs and performance in attention and working memory tasks, which predominantly engage prefrontal cortical areas and fronto-parietal cortical networks. Although it is not possible to directly relate human and nematode phenotypes at the behavioral level, the data obtained in humans do support the nematode-based findings, which suggest an important role for ADD1 in memory. Due to the high degree of conservation at the molecular level between invertebrates and vertebrates, our findings suggest a similar molecular function of ADD1 in nematodes and humans.

In conclusion, this study might contribute to better understand the conserved molecular mechanisms regulating structural plasticity of the synapses that is crucial for memory formation. Furthermore, the development of specific inhibitors of ADD-1 function may provide a powerful clinical approach to block transient traumatic memories and thus prevent for example post-traumatic stress disorders. Similarly, drugs enhancing ADD-1 function may be helpful in treating disorders associated with loss of episodic memory capacity, such as Alzheimer`s disease.

## 5 Experimental procedures

### 5.1.1 General methods and strains used.

Common reagents were obtained from Sigma (Sigma-Aldrich, St. Louis, MO) otherwise indicated. Standard methods were used for maintaining and manipulating *C. elegans* (Brenner 1974). Experiments were conducted at 20°C. The *C. elegans* Bristol strain, variety N2, was used as the wild type reference strain in all experiments. Alleles and transgenes used were: *add-1(tm3760)*, *add-1(tm3760)*; *nuIs25[glr-1::gfp]*, *nuIs25[glr-1::gfp]*, *glr-1(n2461)*, *glr-1(n2461)*; *nuIs25[glr-1::gfp]*, *add-1(tm3760)*; *utrEx20[padd-1::add-1minigene, psur-5::dsred]*, *utrEx26[padd-1::tRFP::add-1minigene, rol-6d]*, *add-1(tm3760)*; *utrEx21 [plim-4::add-1minigene, psur-5::dsred]*, *add-1(tm3760)*; *utrEx22[pnmr-1::add-1minigene, psur-5::dsred]*, *add-1(tm3760)*; *utrEx23[podr-2::add-1minigene, psur-5::dsred]*, *add-1(tm3760)*; *utrEx29[ptdc-1::add-1minigene, psur-5::dsred]*, *add-1(tm3760)*; *utrEx28[prig-3::add-1minigene, psur-5::dsred]*, *add-1(tm3760)*; *utrEx30[padd-1::add-1a, psur-5::dsred]*, *add-1(tm3760)*; *utrEx31[padd-1::add-1b, psur-5::dsred]*, *add-1(tm3760)*; *utrEx38[padd-1::add-1c, psur-5::dsred]*, *utrEx26[padd-1::human add1, psur-5::dsred]*, *add-1(tm3760)*; *utrEx45[ptdc-1::add-1b, psur-5::dsred]*, *add-1(tm3760)*; *utrEx46[pnmr-1::add-1b, psur-5::dsred]*, *add-1(tm3760)*; *utrEx47[prig-3::add-1b, psur-5::dsred]*, *add-1(tm3760)*; *utrEx48[padd-1::trfp::add-1minigene, pmyo-3::gfp]*, *add-1(tm3760)*; *utrEx49[prig-3::add-1a, psur-5::dsred]*, *add-1(tm3760)*; *utrEx50[prig-3::add-1c, psur-5::dsred]*, *glr-1(n2461)*; *nuIs25[glr-1::gfp]*; *utrEx51[prig-3::GFPhp, psur-5::dsred]*; *utrEx41[prig-3::GCaMP3, psur-5::dsred]*; *utrEx41[prig-3::GCaMP3, psur-5::dsred]*, *add-1(tm3760)*; *utrEx43[ptdc-1::GCaMP3, psur-5::dsred]*; *utrEx43[ptdc-1::GCaMP3, psur-5::dsred]*, *add-1(tm3760)*.

Transgenic lines were generated by injecting the indicated DNA at a concentration of 50-100 ng/ $\mu$ l, transformation marker, and 100 ng/ $\mu$ l  $\lambda$  phage/HindIII carrier DNA into both arms of the syncytial gonad as described (Mello *et al.* 1991). The transformation markers *psur-5::mDsRed*, *pmyo-3::gfp* were used at 10 ng/ $\mu$ l concentration, and *pRF4(rol-6D)* was used at 5 ng/ $\mu$ l concentration.

### 5.1.2 Molecular biology.

$\alpha$ -adducin minigene was constructed by fusing a 3.1 kb promoter region with the N-terminal *add-1* cDNA fragment (encoding amino-acids 1 to 534) that is common in all *add-1* isoforms (see Figure 2) together with the C-terminal genomic region of the *add-1* gene using a unique *SacI* site. *tRFP* translational reporter construct was generated by introducing *tRFP* encoding sequence after the start codon of the *add-1* minigene. Splice form specific constructs were generated by replacing the genomic C-terminal end of the *add-1* minigene with the appropriate cDNA.

### 5.1.3 Real-time RT-PCR.

Total RNA was isolated from synchronized adult worms and 400ng total RNA was reverse transcribed using a mix of Random Decamers (Ambion) and Anchored Oligo(dT)<sub>20</sub> Primer (Invitrogen). Real-time PCR was performed using the SyBr Fast Kit (Kapa Biosystems) according to manufacturer's recommendations in a Corbett Research RG-6000A instrument. Expression levels were normalized to *tba-1* and *cdc-42* using a geometric mean of their level of expression.

### 5.1.4 Chemotaxis

Chemotaxis to different compounds was assessed as described previously (Bargmann et al, 1993). A population of well-fed, young adults was washed three times with CTX buffer (5 mM KH<sub>2</sub>PO<sub>4</sub>/K<sub>2</sub>HPO<sub>4</sub> pH 6.0, 1 mM CaCl<sub>2</sub> and 1 mM MgSO<sub>4</sub>) and 100–200 worms were placed at the middle of the test plate. Worms were given a choice between a spot of attractant or repellent in ethanol with 20 mM sodium-azide and a counter spot with ethanol and sodium-azide. The distribution of the worms over the plate was determined after 1 hour and a chemotaxis index was calculated as described (Bargmann et al, 1993).

### 5.1.5 Olfactory conditioning

Olfactory conditioning was assessed as described (Nuttley et al, 2002) with some modifications. Starvation conditioning was performed without food in the presence of 2  $\mu$ l undiluted chemo-attractant spotted on the plate for 1 hour on 10 cm CTX plates (5 mM KH<sub>2</sub>PO<sub>4</sub>/K<sub>2</sub>HPO<sub>4</sub> pH=6.0, 1 mM CaCl<sub>2</sub>, 1 mM MgSO<sub>4</sub>, 2% agar). Naïve and conditioned worms were tested for their chemotaxis towards DA as described above.

Long-term associative memory was tested as shown in Figure 5A. Cycloheximide (800  $\mu\text{g/ml}$ ) and actinomycin D (100  $\mu\text{g/ml}$ ) treatments were performed in all washing steps before and during the conditioning phases. Following conditioning, worms were kept on NGM plates in presence of abundant food for 16 or 24 hours and tested for chemotaxis to DA after the recovery phase.

### 5.1.6 Chemotaxis to water-soluble compounds

Chemotaxis to water-soluble compounds was assessed as described (Wicks et al, 2000). Pairs of opposite quadrants of four-quadrant Petri plates (Falcon X plate, Becton Dickinson Labware) were filled with buffered agar (2% agar, 5 mM  $\text{KH}_2\text{PO}_4/\text{K}_2\text{HPO}_4$  pH 6.0, 1 mM  $\text{CaCl}_2$  and 1 mM  $\text{MgSO}_4$ ), either containing 25 mM NaCl or no salt. Adjacent quadrants were connected with a thin layer of molten agar. A population of well-fed, young adults was washed three times with CTX buffer (5 mM  $\text{KH}_2\text{PO}_4/\text{K}_2\text{HPO}_4$  pH 6.0, 1 mM  $\text{CaCl}_2$  and 1 mM  $\text{MgSO}_4$ ) and 100–200 worms were placed at the intersection of the four quadrants. The distribution of the worms over the four quadrants was determined after 10 minutes. For NaCl conditioning, animals were exposed to 25 mM NaCl in CTX buffer for 4 hours.

#### 5.1.6.1 Locomotory rate assays

Locomotory rate assays were performed on a bacterial lawn as described (Mohri et al, 2005; Sawin et al, 2000). Briefly, worms were grown under uncrowded conditions with or without food on conditioning plates for 1 hour. Two minutes after transfer on 6 cm assay plates seeded with OP50, the number of body bends of 8 animals from each strain was counted for 1 minute.

### 5.1.7 Microscopy.

GFP (or tRFP)-tagged proteins were detected with a Zeiss Axiovert 200M LSM 5 Pascal confocal microscope. Animals were immobilized with sodium-azide and GLR-1::GFP was recorded posterior to the vulva, along the z-axis. Quantification of GLR-1::GFP cluster volume was performed using the ImageJ Object Counter 3D plugin. Total fluorescence intensities in a 50  $\mu\text{m}$  long part of the VNC posterior to the vulva were measured on the projected z-sections using ImageJ. Fluorescence recovery after photobleaching (FRAP) was

conducted on young adult animals that were immobilized with polystyrene microspheres and GLR-1::GFP was recorded posterior to the vulva every 5 seconds for 4 minutes. Bleaching of the region of interest was done with 488 nm laser with 30 pulses at maximum energy. Bleaching of the region of interest was done with 488 nm laser with 30 pulses at maximum energy. Calcium transients using GCaMP3 fluorescence calcium indicator were detected with a Zeiss Axioplan2 Imaging fluorescent microscope. The measurements were conducted on young adult animals, immobilized with polystyrene microspheres and  $\text{Ca}^{2+}$  transients fluorescence signal was recorded in AVA and RIM neurons, every 2 seconds with 150ms exposure, for 400s total (200 cycles). Following recording, images were aligned using the ImageJ Stackreg plugin to compensate for movements of the animals and intensity of the ROI was measured with the Time Series Analyzer plugin. Normalization of the fluorescence signal was performed as described (Phair et al, 2004).

#### 5.1.8 Human studies.

**Sample 1:** We recruited 466 young Swiss subjects at the University of Zurich (351 female and 115 male, with a mean age of 21.6 years,  $\text{SD} \pm 2.6$ ). After complete description of the study, all subjects gave written informed consent. Subjects performed a picture-based episodic memory task as described previously (de Quervain et al, 2007) In short, 30 picture stimuli (10 positive, 10 neutral, 10 negative) that were taken from the International Affective Picture System (IAPS; Lang, P.J., Bradley, M.M., & Cuthbert, B.N. (2008). International affective picture system (IAPS): Affective ratings of pictures and instruction manual. Technical Report A-8. University of Florida, Gainesville, FL.) were presented. After a delay of 10 minutes, subjects were unexpectedly instructed to recall the pictures. The phenotype of interest was episodic memory for visual information, measured as the number of recalled pictures, irrespective of emotional quality. Additionally, concentration and attention were measured with the d2 cancellation test, and working memory was assessed with the digit span test.

**Sample 2:** We recruited 620 young Swiss subjects at the University of Basel (403 female and 217 male, with a mean age of 22.7 years,  $\text{SD} \pm 3.6$ ). After complete description of the study, all subjects gave written informed consent. Subjects were presented 72 IAPS pictures (24 positive, 24 negative and 24 neutral) and, after a 10 minutes delay, they were instructed to write down a short description of the previously seen pictures. As in sample 1, the number of correctly recalled pictures served as phenotype.



### 5.1.9 Array-based SNP genotyping.

Samples were processed as described in the Genome-Wide Human SNP Nsp/Sty 6.0 User Guide (Affymetrix). Briefly, 250ng of DNA was digested in parallel with Sty I and Nsp I restriction enzymes (New England Biolabs, Beverly, MA). Enzyme specific adaptor oligonucleotides were then ligated onto the digested ends and diluted ligation reactions were subjected to PCR with Titanium Taq DNA Polymerase. Three PCR reactions of 100 $\mu$ l were performed for Sty I digested products and four PCR reactions for Nsp I. PCR. Cycling parameters were as follows: initial denaturation at 94°C for 3 minutes, amplification at 94°C for 30 seconds, 60°C for 45 seconds and extension at 68°C for 15 seconds repeated a total of 30 times, final extension at 68°C for 7 minutes. PCR products were combined and purified with the Filter Bottom Plate (Seahorse Bioscience, North Billerica, MA) using Agencourt Magnetic Beads (Beckman Coulter, Fullerton, CA). Around 250  $\mu$ g of purified PCR products were fragmented using 0.5 units of DNase I at 37°C for 35 minutes. Following fragmentation, the DNA was end labeled with 105 units of terminal deoxynucleotidyl transferase at 37°C for 4 hours. The labeled DNA was then hybridized onto Genome-Wide Human SNP 6.0 Array at 50°C for 18 hours at 60 rpm. The hybridized array was washed, stained, and scanned according to the manufacturer's (Affymetrix) instructions using Affymetrix GeneChip Command Console (AGCC, version 3.0.1.1214). Generation of SNP calls and Array quality control were performed using the command line programs of the Affymetrix Power Tools package (version: apt-1.12.0). Contrast QC was chosen as QC metric, using the default value of greater or equal than 0.4. Mean Call Rate for all samples averaged 98.5%. All samples passing QC criteria were subsequently genotyped using the Birdseed (v2) algorithm.

## 6 Acknowledgments

We would like to thank to Anne Spang and Jean Pieters for generously sharing methods, reagents and instruments. We would also like to thank the National Bioresource Project, Japan and the Caenorhabditis Genetic Center for providing nematode strains. This work was supported in part by the Swiss National Science Foundation (SNSF) Sinergia grants CRSIKO\_122691 and CRSI33\_130080 (D.Q. and A.P.). This work is also part of the National Centre of Competence in Research (NCCR) Synapsy and of the the 7th framework programme of the European Union (ADAMS, project number 242257, FP7-HEALTH-2009) (D.Q. and A.P.). VV was supported by the Werner Siemens Foundation PhD grant and Opportunities for Excellence PhD Program of the Biozentrum.

Author contributions: VV performed the experiments, evaluated the results, and wrote the manuscript; LG, FP and PD performed the experiments; CV performed the experiments and evaluated the results; DQ and AP designed and evaluated the experiments and wrote the manuscript; AS designed, performed, and evaluated the experiments and wrote the manuscript.

## 7 References

- Bargmann CI, Hartwig E, Horvitz HR (1993) Odorant-selective genes and neurons mediate olfaction in *C. elegans*. *Cell* **74**: 515-527
- Bednarek E, Caroni P (2011) beta-Adducin Is Required for Stable Assembly of New Synapses and Improved Memory upon Environmental Enrichment. *Neuron* **69**: 1132-1146
- Bennett V, Gardner K, Steiner JP (1988) Brain adducin: a protein kinase C substrate that may mediate site-directed assembly at the spectrin-actin junction. *J Biol Chem* **263**: 5860-5869
- Bloom O, Evergren E, Tomilin N, Kjaerulff O, Löw P, Brodin L, Pieribone VA, Greengard P & Shupliakov O (2003) Colocalization of synapsin and actin during synaptic vesicle recycling. *The Journal of Cell Biology* **161**: 737-747
- Cassata G, Kuhn F, Witmer A, Kirchhofer R, Burglin TR (2000) A steep thermal gradient thermotaxis assay for the nematode *Caenorhabditis elegans*. *Genesis* **27**: 141-144
- Capani F, Martone ME, Deerinck TJ & Ellisman MH (2001) Selective localization of high concentrations of F-actin in subpopulations of dendritic spines in rat central nervous system: a three-dimensional electron microscopic study. *The Journal of comparative neurology* **435**: 156-170
- Chalfie M, Sulston JE, White JG, Southgate E, Thomson JN, Brenner S (1985) The neural circuit for touch sensitivity in *Caenorhabditis elegans*. *The Journal of neuroscience : the official journal of the Society for Neuroscience* **5**: 956-964
- Chen LY, Rex CS, Casale MS, Gall CM, Lynch G (2007) Changes in synaptic morphology accompany actin signaling during LTP. *J Neurosci* **27**: 5363-5372
- Cingolani L (2008) Actin in action: the interplay between the actin cytoskeleton and synaptic efficacy. *Nat Rev Neurosci*
- Citterio L, Tizzoni L, Catalano M, Zerbini G, Bianchi G, Barlassina C (2003) Expression analysis of the human adducin gene family and evidence of ADD2 beta4 multiple splicing variants. *Biochem Biophys Res Commun* **309**: 359-367
- Colbert HA, Bargmann CI (1995) Odorant-specific adaptation pathways generate olfactory plasticity in *C. elegans*. *Neuron* **14**: 803-812

Cowan AE, McIntosh JR (1985) Mapping the distribution of differentiation potential for intestine, muscle, and hypodermis during early development in *Caenorhabditis elegans*. *Cell* **41**: 923-932

de Quervain DJ, Kolassa IT, Ertl V, Onyut PL, Neuner F, Elbert T, Papassotiropoulos A (2007) A deletion variant of the alpha2b-adrenoceptor is related to emotional memory in Europeans and Africans. *Nat Neurosci* **10**: 1137-1139

Drain P, Folkers E, Quinn WG (1991) cAMP-dependent protein kinase and the disruption of learning in transgenic flies. *Neuron* **6**: 71-82

Dillon C & Goda Y (2005) The actin cytoskeleton: integrating form and function at the synapse. *Annu. Rev. Neurosci.* **28**: 25–55

Earnshaw BA, Bressloff PC (2006) Biophysical model of AMPA receptor trafficking and its regulation during long-term potentiation/long-term depression. *J Neurosci* **26**: 12362-12373

Ethell IM & Pasquale EB (2005) Molecular mechanisms of dendritic spine development and remodeling. *Prog. Neurobiol.* **75**: 161–205

Fetcho JR, Cox KJ & O'Malley DM (1998) Monitoring activity in neuronal populations with single-cell resolution in a behaving vertebrate. *The Histochemical journal* **30**: 153–167

Flanagan MD, Lin S (1980) Cytochalasins block actin filament elongation by binding to high affinity sites associated with F-actin. *J Biol Chem* **255**: 835-838

Frost NA, Shroff H, Kong H, Betzig E, Blanpied TA (2010) Single-molecule discrimination of discrete perisynaptic and distributed sites of actin filament assembly within dendritic spines. *Neuron* **67**: 86-99

Fukata Y, Oshiro N, Kinoshita N, Kawano Y, Matsuoka Y, Bennett V, Matsuura Y, Kaibuchi K (1999) Phosphorylation of adducin by Rho-kinase plays a crucial role in cell motility. *J Cell Biol* **145**: 347-361

Gardner K, Bennett V (1987) Modulation of spectrin-actin assembly by erythrocyte adducin. *Nature* **328**: 359-362

Goldstein B (1995) An analysis of the response to gut induction in the *C. elegans* embryo. *Development* **121**: 1227-1236

Gray JM, Hill JJ & Bargmann CI (2005) A circuit for navigation in *Caenorhabditis elegans*. *Proc Natl Acad Sci USA* **102**: 3184–3191

Ha HI, Hendricks M, Shen Y, Gabel CV, Fang-Yen C, Qin Y, Colon-Ramos D, Shen K, Samuel AD, Zhang Y (2010) Functional organization of a neural network for aversive olfactory learning in *Caenorhabditis elegans*. *Neuron* **68**: 1173-1186

Hart AC, Sims S, Kaplan JM (1995) Synaptic code for sensory modalities revealed by *C. elegans* GLR-1 glutamate receptor. *Nature* **378**: 82-85

Hirokawa N, Sobue K, Kanda K, Harada A & Yorifuji H (1989) The cytoskeletal architecture of the presynaptic terminal and molecular structure of synapsin I. *The Journal of Cell Biology* **108**: 111–126

Honkura N, Matsuzaki M, Noguchi J, Ellis-Davies GC, Kasai H (2008) The subspine organization of actin fibers regulates the structure and plasticity of dendritic spines. *Neuron* **57**: 719-729

Hughes CA, Bennett V (1995) Adducin: a physical model with implications for function in assembly of spectrin-actin complexes. *J Biol Chem* **270**: 18990-18996

Kauffman AL, Ashraf JM, Corces-Zimmerman MR, Landis JN, Murphy CT (2010) Insulin signaling and dietary restriction differentially influence the decline of learning and memory with age. *PLoS biology* **8**: e1000372

Kim, S., Nollen, E.A., Kitagawa, K., Bindokas, V.P., and Morimoto, R.I. (2002). Polyglutamine protein aggregates are dynamic. *Nat Cell Biol* **4**, 826-831.

Kimura K, Fukata Y, Matsuoka Y, Bennett V, Matsuura Y, Okawa K, Iwamatsu A, Kaibuchi K (1998) Regulation of the association of adducin with actin filaments by Rho-associated kinase (Rho-kinase) and myosin phosphatase. *J Biol Chem* **273**: 5542-5548

Krucker T, Siggins GR, Halpain S (2000) Dynamic actin filaments are required for stable long-term potentiation (LTP) in area CA1 of the hippocampus. *Proc Natl Acad Sci U S A* **97**: 6856-6861

Kuhara A, Mori I (2006) Molecular physiology of the neural circuit for calcineurin-dependent associative learning in *Caenorhabditis elegans*. *J Neurosci* **26**: 9355-9364

Kuhlman PA, Hughes CA, Bennett V, Fowler VM (1996) A new function for adducin. Calcium/calmodulin-regulated capping of the barbed ends of actin filaments. *J Biol Chem* **271**: 7986-7991

Landis DM, Hall AK, Weinstein LA & Reese TS (1988) The organization of cytoplasm at the presynaptic active zone of a central nervous system synapse. *Neuron* **1**: 201–209

Lang C, Barco A, Zablow L, Kandel ER, Siegelbaum SA, Zakharenko SS (2004) Transient expansion of synaptically connected dendritic spines upon induction of hippocampal long-term potentiation. *Proc Natl Acad Sci U S A* **101**: 16665-16670

- Li W, Tully T, Kalderon D (1996) Effects of a conditional *Drosophila* PKA mutant on olfactory learning and memory. *Learning & memory* **2**: 320-333
- Li X, Matsuoka Y, Bennett V (1998) Adducin preferentially recruits spectrin to the fast growing ends of actin filaments in a complex requiring the MARCKS-related domain and a newly defined oligomerization domain. *J Biol Chem* **273**: 19329-19338
- Lisman J, Raghavachari S (2006) A unified model of the presynaptic and postsynaptic changes during LTP at CA1 synapses. *Sci STKE* **2006**: re11
- MacLean-Fletcher S, Pollard TD (1980) Mechanism of action of cytochalasin B on actin. *Cell* **20**: 329-341
- Matsuoka Y, Hughes CA, Bennett V (1996) Adducin regulation. Definition of the calmodulin-binding domain and sites of phosphorylation by protein kinases A and C. *J Biol Chem* **271**: 25157-25166
- Matsuoka Y, Li X, Bennett V (1998) Adducin is an in vivo substrate for protein kinase C: phosphorylation in the MARCKS-related domain inhibits activity in promoting spectrin-actin complexes and occurs in many cells, including dendritic spines of neurons. *J Cell Biol* **142**: 485-497
- Matsuoka Y, Li X, Bennett V (2000) Adducin: structure, function and regulation. *Cell Mol Life Sci* **57**: 884-895
- Matsuzaki M, Honkura N, Ellis-Davies GC, Kasai H (2004) Structural basis of long-term potentiation in single dendritic spines. *Nature* **429**: 761-766
- Matus A (2000) Actin-based plasticity in dendritic spines. *Science* **290**: 754-758
- Mehren JE, Griffith LC (2004) Calcium-independent calcium/calmodulin-dependent protein kinase II in the adult *Drosophila* CNS enhances the training of pheromonal cues. *The Journal of neuroscience : the official journal of the Society for Neuroscience* **24**: 10584-10593
- Mische SM, Mooseker MS, Morrow JS (1987) Erythrocyte adducin: a calmodulin-regulated actin-bundling protein that stimulates spectrin-actin binding. *J Cell Biol* **105**: 2837-2845
- Mohri A, Kodama E, Kimura KD, Koike M, Mizuno T, Mori I (2005) Genetic control of temperature preference in the nematode *Caenorhabditis elegans*. *Genetics* **169**: 1437-1450
- Morales M, Colicos MA & Goda Y (2000) Actin-dependent regulation of neurotransmitter release at central synapses. *Neuron* **27**: 539-550

Mori I, Sasakura H, Kuhara A (2007) Worm thermotaxis: a model system for analyzing thermosensation and neural plasticity. *Curr Opin Neurobiol* **17**: 712-719

Morrison GE, van der Kooy D (1997) Cold shock before associative conditioning blocks memory retrieval, but cold shock after conditioning blocks memory retention in *Caenorhabditis elegans*. *Behav Neurosci* **111**: 564-578

Morrison GE, van der Kooy D (2001) A mutation in the AMPA-type glutamate receptor, *glr-1*, blocks olfactory associative and nonassociative learning in *Caenorhabditis elegans*. *Behav Neurosci* **115**: 640-649

Nakazawa H, Kaba H, Higuchi T, Inoue S (1995) The importance of calmodulin in the accessory olfactory bulb in the formation of an olfactory memory in mice. *Neuroscience* **69**: 585-589

Nuttley WM, Atkinson-Leadbetter KP, Van Der Kooy D (2002) Serotonin mediates food-odor associative learning in the nematode *Caenorhabditiselegans*. *Proc Natl Acad Sci U S A* **99**: 12449-12454

Okamoto K, Nagai T, Miyawaki A, Hayashi Y (2004) Rapid and persistent modulation of actin dynamics regulates postsynaptic reorganization underlying bidirectional plasticity. *Nat Neurosci* **7**: 1104-1112

Phair RD, Gorski SA, Misteli T (2004) Measurement of dynamic protein binding to chromatin in vivo, using photobleaching microscopy. *Methods Enzymol* **375**: 393-414

Phillips GR, Huang JK, Wang Y, Tanaka H, Shapiro L, Zhang W, Shan WS, Arndt K, Frank M, Gordon RE, Gawinowicz MA, Zhao Y & Colman DR (2001) The presynaptic particle web: ultrastructure, composition, dissolution, and reconstitution. *Neuron* **32**: 63-77

Pielage J, Bulat V, Zuchero JB, Fetter RD, Davis GW (2011) Hts/Adducin controls synaptic elaboration and elimination. *Neuron* **69**: 1114-1131

Piggott BJ, Liu J, Feng Z, Wescott SA & Xu XZS (2011) The Neural Circuits and Synaptic Mechanisms Underlying Motor Initiation in *C. elegans*. *Cell* **147**: 922-933

Pollard TD & Borisy GG (2003) Cellular motility driven by assembly and disassembly of actin filaments. *Cell* **112**: 453-465

Porro F, Rosato-Siri M, Leone E, Costessi L, Iaconcig A, Tongiorgi E, Muro AF (2010) beta-adducin (Add2) KO mice show synaptic plasticity, motor coordination and behavioral deficits accompanied by changes in the expression and phosphorylation levels of the alpha- and gamma-adducin subunits. *Genes Brain Behav* **9**: 84-96

Rabenstein RL, Addy NA, Caldarone BJ, Asaka Y, Gruenbaum LM, Peters LL, Gilligan DM, Fitzsimonds RM, Picciotto MR (2005) Impaired synaptic plasticity and learning in mice lacking beta-adducin, an actin-regulating protein. *J Neurosci* **25**: 2138-2145

Revenu C, Athman R, Robine S & Louvard D (2004) The co-workers of actin filaments: from cell structures to signals. *Nature reviews. Molecular cell biology* **5**: 635–646

Rongo C, Whitfield CW, Rodal A, Kim SK, Kaplan JM (1998) LIN-10 is a shared component of the polarized protein localization pathways in neurons and epithelia. *Cell* **94**: 751-759

Rose JK, Kaun KR, Chen SH, Rankin CH (2003) GLR-1, a non-NMDA glutamate receptor homolog, is critical for long-term memory in *Caenorhabditis elegans*. *J Neurosci* **23**: 9595-9599

Saeki S, Yamamoto M, Iino Y (2001) Plasticity of chemotaxis revealed by paired presentation of a chemoattractant and starvation in the nematode *Caenorhabditis elegans*. *J Exp Biol* **204**: 1757-1764

Sawin ER, Ranganathan R, Horvitz HR (2000) *C. elegans* locomotory rate is modulated by the environment through a dopaminergic pathway and by experience through a serotonergic pathway. *Neuron* **26**: 619-631

Segal DS, Squire LR, Barondes SH (1971) Cycloheximide: its effects on activity are dissociable from its effects on memory. *Science* **172**: 82-84

Sharma K, Fong DK, Craig AM (2006) Postsynaptic protein mobility in dendritic spines: long-term regulation by synaptic NMDA receptor activation. *Mol Cell Neurosci* **31**: 702-712

Squire LR, Barondes SH (1970) Actinomycin-D: effects on memory at different times after training. *Nature* **225**: 649-650

Stetak A, Horndli F, Maricq AV, van den Heuvel S, Hajnal A (2009) Neuron-specific regulation of associative learning and memory by MAGI-1 in *C. elegans*. *PLoS One* **4**: e6019

Stosiek C, Garaschuk O, Holthoff K & Konnerth A (2003) In vivo two-photon calcium imaging of neuronal networks. *Proc Natl Acad Sci USA* **100**: 7319–7324

Tardin C, Cognet L, Bats C, Lounis B, Choquet D (2003) Direct imaging of lateral movements of AMPA receptors inside synapses. *EMBO J* **22**: 4656-4665

Tian L, Hires SA, Mao T, Huber D, Chiappe ME, Chalasani SH, Petreanu L, Akerboom J, McKinney SA, Schreiter ER, Bargmann CI, Jayaraman V, Svoboda K & Looger LL (2009) Imaging neural activity in worms, flies and mice with improved GCaMP calcium indicators. *Nat Meth* **6**: 875–881

Tomioka M, Adachi T, Suzuki H, Kunitomo H, Schafer WR, Iino Y (2006) The insulin/PI 3-kinase pathway regulates salt chemotaxis learning in *Caenorhabditis elegans*. *Neuron* **51**: 613-625



Wicks SR, de Vries CJ, van Luenen HG, Plasterk RH (2000) CHE-3, a cytosolic dynein heavy chain, is required for sensory cilia structure and function in *Caenorhabditis elegans*. *Dev Biol* **221**: 295-307

Yuste R & Bonhoeffer T (2004) Genesis of dendritic spines: insights from ultrastructural and imaging studies. *Nat Rev Neurosci* 5: 24–34



## **Epigenetics of human memory: Linking memory to the fifth base**

One of the most intriguing and fundamental properties of brain function is the ability to sustain long-term changes in patterns of neuronal activity, a phenomenon broadly defined as memory. Human memory once formed, can last from minutes to years. This suggests the existence of multiple mechanisms that alter the neuronal function and ultimately generate short-to-long lasting changes in the brain. The exact nature of those processes underlying neural plasticity has been intensively investigated in the last years. They seem to include complex changes in gene expression; protein synthesis; anatomical and cellular structure.

The main question is what are the mechanisms that can respond on a short timescale that is associated with the phenomena of memory formation, while persisting over long timescale for which memory is maintained. Epigenetic changes maintain alterations in gene expression in the absence of the original signal through self-perpetuation. Intuitively, this idea of persistent change induced by short event is parallel to the long-term effects involved in memory.

Transcriptional regulation events are thought to be central in memory processes. In order to streamline and maintain de novo expression profiles on certain loci, epigenetic machinery is recruited together with/or ahead of the transcriptional one. Little is known about the mechanisms that enable maintenance and propagation of introduced epigenetic changes. GWAS studies related to various learning disability disorders (mental retardations) pointed in

many cases to genes that affect epigenetic changes. Recent findings also emphasized the importance of these alterations for neuronal and synaptic plasticity. Never the less, it is still unclear whether the importance of epigenetic regulation is merely reflecting the complexity of transcriptional regulation in CNS, or it indicates the special and specific function of epigenetic mechanisms in memory control.

The methylation of cytosine nucleotides in DNA to form 5-methyl- cytosine, which in mammalian cells is mainly confined to CpG dinucleotides (the fifth base), is viewed as the most stable and long-lasting epigenetic modification. However the precise mechanism by which DNA methylation marks are set, maintained and erased are largely unknown.

The aim of this project is to address a slightly different set of questions concerning the extents to which DNA methylation marks can affect the neural functions of cognitive processes. The methylation status of several genes involved in cognitive processes and in behavioral control has been reported recently by several groups to vary according to postnatal environmental conditions. We hypothesize that these epigenetic stages, via plastic regulation of gene expression and/or gene-gene interactions can significantly modulate memory cascades. Neural activity ultimately induces changes in gene expression that are crucial for establishing and maintaining long-term neuronal plasticity in the adult brain. This is intuitively, as stated before, very similar to context of memory formation, recall and consolidation. In recent years, neuroscience has gained a relatively deep understanding of how memories are formed. In stark contrast is our limited understanding of how these same memories are maintained. Epigenetic modifications of DNA could be crucial for understanding the molecular basis of complex phenotypes. But, instead of revealing a simple predictive code that is shared by many genes, in-depth observation of epigenomic patterns highlights the unique complexity of each transcriptional unit and its associated transcriptional regulatory machinery. This ensures a proper response to cellular signals. In this project we are trying to underpin the link between traumatic memory and PTSD in genocide survivors and

**DNA methylation at glucocorticoid receptor gene promoter is linked to the PTSD risk in  
genocide survivors**

DNA methylation epigenetic states. Such associations could be then taken one step “back” to the context of the genomic DNA sequence, thus getting insights into mechanisms that loop epigenetic variation as a driving force of the phenotypic plasticity with development, adaptation and disease.

UNDER SUBMISSION



## **DNA methylation at glucocorticoid receptor gene promoter is linked to the PTSD risk in genocide survivors**

Vanja Vukojevic<sup>1,2</sup>, Iris T. Kolassa<sup>3</sup>, Angela Heck<sup>1,5,6</sup>, Matthias Fastenrath<sup>1,4</sup>, Leo Gschwind<sup>1,4</sup>, Christian Vogler<sup>1,5,6</sup>, Philippe Demougin<sup>1,2</sup>, Fabian Peter<sup>1,2</sup>, Attila Stetak<sup>1,2,5</sup>, Thomas Elbert<sup>7</sup>, Dominique J.-F. de Quervain<sup>4,5,6</sup>, Andreas Papassotiropoulos<sup>1,2,5,6</sup>

<sup>1</sup> *University of Basel, Department of Psychology, Division of Molecular Neuroscience, Basel, Switzerland*

<sup>2</sup> *University of Basel, Department Biozentrum, Life Sciences Training Facility, Basel, Switzerland*

<sup>3</sup> *Clinical & Biological Psychology, Institute for Psychology & Education, University of Ulm, Ulm, Germany*

<sup>4</sup> *University of Basel, Department of Psychology, Division of Cognitive Neuroscience, Basel, Switzerland*

<sup>5</sup> *University of Basel, Psychiatric University Clinics, Basel, Switzerland*

<sup>6</sup> *University of Basel, Transfaculty Research Platform, Basel, Switzerland*

<sup>7</sup> *Clinical Psychology & Neuropsychology, University of Konstanz, Konstanz, Germany*

## 8 Abstract

Stress induces a complex set of mechanisms that affect the entire organism. The primary function of those changes is to prepare the organism for the direct consequences of stressful events and to ensure a quick return to homeostasis. Additionally, stress is triggering long-term adaptive responses, which result in enhanced memory of stressful events. Failing to recover from the initial response and to keep the adaptive biological alterations under control leads to impaired homeostasis, results in disorders like posttraumatic stress disorder (PTSD). Studies with PTSD patients point to impaired physiological and cognitive balance. One of the critical symptoms is loss of the auto-regulation of the stress-induced alterations in HPA (hypothalamic-pituitary-adrenal axis) signaling and increased inhibition of the HPA axis. These changes are maintained over a long period of time, although the underlying mechanisms remain unclear.

In the present study we investigated epigenetic alterations of the glucocorticoid receptor (GR) gene promoter in saliva samples from survivors of the Rwandan genocide. We found a strong, negative correlation of PTSD symptoms like intrusions, avoidance, and PTSD diagnosis with DNA methylation of the GR gene promoter in genocide survivors. Furthermore, the epigenetic changes were specific to the NGFI transcriptional factor-binding site of the GR promoter and also correlate with GR gene expression. Additionally, we detected a significant negative correlation of *LINE-1* element methylation with PTSD risk and avoidance symptoms.

Together, our data suggests that epigenetic alterations of glucocorticoid receptor gene and genome-wide in *LINE-1* elements could be important for pathophysiology of PTSD and may offer new targets for PTSD diagnosis and treatment. This study also suggests an intriguing possibility of using peripheral tissues for finding epigenetic signatures of some life experiences and complex memory processes.

## 9 Introduction

Severe traumatic experiences can lead to development of posttraumatic stress disorder (PTSD). It is characterized by the presence of three distinct, but co-occurring, symptom clusters. *Intrusions* describe spontaneous, often insuppressible re-experience of the traumatic memory. *Avoidance* involves restricting thoughts and distancing oneself from reminders of the event, as well as more generalized emotional and social withdrawal. *Hyperarousal* symptoms reflect more overt physiological manifestations, such as insomnia, irritability, impaired concentration, hypervigilance, and increased startle responses (Yehuda & LeDoux, 2007b). In contrast to the auto-regulation of stress-initiated response by cortisol negative-feedback inhibition (Munck *et al*, 1984), PTSD studies pointed to impeded physiological and cognitive balance. Although early reports hypothesized the set of mechanisms in PTSD to be similar to ones of classic model of stress (Yehuda *et al*, 1998), this proved to be only partially true. PTSD cases show chronic physiological hyperarousal and elevated catecholamine levels but unexpectedly lower basal level of cortisol (Kardiner, 1941; Mason *et al*, 1986; Pitman & Orr, 1990; Yehuda, 1998; Kanter *et al*, 2001; Marshall *et al*, 2002), despite the levels corticotrophin-releasing factor (CRF) seem to be elevated (Bremner *et al*, 1997; Baker *et al*, 1999). Furthermore, PTSD was associated with enhanced cortisol negative-feedback inhibition (de Quervain *et al*, 2009b; Yehuda & LeDoux, 2007a), in contrast to the attenuated one seen in animal models of chronic stress and patients with depression (Holsboer, 2003). The enhanced inhibition of the HPA axis is possibly mediated by exaggerated GR responsiveness (Yehuda *et al*, 1993; 2004). This is also reflected in decreased cortisol levels in dexamethasone (DEX) suppression test in PTSD cases as compared to controls (Yehuda *et al*, 1995; Goenjian *et al*, 1996; Stein *et al*, 1997).

The etiology of observed HPA axis alterations are unclear. Several studies implied reduced cortisol excretion after the trauma to be associated with increased risk of subsequent development of PTSD (McFarlane *et al*, 1997; Yehuda *et al*, 1998; Delahanty *et al*, 2000). This could also explain significant individual variability and why only 25% of cases experiencing traumatic events actually progress in the PTSD. The state of continuous enhanced negative feedback of the HPA axis, through glucocorticoid receptor signaling, could



attenuate the efforts to re-establish the stress-impaired homeostasis. Given the nature of glucocorticoid signaling on memory formation and maintenance (Roozendaal *et al*, 2009), this could also in return boost the vicious cycle of retrieval, re-experience and reconsolidation of aversive memories (Mcgaugh & Roozendaal, 2002b; de Quervain *et al*, 2009a).

A significant contribution has been made about the effects of the neuroendocrinological impairments in the PTSD. Though it remains unclear what are their underlying mechanisms of origin and stability over extensive period of time, post the traumatic experience (Yehuda *et al*, 2007). A wide range of biological contributors could have an impact on the observed HPA axis alterations. Studies with monozygotic twins discordant for PTSD, provided compelling evidence for the link between genetic factors and PTSD (True *et al*, 1993; Xian *et al*, 2000; Stein *et al*, 2002). Segman and colleagues found a correlation between variable number of tandem repeats in dopamine transporter gene and PTSD risk (Segman & Shalev, 2003). Previously we reported an association between  $\alpha 2b$ -adrenoreceptor deletion variant and emotional memories in traumatized Rwandese, and more recently we also related a genetic variant of the PKC $\alpha$  gene to traumatic memory and to the risk for PTSD survivors of the Rwandan genocide (de Quervain *et al*, 2007; de Quervain & Kolassa, 2012). The polymorphisms in the GR gene were reported not to be significantly associated to the PTSD diagnosis (Bachmann & Sedgley, 2005). Although genetic studies so far provided an important contribution to etiology and variability in PTSD, the biological mechanisms underlying the core symptoms remained unexplained.

Epigenetic mechanisms provide pathways for self-perpetuating transcriptional alternations driven by environmental signals (Squire, 1987; Dulac, 2010). Several studies implicated DNA methylation as a key mechanism for programming of HPA axis activity by early life events (i.e., differential maternal care and early life stress) in rats (Weaver *et al*, 2004) and mice (Murgatroyd *et al*, 2009). Early life stress and childhood abuse were also shown to impact epigenetic programming of the HPA axis in humans (Oberlander *et al*, 2008; McGowan *et al*, 2009b). Thus, those mechanisms could explain how traumatic experiences generate changes in the brain that are maintained over long period of time, in the absence of the initial signal. Sustained alternations in the GR expression could cause long-term changes in neuroendocrine system signaling. Consequently this would have a strong impact on physiological and memory processes, giving a base for development of permanent impaired condition like posttraumatic stress disorder.

In the present study we investigated epigenetic alterations of the human glucocorticoid receptor gene (*NR3C1*, nuclear receptor subfamily 3, group C, member 1) promoter in survivors of the Rwandan genocide. We found a strong, negative correlation of PTSD symptoms and diagnosis with DNA methylation at GR gene promoter. Furthermore, the epigenetic changes are specific to the NGFI transcriptional factor-binding site of the GR promoter and also correlate with GR gene expression. Furthermore, we detected a significant correlation of *Long Interspersed Element 1* (*LINE-1*, *LI*) global methylation and PTSD symptoms, possibly pointing to the increased genomic instability in post-traumatic-stress disorder patients. Our study suggests that epigenetic alterations in the glucocorticoid receptor gene and genome-wide in *LINE-1* elements could be important for pathophysiology of PTSD and may offer new targets for PTSD diagnosis and treatment.

## 10 Results

### 10.1.1 DNA methylation of the GR promoter gene in traumatized survivors of the Rwandan genocide

We hypothesized that epigenetic regulation of the GR promoter and consequently alternations in the GR expression could be related to the risk for PTSD, possibly through sustained changes in the HPA axis activity. Therefore, we tested if the DNA methylation at the glucocorticoid receptor gene promoter could be linked to traumatic experiences and PTSD risk. The promoter region of the *NR3C1* gene that we have investigated is illustrated on the Figure 1. It spans the exon 1F region, a human homologue of the rat exon 1-7, previously reported as differentially methylated (Oberlander *et al*, 2008; McGowan *et al*, 2009a). The analysis covered 8 CpGs, with the NGFI-A (Nerve Growth Factor Inducible A) consensus binding sequence encompassing CpG positions 3 and 4.

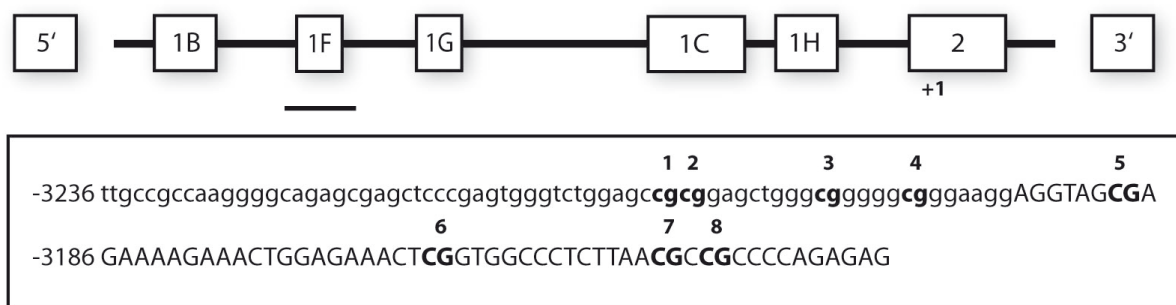


**Figure 1. Human *NR3C1* gene and the CpG region analyzed by bisulfite pyrosequencing**

5' region of the *NR3C1* gene contains multiple first exons, corresponding to multiple transcriptional start sites and multiple mRNA splice variants (Breslin, 2001; Francis, 1999).

The region analyzed by pyrosequencing is illustrated. Numbering is relative to TSS +1 located in exon 2. The underlined sequence represents the potential NGFI-A binding site. Adapted from Oberlander et al (Oberlander *et al*, 2008).

We tested this hypothesis in 162 refugees who have fled from the Rwandan civil war and have been living in the Nakivale refugee camp in Uganda during the time of investigation. All subjects had experienced highly aversive situations and were examined by trained experts with a structured interview based on the Posttraumatic Diagnostic Scale (Foa *et al*, 1997). The population consisted of 104 subjects fulfilling the diagnostic criteria of *DSM-IV* for lifetime post-traumatic stress disorder, as well as 58 individuals don't meeting the *DSM-IV* diagnostic criteria for PTSD (61.5% with PTSD life diagnosis; 38.5% subjects with current PTSD according to *Diagnostic and Statistical Manual of Mental Disorders*, Fourth Edition (DSM-IV, 2000)). The Table S1 illustrates association of GR gene promoter DNA methylation with symptom clusters of PTSD in traumatized Rwandese. Remarkably, significant association was almost exclusive to the CpG3, which is embedded in the NGFI-A consensus binding sequence. Methylation at this site was negatively associated with symptoms of re-experiencing traumatic events (intrusions) ( $P = 0.006$ ,  $\rho = -0.225$ , Table S1; Figure 2). Furthermore, CpG3 site of the glucocorticoid receptor promoter was also associated with increased avoidance symptoms ( $P = 0.009$ ,  $\rho = -0.204$ , Table 1; Figure 2) and with total score of the PDS scale ( $P = 0.005$ ,  $\rho = -0.203$ , Table S1; Figure 2). Finally, hypomethylation at the CpG3 of the *NR3C1* gene promoter is strongly associated with the posttraumatic stress disorder risk ( $P = 0.05$ ; means:  $3.75 \pm 0.25$  and  $2.82 \pm 0.17$ , for PTSD positive and PTSD negative cases, respectively).

PTSD - Symptome clusters		NR3C1_CpG1	NR3C1_CpG2	NR3C1_CpG3	NR3C1_CpG4	NR3C1_CpG5	NR3C1_CpG6	NR3C1_CpG7	NR3C1_CpG8
SUM of INTRUSIONS	Correl. Coeff.	-.155*	-0.009	-.214**	-0.025	-0.09	-0.006	-0.07	-0.065
	Sig.	0.049	0.907	0.006	0.753	0.254	0.941	0.378	0.413
	N	162	162	162	162	162	162	162	162
SUM of AVOIDANCE	Correl. Coeff.	-0.072	-0.023	-.183*	0.021	-0.07	0.006	0.03	0.025
	Sig.	0.361	0.77	0.02	0.787	0.374	0.935	0.709	0.753
	N	162	162	162	162	162	162	162	162
SUM of HYPERAROUSAL	Correl. Coeff.	-0.097	-0.066	-0.145	-0.011	-0.067	-0.039	-0.045	-0.009
	Sig.	0.221	0.401	0.066	0.893	0.399	0.622	0.567	0.906
	N	162	162	162	162	162	162	162	162
SUM_PDS	Correl. Coeff.	-0.124	-0.036	-.207**	-0.014	-0.096	-0.005	-0.03	-0.016
	Sig.	0.115	0.651	0.008	0.863	0.222	0.945	0.706	0.843
	N	162	162	162	162	162	162	162	162

\*\* Correlation is significant at the 0.01 level (2-tailed, Spearman's rho).

\* Correlation is significant at the 0.05 level (2-tailed, Spearman's rho).

**Table S1. Association of PTSD symptom clusters and DNA methylation at the NR3C1 gene promoter in Rwanda sample (n=162)** \*Sum of specific symptom clusters corrected for total number of traumatic events in a lifetime.

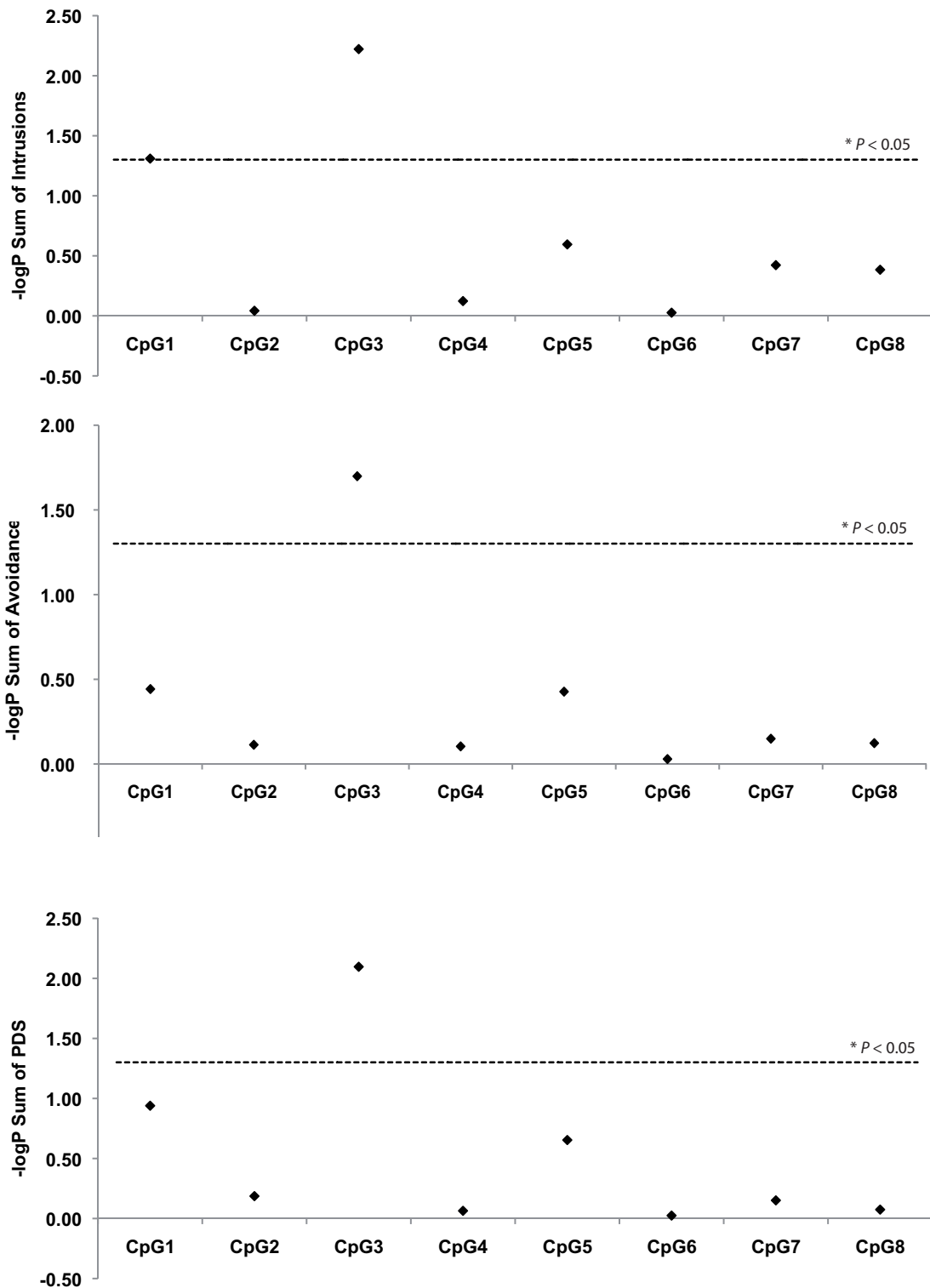


**Figure 2. DNA Methylation association of *NR3C1* promoter region and PTSD symptom clusters: Intrusions, Avoidance and Sum of PDS scale** Significance of the association (expressed as  $-\log P$ ) between cytosine methylation of 8 CpGs in the promoter

region of human NR3C1 gene (as described under Figure 1) and PTSD symptoms intrusions, avoidance as well as Sum of PDS scale. The CpGs are ordered by genomic position. The horizontal line indicates the  $P < 0.05$  significance threshold corrected for the number of effectively independent multiple comparisons. ( $n=162$ ) \*Sum of specific symptom clusters corrected for total number of traumatic events in a lifetime.

Gender did not influence the epigenetic effect on traumatic memory or PTSD risk (gender x CpG3 methylation interaction  $P > 0.5$ ). NR3C1 CpG3 was not associated with hyperarousal symptoms or with the number of experienced event types ( $P > 0.6$ ). Also, DNA methylation at position CpG1 in the examined region of the NR3C1 gene promoter was border line associated with intrusion symptoms ( $P = 0.049$ ,  $\rho = -0.185$ , Table 1). Thus, DNA methylation at the promoter region of glucocorticoid receptor gene is strongly associated with symptoms and risk of PTSD. These findings could be very important for understanding long-term alterations of the HPA axis that are at the core of the posttraumatic stress disorder.

### **10.1.2 Expression of the GR correlates with DNA methylation at the NR3C1 gene promoter**

DNA methylation at the NR3C1 gene promoter CpG3 site strongly correlates with PTSD symptom clusters like intrusions and PTSD risk. This CpG site is encompassed by the NGFI-A transcriptional factor consensus binding sequence, previously reported as important for transcriptional regulation of the glucocorticoid receptor gene (Weaver *et al*, 2004; Turner, 2005). Therefore, we tested if DNA methylation on CpG3 site of the NR3C1 could be associated with the expression of the glucocorticoid receptor. For this purpose, we recruited additional 25 healthy individuals, from which we collected both saliva samples for DNA and RNA isolations. We designed qPCR assays against splice variants containing exon 1F as well as splice variants containing constitutive exon 2 (a measure of total GR expression). Indeed, DNA methylation at the CpG3 correlated strongly both with exon 1F variants and total GR expression ( $P=0.001$ ,  $R^2=0.559$ , Figure 3A and  $P=0.001$ ,  $R^2=0.587$ , Figure 3B; respectively). Furthermore, the expression levels as assayed against exon 1F and total GR expression also correlate ( $P=0.001$ ,  $R^2=0.573$ ). In conclusion, DNA methylation at the NGFI-A

transcriptional factor-binding site of the *NR3C1* gene is negatively associated with the expression of the *NR3C1* gene in saliva. Thus, this suggests that epigenetic modifications at the GR locus could have functional consequences through impact on GR expression.

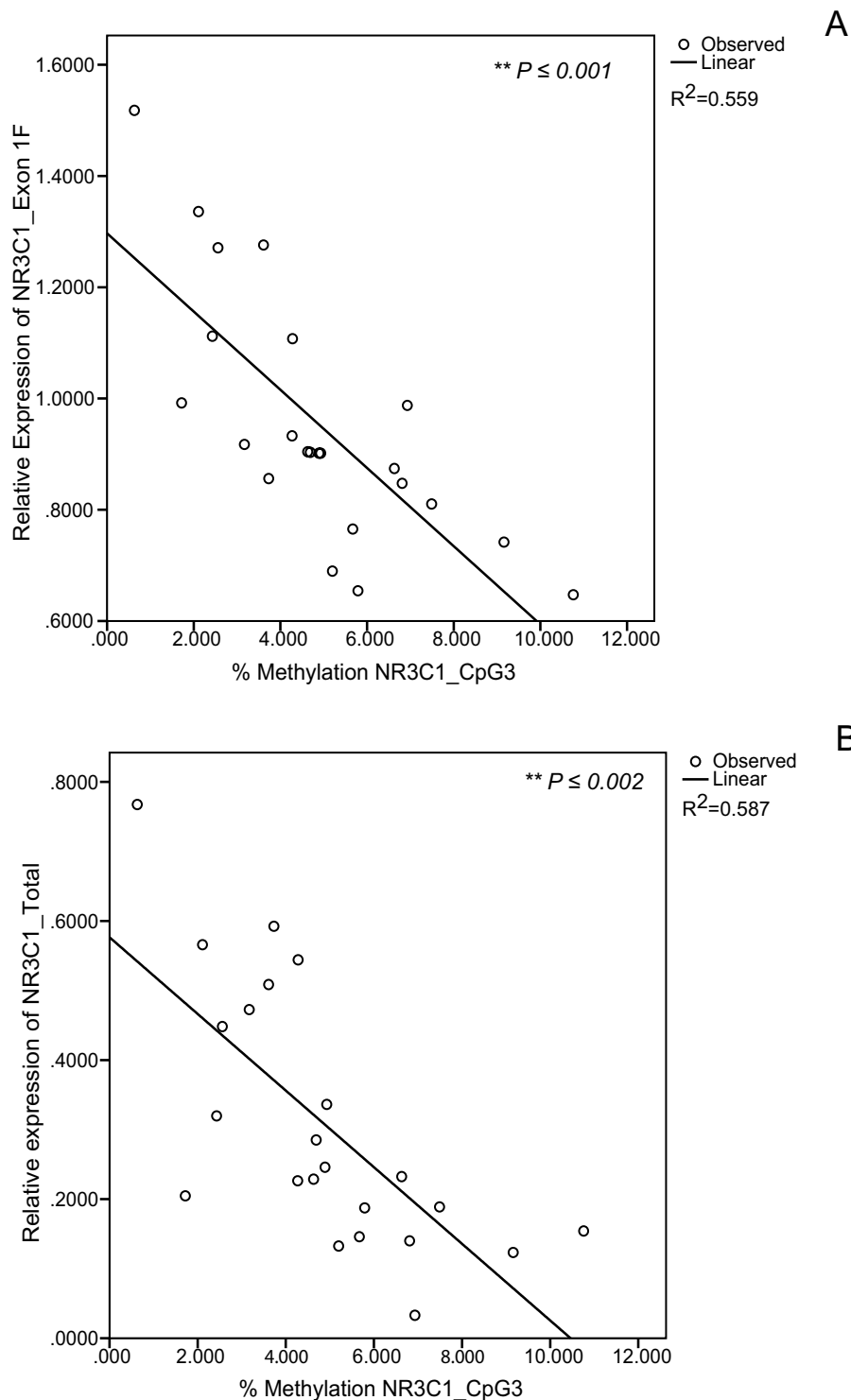


**Figure 3. Linear regression of *NR3C1* CpG3 DNA methylation and expression of glucocorticoid receptor CpG3 methylation is negatively correlated with expression of exon**



1F containing splice variant of the GR (2A) as well as total GR expression based on exon 2 (2B) ( $n=25$ )

### 10.1.3 *LINE-1* element methylation

Following, we tested if there is a difference in total genomic DNA methylation load between the two distinct populations. Long Interspersed Element 1 retrotransposon is the most abundant element in the human genome covering more than 17% of genomic sequence (Ewing & Kazazian, 2010). Therefore, we quantified global methylation of *LINE-1* genomic element by qPCR coupled with high resolution melting (HRM). HRM is a powerful technique that enables very precise monitoring of "melting" of the PCR products in real time. Given that the melting profiles are highly sequence specific, bisulfite PCR coupled with qPCR-HRM enables very precise quantification of DNA methylation.

<b>PTSD - Symptome clusters</b>	<b>LINE-1 Methylation</b>	
<b>SUM of INTRUSIONS‡</b>	Correl. Coeff. Sig. N	-0.123 0.359 58
<b>SUM of AVOIDANCE‡</b>	Correl. Coeff. Sig. N	-.350** 0.007 58
<b>SUM of HYPERAROUSAL‡</b>	Correl. Coeff. Sig. N	-0.246 0.062 58
<b>SUM_PDS‡</b>	Correl. Coeff. Sig. N	-.270* 0.04 58
<b>NR3C1_CpG3 Methylation</b>	Correl. Coeff. Sig. N	-0.038 0.776 59

\*\* Correlation is significant at the 0.01 level (2-tailed, *Spearman's rho*).

\* Correlation is significant at the 0.05 level (2-tailed, *Spearman's rho*).

**Table 1. Association of PTSD symptom clusters and DNA methylation of *LINE-1* element promoter in Rwanda sample ( $n=59$ )** ‡Sum of specific symptom clusters corrected for total number of traumatic events in a lifetime.

Interestingly, we found association of *LINE-1* element global DNA methylation against symptom clusters of PTSD in traumatized Rwandese. Specifically, we observed significant correlation with avoidance symptoms ( $P = 0.003$ ; sum of PDS scale  $P = 0.04$ , Table 1). Global methylation of *LINE-1* genomic element was borderline associated with hyperarousal symptoms ( $P = 0.058$ , Table 1), but no significantly associated with symptoms of re-experiencing traumatic events (intrusions,  $P = 0.972$ , Table 1). Furthermore, hypomethylation of the Long Interspersed Element 1 was strongly associated with the current PTSD diagnosis (Table 2,  $P = 0.003$ ,  $n=60$ ). Finally, there was no significant correlation of global *LINE-1* methylation and the methylation at the NR3C1 promoter or the total sum of traumatic events ( $P = 0.862$  and  $P = 0.753$ , respectively).

PTSD_Current_DSM-IV	LINE-1 genomic element methylation %		
	Mean	Std. Dev.	N
0	96.8*	3.8	41
1	91.6*	3.2	19

\*  $P = 0.003$ , Mann-Whitney U Test

**Table 2. *LINE-1* element methylation is associated with PTSD ( $n=59$ )** PTSD positive and negative diagnosis according to *DSM-IV* criteria are marked 0 and 1, respectively. ‡Sum of specific symptom clusters corrected for total number of traumatic events in a lifetime.

## **11 Discussion**

The present study indicates that DNA methylation at the glucocorticoid receptor gene is linked to traumatic memories, PTSD symptoms and risk in the heavily traumatized genocide survivors. Importantly, the hypomethylation at the examined region of the *NR3C1* promoter is almost exclusively restricted to the NGFI transcriptional factor consensus binding sequence. Furthermore, DNA methylation at this site strongly correlates with the expression of the glucocorticoid receptor. Thus, epigenetically driven, long-lasting alternations in the GR expression could impede HPA axis regulation, impacting physiological and memory processes, and possibly contributing to the development of posttraumatic stress disorder.

Several studies with PTSD patients pointed that increased negative feedback on the HPA axis, as one of the core PTSD symptoms is strongly mediated via enhanced GR responsiveness (Yehuda *et al*, 1993; 1991; 2004). Additionally, reports with animal models of PTSD also pointed to increased HPA axis inhibition and up-regulated GR expression in the hippocampus (Liberzon *et al*, 1999; Kohda *et al*, 2007). However, it remains unclear how are these alterations maintained over-time. Our current study suggests a link between epigenetic regulation of the glucocorticoid receptor gene and posttraumatic stress disorder risk. Furthermore, site-specific DNA methylation of the GR gene promoter is not only associated with the PTSD risk, but also with specific symptom clusters like intrusions or avoidance. Uncontrollable, easy reactivation and re-experience of traumatic events is one of the core marks of the PTSD (Brewin, 2001; Michael *et al*, 2005; de Quervain *et al*, 2009a). It would be important to examine if epigenetic changes of GR promoter are mirrored in the brain regions like amygdala, thus possibly resulting in enhanced re-experience and re-consolidation of traumatic memories. Additionally, resulting HPA axis impairment could contribute to the persistence of avoidance symptoms, leading to systemic emotional and social withdrawal.

The epigenetically altered HPA axis may be a part of biological responses initiated with traumatic events or it may rather reflect the pre-existing vulnerability that impedes the

process of biological recovery from stress (Resnick *et al*, 1995; Yehuda *et al*, 1998; Mcgaugh & Roozendaal, 2002a). Mentioned animal models of PTSD showed persistent PTSD-like impairments in the absence of obvious early life adversity. In our current study it was possible to compare persons who had developed PTSD after experiencing traumatic events to severely trauma-exposed controls without PTSD. The differences in GR promoter methylation were strongly correlated with PTSD symptoms and diagnosis, independently to the number of experienced traumatic events. This could be due to known ceiling effects, but could also indicate that hypomethylation at GR promoter is a pre-acquired risk factor. Unfavorable life experiences (e.g. poor life conditions, hunger and adverse events) prior the Rwandan genocide could contribute to pre-acquired epigenetic differences at the GR locus and thus vulnerability to traumatic events. However, the possibility that epigenetic mechanisms are rather initiated by traumatic experiences couldn't be excluded by our and previous studies. Future studies should help us examine the origins and the function of epigenetic changes at glucocorticoid receptor gene for the development and progress of PTSD. Larger, longitudinal studies, including sampling before and after traumatic experiences, combined with animal models (e.g. inhibitory avoidance paradigm in rats) could help us underpin the underlying etiology and mechanisms of epigenetic modifications in PTSD.

Additionally, we found that global *LINE-1* promoter methylation is also correlating with PTSD risk and symptoms like avoidance. Long Interspersed Element-1 is often used as a global methylation marker (Morales, 2002a; Kim *et al*, 2009a; Xie *et al*, 2009). Although these ancient genomic elements affect the genome stability through retrotransposition-dependent expression of *LINE-1* RNA and encoded proteins (Bourc'his & Bestor, 2004), the activity of *LINE-1* elements is not completely disabled in mammals (Brouha *et al*, 2002; Ostertag & Kazazian, 2001; Prak *et al*, 2003). Several cellular mechanisms, including L1 promoter DNA methylation, regulate both the activation and the repression of these elements in vivo (Fedorov, 2008). Moreover, a few studies suggested that this mechanisms could be modulated by environment (Bollati *et al*, 2007; Baccarelli *et al*, 2009; Capomaccio *et al*, 2010). Additionally, recent study in U.S. military service members deployed to Iraq or Afghanistan, reported hypomethylation in PTSD cases versus controls (post-deployment vs. pre-deployment) (Rusiecki *et al*, 2012). Thus, the negative correlation of *LINE-1* methylation with PTSD symptoms could be a potential biological marker for increased stress, and possibly its consequences on genome stability. Future experiments are needed to underpin the causes and functional meaning of the observed changes in the *LINE-1* element methylation relative to traumatic experiences and PTSD. It has to be determined if

these changes are also reflected in the activity of these elements, for example in terms of new retro-transpositions frequency. Additionally, it would be interesting to closely examine the relations of multiple epigenetic mechanisms in PTSD and their contributions to PTSD symptoms and risk.

Finally, the DNA and RNA samples used in this study were extracted from the periphery (saliva) as opposed to the brain. For the scientific community interested in finding epigenetic signatures of life experiences and complex cognitive processes this raises very important issues. Although the epigenetic patterns (including DNA methylation) are showing significant tissue specificity, several points suggest the possible use of non-brain tissues for epigenetic studies of at least some psychiatric disorders. First, a few available whole methylome studies (Davies *et al*, 2012; Ladd-Acosta *et al*, 2007; Mill *et al*, 2008; Maunakea *et al*, 2010; Lister *et al*, 2009) suggest that DNA methylation signatures show high tissue specificity in rather poor CG regions, especially CG Island (CGI) Shores, 3' regions, but as well CG rich intragenic CGI. On the other hand, genomic regions with high CG content like the promoter CG Islands (interestingly, this is the case with *NR3C1* gene promoter) generally show steady epigenetic signatures across brain tissues and periphery. Second, the pattern of relative inter-individual variability by feature is the same across tissues, with a significant correlation between different tissues. Third, in relation to these observations comes the question of what is the range of tissues to be likely affected by certain complex processes. It could be possible that systemic disorders (e.g. stress or traumatic experience), may lead to overlapping epigenetic patterns. Our study together with several other human studies that we discussed before suggests the intriguing possibility to use the peripheral epigenetic markers for studies of some complex psychiatric disorders. However, future studies should carefully and moreover longitudinally address the relations of intra-individual epigenetic differences, both developmentally and adaptively.

In summary, the present study suggests that epigenetic regulation of the glucocorticoid receptor promoter is important for PTSD symptoms and risk. Furthermore, global *LINE-1* hypomethylation is also associated to the disorder symptoms and risk, possibly pointing to effects of stress and trauma on genomic stability. Taken together, this study may be important for the understanding of posttraumatic stress disorder, reflecting risk, complex and broad symptomatology, and possibly offer new diagnostic markers and treatments.

## 12 Material and methods

### 12.1.1 Subjects: Rwanda Sample

The main cohort used in the epigenetic study included 162 Rwandese, survivors of the Rwanda genocide (86 females, 76 males; median age 31 y; range, 12–34 y). The sample was structured so that participants were sampled proportionally to population size, from all zones of the large area of the Nakivale refugee camp. Additionally, in order to exclude genetic relatives in the samples, only one person per household was interviewed. Candidates exhibiting current alcohol abuse and acute psychotic symptoms were excluded. All subjects had experienced highly aversive traumatic situations and were examined in 2006/2007 by trained experts, using a structured interview based on the Posttraumatic Diagnostic Scale (PDS) (Foa *et al*, 1997) with the help of trained interpreters. A checklist of 36 war- and non-war-related traumatic event types (e.g., injury by weapon, rape, accident) was used to assess traumatic events (de Quervain *et al*, 2007; de Quervain & Kolassa, 2012; Neuner *et al*, 2004). Traumatic load was estimated by assessing the number of different traumatic event types experienced or witnessed. This measure is considered more reliable than assessing the frequency of traumatic events (Neuner *et al*, 2004). For assessing depressive symptoms, the depression section of the Hopkins Symptom Checklist (HSCL-D) was used (Derogatis *et al*, 1974). A subset of this sample has been analyzed in previous studies (Kolassa *et al*, 2010a; de Quervain & Kolassa, 2012). All the procedures were conducted with the approval of the Ethics Committees of the University of Konstanz and the Mbarara University of Science and Technology, Mbarara, Uganda.

A form of a standardized interview was used for completing the PDS and event list. All Interviewers first went through a 6-wk course training on principles of quantitative data collection and interviewing techniques. The translation of the instruments into Kinyarwanda was done using several steps of translations, blind back-translations, and subsequent corrections by independent groups of translators (Onyut, 2004). Following the translations,

the psychometric properties of the translated scales were investigated in a validation study including a retest spanning a 2-wk period and a cross-validation with expert rating (Neuner *et al*, 2008).

Subjects were selected to have experienced no more than 16 traumatic event types, to avoid known ceiling effects (Kolassa *et al*, 2010b). Saliva samples were collected from all subjects, using an Oragene DNA Kit (DNA Genotek, Ottawa, Ontario CA).

### **12.1.2 DNA isolation and bisulfite conversion**

DNA was initially extracted using precipitation protocol recommended by the producer. In order to obtain high purity DNA prior bisulfite conversion, samples were additionally re-purified. For this purpose 2µg of DNA isolated with Oragene procedure, was incubated overnight on 50°C with proteinase K (Lysis buffer: 30 mM Tris·Cl; 10 mM EDTA; 1% SDS, pH 8,0; 150ng/µl Proteinase K), agitated by gentle orbital shaking. Following, the DNA was purified using Genomic DNA Clean & Concentrate Kit (Zymo Research, Irvine, California USA). The quality and concentration were assessed using gel electrophoresis and fluorometry (Qubit dsDNA BR Assay Kit; Invitrogen, Carlsbad, CA USA), respectively. 500ng of high purity, intact DNA was used for bisulfite conversion using EZ DNA Methylation-Gold kit (Zymo Research) by standard protocol. Bisulfite DNA quality and concentration was determined using RNA Pico 6000 Kit on Bioanalyzer 2100 instrument (Agilent Technologies, Santa Clara, CA USA) and Nanodrop 2000 (ThermoScientific, Waltham, MA USA). An external control sample was always converted in parallel to assess possible variations in conversion reactions. Randomly chosen 48 samples were reconverted and measured as an additional control. Bisulfite-converted (BSC) samples were normalized to 10ng/µl.

### **12.1.3 Pyrosequencing analysis**

The methylation status of CpG-rich region of the human *NR3C1* gene, including exon 1F and NGFI binding site (Turner, 2005; Oberlander *et al*, 2008) was quantified by bisulfite pyrosequencing (Tost & Gut, 2007). Primers were designed according to recommendations of Wojdacz *et al* (Wojdacz *et al*, 2008; 2009): NR3C1\_Q-CpG\_FW, 5'-GTTATTCGTAGGGGTATTG-3' and NR3C1\_Q-CpG\_RV, 5'-biot-CAACTCCCCAAAAAAAAAAAAA-3' (Microsynth, Balgach, Switzerland). 206bp *NR3C1* promoter fragment was amplified using AmplyTaq Gold Kit from Applied Biosystems (Life Technologies, Grand Island, NY USA). PCR was done in 30µl reactions containing: 1x PCR Buffer II, 300µM dNTPs, final 3.5mM MgCl<sup>2</sup>, 200µM of each primer, 20ng of BSC DNA. We used the following cycling conditions: 95°C, 15 min – 50 x (95°C, 30s - 55°C, 30s - 72°C, 30s) – 72°C, 10min. PCR products were purified and sequenced using a PyroMark ID System (Biotage, Foxboro, MA USA) following the manufacturer's suggested protocol and two sequencing primers: NR3C1\_S2, 5'-GAGTGGGTTTGGAGT-3' and NR3C1\_S3, 5'-AGAAAAGAAATTGGAGAAATT-3' (Microsynth) as in Oberlander *et al* 2008 (Oberlander *et al*, 2008). Testing for PCR temperature bias and calibration was done by introducing a series of calibrator samples with known methylation levels. Briefly, we prepared un-methylated standards by using two rounds of linear whole genome amplification with Ovation WGA System Kit (Nugen, San Carlos, CA USA), starting from 10ng of DNA, as recommended by manufacturer. Methylated standards were made using CpG Methyltransferase assay with M.SssI (M0226M, New England Biolabs, Beverly, MA) starting from 2µg of purified DNA, following the standard protocol. Bisulfite conversion of standard samples was done as described above. All samples were analyzed in quadruplicates.

#### 12.1.4 LINE-1 HRM qPCR analysis

The methylation of Long Interspersed Element 1 was used to estimate the whole genome methylation (Yang *et al*, 2004). Analysis was performed on a subset of samples from Rwanda genocide survivors' pool described above ( $n=60$ ; 29 males, 31 females; median age 31 y; range, 12–34 y). A pyrosequencing assay from Kim *et al* (Kim *et al*, 2009a) was adopted for High Resolution Melting (HRM) quantitative methylation analysis (Kristensen *et al*, 2008; Stanzer *et al*, 2010; Tse *et al*, 2011). Briefly, *LINE-1* HRM assay was performed using primers: *LINE-1*\_HRM\_FW 5'-TTTTGAGTTAGGTGTGGGATATA-3' and *LINE-*



*I\_HRM\_RV* 5'-AAAATCAAAAATTCCTTTC-3' (Microsynth). qPCR followed by HRM was performed on Rotor-Gene 6000A instrument (Corbett Life Science, Mortlake NSW, Australia). qPCR was done in a 15- $\mu$ l reaction volume with 10 ng of BSC DNA and 200 $\mu$ M of each primer, using SensiMix HRM kit (Bioline, London, UK). Following cycling conditions were used: 95°C, 10min – 40 x (95°C, 15s - 56.5°C, 10s - 72°C, 15s) – 72°C, 5 min. Subsequently high resolution melting (HRM) step was performed. The HRM analysis was initiated by denaturing all products at 95°C for 1 min, followed by annealing at 40°C for 1 min. After fast ramping to 55°C, HRM was performed: 55°C to 95°C, rising by 0.1°C / s. Fluorescence data were collected at 25 acquisitions per second. Methylation standards (0%, 30%, 50%, 70%, 90%, 100%) used to calibrate the HRM curves and quantify the methylation of the samples were prepared as described above.

Fluorescence data were analyzed using Corbett Rotor-Gene 6000 Application Software, version 1.7 (Corbett) and TeeChart Office (Steema Software, Girona, Spain). Methylation values of standard samples were plotted against peak heights as well a surface-area below normalized HRM curves. These standard curves were used for quantification of *LINE-1* methylation in test samples. All samples were done in quadruplicates. Assay was additionally validated with bisulfite pyrosequencing as previously described (Kim *et al*, 2009b), with the exception that bisulfite PCR was prepared as described above for HRM qPCR.

### **12.1.5 RNA isolation and expression analysis**

RNA was isolated from Oragene RNA Self-Collection Kits. Promptly after collection, samples were mixed for 10s by vortexing, incubated at 50°C in a water-bath for 2.5hr and stored at -80°C until further analysis. For the isolation procedure samples were processed in 250 $\mu$ l aliquots. Briefly, samples were again incubated in the water-bath on 90°C for 15 minutes and then cooled to the RT. Following, 750 $\mu$ l of TRIReagent LS (Ambion, Life Technologies) was added to each sample and homogenization was done for 1min on 28Hz using TissueLyser II (Qiagen AG, Hilden, Germany). After homogenization, 1000 $\mu$ l of absolute ethanol was added to the sample and mixed. Finally, the mixture was loaded on Zymo-Spin IIC column and RNA was further purified using Direct-zol kit (ZymoResearch)

following the recommended procedure, including DNase I treatment. The concentration and quality of the RNA was determined using Nanodrop 2000 (ThermoScientific) and RNA Nano 6000 Kit on Bioanalyzer 2100 instrument (Agilent).

For reverse transcription, 350ng total RNA was denaturated for 8min at 70°C followed by ice incubation in the presence of 25ng Anchored Oligo(dT)20 Primer (Invitrogen) and 75ng Random Decamers Primers (Ambion). In the RT reaction, cDNA was generated in 25µl reaction using Super RT kit (HT Biotechnology, Santa Cruz, CA USA). Upon completion of the reaction, the volume was adjusted to 200µl in Lambda DNA solution (5ng/µl final concentration; Promega, Fitchburg, WI USA). The primers were designed against splice variants that contain exon 1F of the *NR3C1* gene: NR3C1\_1F\_FW, 5'-GTTGATATTCAGTGGGA-3' and NR3C1\_1F\_RV, 5'-CTTGGAGTCTGATTGAGA-3' (Microsynth). Additionally total expression of the GR gene was determined against exon 2: NR3C1\_2\_FW, 5'-CTTCAGAACAGCAACATT-3' and NR3C1\_2\_RV, 5'-GACTCTCATTCGTCTCTT-3' (Microsynth). The expression levels were normalized to *RPLPO* gene (human large ribosomal protein) using the following primers: RPLP0-Ex3-4\_FW, 5'-CTCTGGAGAAACTGCTGC-3' and RPLP0-Ex3-4\_RV, 5'-TGATCTCAGTGAGGTCC-3' (Sigma Aldrich, St.Louis, MI USA). qPCR was performed using the Power SYBR Green PCR Master Mix (Life Technologies) according to standard recommendations, in 12µl final volume of reaction, using 2µl of cDNA template, on Corbett Research RG-6000A instrument. Cycling conditions were as follows: 95°C, 60s – 40x (95°C, 3s - 56°C, 10s – 72°C, 4s) followed by a melting curve analysis (61°C to 95°C, rising by 0.7°C / 3s) to attest amplification specificity. Threshold cycles (crossing point) were determined using Rotor-Gene software version 6.1. Expression levels were normalized to *RPLPO* gene using a geometric mean of their level of expression (Vandesompele *et al*, 2002). Fold differences were calculated using the delta-delta Ct method (Pfaffl, 2001) with the help of qBasePlus software (Biogazelle, Ghent, NL).

### 12.1.6 Statistical analyses

All statistical analyses were done with software packages SPSS Statistics (version 20, SPSS Inc., Chicago, Illinois) and R (R Development Core Team 2012). Non-parametric methods were used wherever appropriate. Corrected significance threshold was set to  $P < 0.05$ .

### **13 Acknowledgments**

This work was funded by the Swiss National Science Foundation (Sinergia grants CRSIK0\_122691, CRSI33\_130080 to D.Q. and A.P.); by the 7th framework program of the European Union (ADAMS project, HEALTH-F4-2009-242257); by the National Center for Competence in Research SYNAPSY; and by the German Research Foundation (DFG; grants to I.K. and T.E.). VV was supported by the Werner Siemens Foundation (Zug, Switzerland) PhD grant and Opportunities for Excellence PhD Program of the Biozentrum. VV, DdQ, AP, ITK, TE, AS designed the study, analyzed data, and wrote the paper. VV, PD performed the experiments. AH, MF, LG, CV contributed to data analysis. VV, PD, FP contributed to methods and analytic tools. The authors declare that they have no competing interests.

## 14 References

- Baccarelli A, Wright RO, Bollati V, Tarantini L, Litonjua AA, Suh HH, Zanobetti A, Sparrow D, Vokonas PS & Schwartz J (2009) Rapid DNA methylation changes after exposure to traffic particles. *Am. J. Respir. Crit. Care Med.* **179**: 572–578
- Bachmann A & Sedgley R (2005) T.L. Jackson, . Glucocorticoid receptor polymorphisms and post-traumatic stress disorder. *Psychoneuroendocrinology* **3**: 297–306
- Baker DG, West SA, Nicholson WE, Ekhaton NN, Kasckow JW, Hill KK, Bruce AB, Orth DN & Geraciotti TD (1999) Serial CSF corticotropin-releasing hormone levels and adrenocortical activity in combat veterans with posttraumatic stress disorder. *Am J Psychiatry* **156**: 585–588
- Bollati V, Baccarelli A, Hou L, Bonzini M, Fustinoni S, Cavallo D, Byun H-M, Jiang J, Marinelli B, Pesatori AC, Bertazzi PA & Yang AS (2007) Changes in DNA methylation patterns in subjects exposed to low-dose benzene. *Cancer Research* **67**: 876–880
- Bourc'his D & Bestor TH (2004) Meiotic catastrophe and retrotransposon reactivation in male germ cells lacking Dnmt3L. *Nature* **431**: 96–99
- Bremner JD, Licinio J, Darnell A, Krystal JH, Owens MJ, Southwick SM, Nemeroff CB & Charney DS (1997) Elevated CSF corticotropin-releasing factor concentrations in posttraumatic stress disorder. *Am J Psychiatry* **154**: 624–629
- Breslin MB (2001) Multiple Promoters Exist in the Human GR Gene, One of Which Is Activated by Glucocorticoids. *Mol Endocrinol* **15**: 1381–1395
- Brewin CR (2001) A cognitive neuroscience account of posttraumatic stress disorder and its treatment. *Behav Res Ther* **39**: 373–393
- Brouha B, Meischl C, Ostertag E, de Boer M, Zhang Y, Neijens H, Roos D & Kazazian HH (2002) Evidence consistent with human L1 retrotransposition in maternal meiosis I. *Am J Hum Genet* **71**: 327–336

**DNA methylation at glucocorticoid receptor gene promoter is linked to the PTSD risk in  
genocide survivors**

- Capomaccio S, Verini-Supplizi A, Galla G, Vitulo N, Barcaccia G, Felicetti M, Silvestrelli M & Cappelli K (2010) Transcription of LINE-derived sequences in exercise-induced stress in horses. *Anim. Genet.* **41 Suppl 2**: 23–27
- Davies MN, Volta M, Pidsley R, Lunnon K, Dixit A, Lovestone S, Coarfa C, Harris RA, Milosavljevic A, Troakes C, Al-Sarraj S, Dobson R, Schalkwyk LC & Mill J (2012) Functional annotation of the human brain methylome identifies tissue-specific epigenetic variation across brain and blood. *Genome Biol* **13**:R43
- de Quervain v et al., 2012. PKCa is genetically linked to memory capacity in non-traumatized individuals and to traumatic memory and PTSD risk in genocide survivors. *PNAS*, in press
- de Quervain D, Aerni A, Schelling G & Roozendaal B (2009a) Glucocorticoids and the regulation of memory in health and disease. *Frontiers in Neuroendocrinology* **30**: 358–370
- de Quervain DJ-F, Aerni A, Schelling G & Roozendaal B (2009b) Glucocorticoids and the regulation of memory in health and disease. *Frontiers in Neuroendocrinology* **30**: 358–370
- de Quervain DJ-F, Kolassa I-T, Ertl V, Onyut PL, Neuner F, Elbert T & Papassotiropoulos A (2007) A deletion variant of the alpha2b-adrenoceptor is related to emotional memory in Europeans and Africans. *Nature Publishing Group* **10**: 1137–1139
- Delahanty DL, Raimonde AJ & Spoonster E (2000) Initial posttraumatic urinary cortisol levels predict subsequent PTSD symptoms in motor vehicle accident victims. *BPS* **48**: 940–947
- Derogatis LR, Lipman RS, Rickels K, Uhlenhuth EH & Covi L (1974) The Hopkins Symptom Checklist (HSCL): a self-report symptom inventory. *Behavioral science* **19**: 1–15
- American Psychiatric A. 2000. *Diagnostic and statistical manual of mental disorder, fourth edition (DSM-IV)*, Washington, DC, 1994 (Washington, DC)
- Dulac C (2010) Brain function and chromatin plasticity. *Nature* **465**: 728–735
- Ewing AD & Kazazian HH (2010) High-throughput sequencing reveals extensive variation in human-specific L1 content in individual human genomes. *Genome Research* **20**: 1262–1270
- Fedorov AV (2008) [Regulation of mammalian LINE1 retrotransposones transcription]. *Tsitologiya* **50**: 1011–1022
- Foa E, Cashman L & Jaycox L (1997) Perry validation of a self-report measure of posttraumatic stress disorder: The Posttraumatic Diagnostic Scale. *Psychol Assess* **9**: 445–451
- Francis D (1999) Nongenomic Transmission Across Generations of Maternal Behavior and Stress Responses in the Rat. *Science* **286**: 1155–1158

- Goenjian AK, Yehuda R, Pynoos RS, Steinberg AM, Tashjian M, Yang RK, Najarian LM & Fairbanks LA (1996) Basal cortisol, dexamethasone suppression of cortisol, and MHPG in adolescents after the 1988 earthquake in Armenia. *Am J Psychiatry* **153**: 929–934
- Holsboer F (2003) Corticotropin-releasing hormone modulators and depression. *Current opinion in investigational drugs (London, England : 2000)* **4**: 46–50
- Kanter ED, Wilkinson CW, Radant AD, Petrie EC, Dobie DJ, McFall ME, Peskind ER & Raskind MA (2001) Glucocorticoid feedback sensitivity and adrenocortical responsiveness in posttraumatic stress disorder. *BPS* **50**: 238–245
- Kardiner, A., 1941. *The Traumatic Neuroses of War*, (New York: Hoeber).
- Kim M-J, White-Cross JA, Shen L, Issa J-PJ & Rashid A (2009a) Hypomethylation of long interspersed nuclear element-1 in hepatocellular carcinomas. *Mod Pathol* **22**: 442–449
- Kim M-S, Kondo T, Takada I, Youn M-Y, Yamamoto Y, Takahashi S, Matsumoto T, Fujiyama S, Shiode Y, Yamaoka I, Kitagawa H, Takeyama K-I, Shibuya H, Ohtake F & Kato S (2009b) DNA demethylation in hormone-induced transcriptional derepression. *Nature* **461**: 1007–1012
- Kohda K, Harada K, Kato K, Hoshino A, Motohashi J, Yamaji T, Morinobu S, Matsuoka N & Kato N (2007) Glucocorticoid receptor activation is involved in producing abnormal phenotypes of single-prolonged stress rats: a putative post-traumatic stress disorder model. *Neuroscience* **148**: 22–33
- Kolassa I-T, Ertl V, Eckart C, Glöckner F, Kolassa S, Papassotiropoulos A, de Quervain DJ-F & Elbert T (2010a) Association study of trauma load and SLC6A4 promoter polymorphism in posttraumatic stress disorder: evidence from survivors of the Rwandan genocide. *The Journal of clinical psychiatry* **71**: 543–547
- Kolassa I-T, Kolassa S, Ertl V, Papassotiropoulos A & de Quervain DJ-F (2010b) The risk of posttraumatic stress disorder after trauma depends on traumatic load and the catechol-o-methyltransferase Val(158)Met polymorphism. *BPS* **67**: 304–308
- Kristensen LS, Mikeska T, Krypuy M & Dobrovic A (2008) Sensitive Melting Analysis after Real Time-Methylation Specific PCR (SMART-MSP): high-throughput and probe-free quantitative DNA methylation detection. *Nucleic Acids Research* **36**: e42–e42
- Ladd-Acosta C, Pevsner J, Sabunciyan S, Yolken RH, Webster MJ, Dinkins T, Callinan PA, Fan J-B, Potash JB & Feinberg AP (2007) DNA methylation signatures within the human brain. *Am J Hum Genet* **81**: 1304–1315
- Liberzon I, López JF, Flagel SB, Vázquez DM & Young EA (1999) Differential regulation of hippocampal glucocorticoid receptors mRNA and fast feedback: relevance to post-traumatic stress disorder. *J. Neuroendocrinol.* **11**: 11–17

**DNA methylation at glucocorticoid receptor gene promoter is linked to the PTSD risk in  
genocide survivors**

- Lister R, Pelizzola M, Downen R & Hawkins R (2009) Human DNA methylomes at base resolution show widespread epigenomic differences. *Nature* **462**: 315–322
- Marshall RD, Blanco C, Prinz D, Liebowitz MR, Klein DF & Coplan J (2002) A pilot study of noradrenergic and HPA axis functioning in PTSD vs. panic disorder. *Psychiatry research* **110**: 219–230
- Mason JW, Giller EL, Kosten TR, Ostroff RB & Podd L (1986) Urinary free-cortisol levels in posttraumatic stress disorder patients. *J. Nerv. Ment. Dis.* **174**: 145–149
- Maunakea A, Nagarajan R & Bilenky M (2010) Conserved role of intragenic DNA methylation in regulating alternative promoters. *Nature* **466**: 253–257
- McFarlane A, Atchison M & Yehuda R (1997) The acute stress response following motor vehicle accidents and its relation to PTSD. In pp 437–441.
- Mcgaugh JL & Roozendaal B (2002a) Role of adrenal stress hormones in forming lasting memories in the brain. *Curr. Opin. Neurobiol.* **12**: 205–210
- Mcgaugh JL & Roozendaal B (2002b) Role of adrenal stress hormones in forming lasting memories in the brain. *Curr. Opin. Neurobiol.* **12**: 205–210
- Mcgowan PO, Sasaki A, D'alessio AC, Dymov S, Labonté B, Szyf M, Turecki G & Meaney MJ (2009a) Epigenetic regulation of the glucocorticoid receptor in human brain associates with childhood abuse. *Nat Neurosci* **12**: 342–348
- Mcgowan PO, Sasaki A, D'alessio AC, Dymov S, Labonté B, Szyf M, Turecki G & Meaney MJ (2009b) Epigenetic regulation of the glucocorticoid receptor in human brain associates with childhood abuse. *Nat Neurosci* **12**: 342–348
- Michael T, Ehlers A, Halligan SL & Clark DM (2005) Unwanted memories of assault: what intrusion characteristics are associated with PTSD? *Behav Res Ther* **43**: 613–628
- Mill J, Tang T, Kaminsky Z, Khare T, Yazdanpanah S, Bouchard L, Jia P, Assadzadeh A, Flanagan J, Schumacher A, Wang S-C & Petronis A (2008) Epigenomic profiling reveals DNA-methylation changes associated with major psychosis. *Am J Hum Genet* **82**: 696–711
- Morales JF (2002a) Environmental factors affecting transcription of the human L1 retrotransposon. I. Steroid hormone-like agents. *Mutagenesis* **17**: 193–200
- Munck A, Guyre PM & Holbrook NJ (1984) Physiological functions of glucocorticoids in stress and their relation to pharmacological actions. *Endocr Rev* **5**: 25–44
- Murgatroyd C, Patchev AV, Wu Y, Micale V, Bockmühl Y, Fischer D, Holsboer F, Wotjak CT, Almeida OFX

- & Spengler D (2009) Dynamic DNA methylation programs persistent adverse effects of early-life stress. *Nat Neurosci* **12**: 1559–1566
- Neuner F, Onyut PL, Ertl V, Odenwald M, Schauer E & Elbert T (2008) Treatment of posttraumatic stress disorder by trained lay counselors in an African refugee settlement: a randomized controlled trial. *Journal of consulting and clinical psychology* **76**: 686–694
- Neuner F, Schauer M, Karunakara U, Klaschik C, Robert C & Elbert T (2004) Psychological trauma and evidence for enhanced vulnerability for posttraumatic stress disorder through previous trauma among West Nile refugees. *BMC psychiatry* **4**: 34
- Oberlander TF, Weinberg J, Papsdorf M, Grunau R, Misri S & Devlin AM (2008) Prenatal exposure to maternal depression, neonatal methylation of human glucocorticoid receptor gene (NR3C1) and infant cortisol stress responses. *epigenetics* **3**: 97–106
- Onyut L (2004) The Nakivale Camp Mental Health Project: Building local competency for psychological assistance to traumatised refugees. *Intervention Amstelveen* **2**: 90–107
- Ostertag EM & Kazazian HH Jr (2001) Biology of mammalian L1 retrotransposons. *Annual review of genetics* **35**: 501–538
- Pfaffl MW (2001) A new mathematical model for relative quantification in real-time RT-PCR. *Nucleic Acids Research* **29**: e45
- Pitman RK & Orr SP (1990) Twenty-four hour urinary cortisol and catecholamine excretion in combat-related posttraumatic stress disorder. *BPS* **27**: 245–247
- Prak ETL, Dodson AW, Farkash EA & Kazazian HH (2003) Tracking an embryonic L1 retrotransposition event. *Proc Natl Acad Sci USA* **100**: 1832–1837
- Resnick HS, Yehuda R, Pitman RK & Foy DW (1995) Effect of previous trauma on acute plasma cortisol level following rape. *Am J Psychiatry* **152**: 1675–1677
- Roosendaal B, McEwen BS & Chattarji S (2009) Stress, memory and the amygdala. *Nat Rev Neurosci* **10**: 423–433
- Rusiecki JA, Chen L, Srikantan V, Zhang L, Yan L, Polin ML & Baccarelli A (2012) DNA methylation in repetitive elements and post-traumatic stress disorder: a case-control study of US military service members. *Epigenomics* **4**: 29–40
- Segman RH & Shalev AY (2003) Genetics of posttraumatic stress disorder. *CNS spectrums* **8**: 693–698
- Squire L (1987) *Memory and Brain* - Larry R. Squire - Google Books Oxford University Press
- Stanzer S, Balic M, Strutz J & Heitzer E (2010) Rapid and reliable detection of LINE-1 hypomethylation using high resolution melting analysis. *Clinical ...*



**DNA methylation at glucocorticoid receptor gene promoter is linked to the PTSD risk in  
genocide survivors**

- Stein MB, Jang KL, Taylor S, Vernon PA & Livesley WJ (2002) Genetic and environmental influences on trauma exposure and posttraumatic stress disorder symptoms: a twin study. *Am J Psychiatry* **159**: 1675–1681
- Stein MB, Yehuda R, Koverola C & Hanna C (1997) Enhanced dexamethasone suppression of plasma cortisol in adult women traumatized by childhood sexual abuse. *BPS* **42**: 680–686
- Tost J & Gut IG (2007) DNA methylation analysis by pyrosequencing. *Nat Protoc* **2**: 2265–2275
- True WR, Rice J, Eisen SA, Heath AC, Goldberg J, Lyons MJ & Nowak J (1993) A twin study of genetic and environmental contributions to liability for posttraumatic stress symptoms. *Arch. Gen. Psychiatry* **50**: 257–264
- Tse MY, Ashbury JE, Zwingerman N, King WD, Taylor SAM & Pang SC (2011) A refined, rapid and reproducible high resolution melt (HRM)-based method suitable for quantification of global LINE-1 repetitive element methylation. *BMC Res Notes* **4**: 565
- Turner JD (2005) Structure of the glucocorticoid receptor (NR3C1) gene 5' untranslated region: identification, and tissue distribution of multiple new human exon 1. *Journal of Molecular Endocrinology* **35**: 283–292
- Vandesompele J, De Preter K, Pattyn F, Poppe B, Van Roy N, De Paepe A & Speleman F (2002) Accurate normalization of real-time quantitative RT-PCR data by geometric averaging of multiple internal control genes. *Genome Biol* **3**: RESEARCH0034
- Weaver ICG, Cervoni N, Champagne FA, D'Alessio AC, Sharma S, Seckl JR, Dymov S, Szyf M & Meaney MJ (2004) Epigenetic programming by maternal behavior. *Nat Neurosci* **7**: 847–854
- Wojdacz TK, Borgbo T & Hansen LL (2009) Primer design versus PCR bias in methylation independent PCR amplifications. *epigenetics* **4**: 231–234
- Wojdacz TK, Hansen LL & Dobrovic A (2008) A new approach to primer design for the control of PCR bias in methylation studies. *BMC Res Notes* **1**: 54
- Xian H, Chantarujikapong SI, Scherrer JF, Eisen SA, Lyons MJ, Goldberg J, Tsuang M & True WR (2000) Genetic and environmental influences on posttraumatic stress disorder, alcohol and drug dependence in twin pairs. *Drug and alcohol dependence* **61**: 95–102
- Xie H, Wang M, Bonaldo MDF, Smith C, Rajaram V, Goldman S, Tomita T & Soares MB (2009) High-throughput sequence-based epigenomic analysis of Alu repeats in human cerebellum. *Nucleic Acids Research* **37**: 4331–4340
- Yang AS, Estéicio MRH, Doshi K, Kondo Y, Tajara EH & Issa J-PJ (2004) A simple method for estimating global DNA methylation using bisulfite PCR of repetitive DNA elements. *Nucleic Acids Research* **32**: e38

- Yehuda R (1998) Psychoneuroendocrinology of post-traumatic stress disorder. *Psychiatr. Clin. North Am.* **21**: 359–379
- Yehuda R & LeDoux J (2007a) Response variation following trauma: a translational neuroscience approach to understanding PTSD. *Neuron* **56**: 19–32
- Yehuda R & LeDoux J (2007b) Response variation following trauma: a translational neuroscience approach to understanding PTSD. *Neuron* **56**: 19–32
- Yehuda R, Boisoineau D, Lowy MT & Giller EL (1995) Dose-response changes in plasma cortisol and lymphocyte glucocorticoid receptors following dexamethasone administration in combat veterans with and without posttraumatic stress disorder. *Arch. Gen. Psychiatry* **52**: 583–593
- Yehuda R, Boisoineau D, Mason JW & Giller EL (1993) Glucocorticoid receptor number and cortisol excretion in mood, anxiety, and psychotic disorders. *BPS* **34**: 18–25
- Yehuda R, Halligan SL, Golier JA, Grossman R & Bierer LM (2004) Effects of trauma exposure on the cortisol response to dexamethasone administration in PTSD and major depressive disorder. *Psychoneuroendocrinology* **29**: 389–404
- Yehuda R, Lowy MT, Southwick SM, Shaffer D & Giller EL (1991) Lymphocyte glucocorticoid receptor number in posttraumatic stress disorder. *Am J Psychiatry* **148**: 499–504
- Yehuda R, McFarlane AC & Shalev AY (1998) Predicting the development of posttraumatic stress disorder from the acute response to a traumatic event. *BPS* **44**: 1305–1313
- Yehuda R, Morris A, Labinsky E, Zemelman S & Schmeidler J (2007) Ten-year follow-up study of cortisol levels in aging holocaust survivors with and without PTSD. *J. Traum. Stress* **20**: 757–761



